2012

The Diversity of Cortical Interneurons

Miho Nakajima

THE DIVERSITY OF CORTICAL INTERNEURONS

A Thesis Presented to the Faculty of

The Rockefeller University

in Partial Fulfillment of the Requirements for

the degree of Doctor of Philosophy

by

Miho Nakajima

June 2012

THE DIVERSITY OF CORTICAL INTERNEURONS

Miho Nakajima, Ph.D.

The Rockefeller University 2012

The cortex is involved in diverse higher cognitive processes including decision making, motor planning, sensory discrimination, and memory consolidation. The cortical interneurons are key elements of the cortical system. These interneurons stabilize networks, but at the same time they also add non-linear effects to the excitatory system to make the cortical network more dynamic. To achieve this, cortical interneurons form a very heterogeneous group, making it hard to classify them without markers. We took a BACtrap approach performing translating ribosome affinity purifications on transgenic mice with Bacterial artificial chromosome, for systematic discovery of markers for different cell types.

First, we generated BACtrap lines for known markers of mixed interneuron populations. After IHC (immnohistochemistry) characterization of each line, we picked 4 lines for Dlx1, Nek7, Htr3a and Cort genes for further studies. We collected mRNAs from targeted neurons in each line and performed gene profiling. Based on IHC and gene profiling studies, we found that each of the 4 lines labeled different but overlapping interneuron populations in the cortex.

Second, we performed a comparative microarray analysis to find genes that showed differential enrichment in each of the 4 populations and we found ~20 genes as candidate marker genes. To examine their potential role as marker genes, we generated BAC

transgenic mice for these candidate genes and also examined their DRP (Density Recovery Profile) on ISH images from the ABA (Allen Brain Atlas). We found that a number of candidate genes showed regular spacing of cell bodies, suggesting that those genes might label a functionally homogenous group.

Third, we characterized new Cre lines for candidate marker genes, Rbp4 and Oxtr, to investigate their cell types and functional roles by using Cre/loxP system. Both Rbp4 and Oxtr Cre are heterogeneous in terms of their neurochemical profiles, but DRP analysis on Oxtr Cre neurons suggested their potential to be a functionally homogenous group. Cre dependent AAV injection also revealed a tiling property of Oxtr Cre neurons in the somatosensory cortex. Connectivity of three different Cre lines (Rbp4, Oxtr, Htr3a) was also examined using retrograde monosynaptic rabies virus tracers. Although three lines expressed Cre proteins in different interneuron populations, the presynaptic inputs were almost identical except for a few differences. However, each line had a different preference in inputs and we found line specific inputs from the hippocampus and the dopaminergic nuclei.

In short, we carried out systematic marker searches and the generation of transgenic mice. Our findings suggest the existence of better markers for interneuron cell types, and we also showed that a group that is heterogeneous at the cellular level could work as a functionally homologous group. New interneuronal Cre lines showed a few differences in presynaptic inputs and created new opportunities for us to understand the functional differences of distinct cell types.

ACKNOWLEDGEMENTS

It was a challenging for me to live and study outside Japan speaking in English, but with the hospitality and friendliness of the people in science and NY, I've never felt homesick and always felt lucky for my opportunities to do neuroscience in the best place in the world. I would like to thank so many people for that.

First, I would like to thank my advisor, Prof. Nathaniel Heintz. Nat understood what I wanted to study from the day we talked for the first time, and he let me do what I was interested in. I am quite stubborn when it comes to the subjects, but he has never pushed me do something I am not interested in. He guided me and showed me the new possibilities of studies. I could do something nobody else could do in the world, with his resource and techniques. I also would like to thank my committee members Dr. Cori Bargmann, Dr. Paul Greengard, Dr. Gordon Fishell and Dr. Stewart Anderson for their time to guide me through my thesis, helping me understand how science works and how important the presentation is. Especially Dr. Fishell invited me to his lab meetings and gave me the great opportunities to talk with interneuron specialists.

I couldn't do anything without the support from my family in Japan. My parents, Ryoichi Nakajima and Chiaki Nakajima, my sister, Sachiko Nakajima and my niece, Sou Nakajima are the ones who gave me inspiration and taught me how interesting the research is. They are the reason why I am here to study one of the most difficult subjects in the world, brain. They understood my passion and never complained even though I couldn't do anything for them and couldn't go home for a couple of years.

I also thank all my friends in Rockefeller. My lab member, Pinar Ayata and Prerana Shrestha are the best friends in NY. They are always besides me when I am in trouble. My bay mates, Joseph Dougherty and Hirofumi Nakayama are the best partners for discussion. They knew so many scientific facts and discussion with them were always fun and very useful. I would like to thank all other Heintz lab members, past and present for their scientific advice and good times in the lab. I also thank all my beer mates, especially Chan Tan and Pat in the faculty club. Faculty club is my favorite place in NY, and drinking beer and talking science is my best combination. They will be my life-long friends.

Last but not least I would like to thank my boyfriend, Jonathan O'brien. After I met him, my life has changed. I could expand my friends outside science and his interests in literature, history and philosophy gave me great inspiration. He also read my thesis and corrected my grammar, even though he is a lawyer.

TABLE OF CONTENTS

LIST OF FIGURES

LIST OF TABLES

Chapter 1
Introduction

1-1: Prologue

The intricacy of vertebrate neural networks can make vertebrates' movements more complicated and sophisticated. This intricacy is mainly supported by the plasticity and the diversity of neurons and the complex and dynamic circuits into which neurons are organized. To understand the diversity of neurons, the term, "Cell Type", has been used to classify neurons based on their morphologies, firing patterns, connections and cytochemical markers. A cell type is the elementary computational element in the brain machine and identification of the functionally distinct cell types is critical to any bottom-up understanding of neural networks. Some major cell types were already described in the late 19th century by Ramon y Cajal using Golgi staining (Cajal 1899). However due to the plasticity of neurons and the lack of information on the neural networks, we still don't know how to define cell types and how many cell types exist, especially in the cortex. This problem is being discussed intensively in the cortical interneuron area (Nelson, Sugino et al. 2006; Ascoli, Alonso-Nanclares et al. 2008) and retina study (Stevens 1998; Masland 2001; Masland 2004). Much progress has been made on retina cell types owing to its accessibility to physiological stimuli, clearly defined laminar structure, cellular morphologies and cellular function. 55-60 distinct retinal cell types have already been identified (Masland 2001; Siegert, Scherf et al. 2009). If retinal

organization is similar to the cortex, this number could suggest that there are about 1000 cell types in the cortex (Stevens 1998).

1-2: Cell Types in Retina

A mammalian retina contains five major classes of neurons divided into ~60 different types based on their morphologies (Masland 2001; Masland 2004). Three methods are used to confirm the cell types, not the variants of the single types. The first method is based on neurons' stratification pattern. Stratifications of retinal neurons put physical limits on the contact they could have. The second method is the observation of neurons' distinct neurochemical and morphological properties. And the third method of confirmation is to examine the coverage of the retina. In other words, avoidance of axonal terminals or dendritic arbors in the group (tiling), or regular spacing of cell bodies, could be observed in neurons to cover the whole retina without too much redundancy. Cells of a correctly identified type have a regular mosaic, while a mixture of cells from different types shows random spacing.

How cells discriminate cells of the same types from other types is still a mystery. However, recently, a couple of genes including Down syndrome cell adhesion molecule (DSCAM) (Matthews, Kim et al. 2007), Tricornered (TRC), furry (fry) (Emoto, He et al. 2004), and the target genes of rapamycin complex 2 (TORC2) (Koike-Kumagai, Yasunaga et al. 2009), were identified as tiling regulator genes in *D. melanogaster*. The knock-out of mammalian homolog of DSCAM gene also showed fasciculation of dendrites and loss of mosaic pattern of cell bodies in retina, which indicates similar tiling

mechanisms are conserved across species (Fuerst, Koizumi et al. 2008). Recently two related transmembrane proteins, MEGF10 and MEGF11 were shown to have critical roles in the formation of mosaics of two retinal interneuron subtypes through their homotypic interactions in mouse retina (Kay, Chu et al. 2012).

As a measurement of tiling, Density Recovery Profile (DRP) method was developed and is used to measure the randomness of the cell bodies spacing (Figure 1.1).

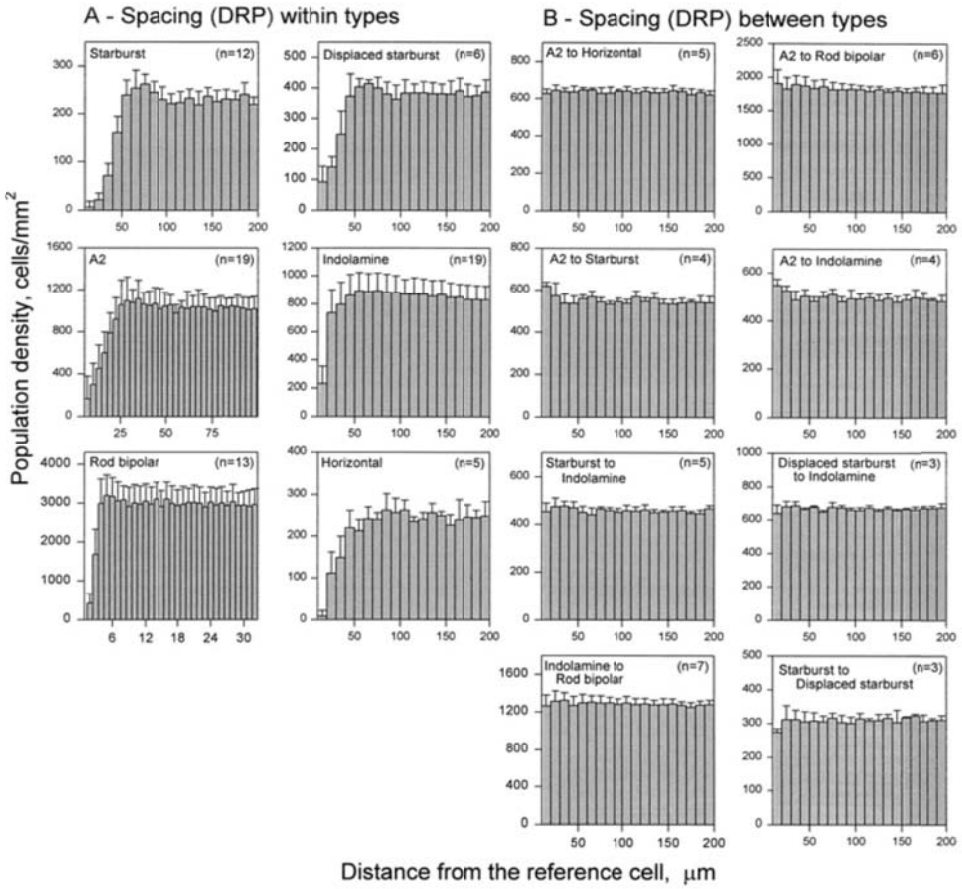

Figure 1.1: The Density Recovery Profiles (DRPs) for Six Types of Retinal Neurons.

(A) The spacing of cells with respect to other cells of the same type. Neurons which belong to the same cell type have a zone of exclusion for other homotypic cells and showed low density in the short distance (B) Cells from mixed populations of different cell types don't show repulsions among them and have random distribution. There are no differences from the average density regardless of the distance.

1-3: Organization of the Mammalian Cortex

The cortex, although heterogeneous at the cellular level, has a well-organized topographic structure. The cortex can be divided into 6 layers along the radial axis and each layer consists of different neuronal cell types. A strong vertical organization (column) is also apparent and this column spans all layers. Neurons in the same column tend to be connected and have similar response properties regardless of layers. Layer 4 is the major thalamocortical input layer and it sends information to superficial layer 2/3 in the same column. Layer 2/3 is involved in corticocortical connectivity and provides two-thirds of the input to all neurons in the cortex. Layer 2/3 also connects to layer 5 which is the major output layer that sends long subcortical and callosal projections. Layer 6 primarily sends feedback to the thalamus. Layer 1 contains a high density of axons originating from projection neurons of different cortical areas and extensions of apical dendrites of neurons in the same column. Layer 1 also has scattered reelin positive Cajal-Retzius interneurons which sends dense horizontal axons (Shepherd 2003).

The cortex can be divided into functionally distinct areas, referred to as cortical areas, via the tangential axis. Cortical areas can be categorized into three main groups: 1) sensory 2) motor 3) association. The sensory areas, such as the primary somatosensory cortex, the primary auditory cortex, and the primary visual cortex, receive and process sensory inputs. The motor cortices, referred to as the primary motor cortex and the premotor cortex, execute and regulate movements. Association cortices execute higher processing of information, affect sensory perception, and plan motor outcomes. They are also

involved in abstract thinking and language. Association cortices include the prefrontal cortex and the secondary motor/somatosensory cortex.

It is well established that neurons in the cortex are divided broadly into two major classes: glutamatergic excitatory projection neurons (pyramidal cells) and γ-aminobutyric acid (GABA)ergic inhibitory local circuit neurons (interneurons). Henceforth, I will refer to interneurons as GABAergic local circuit neurons. Pyramidal cells specialize in the transfer of information between different areas, whereas interneurons primarily contribute to local neural assemblies to modulate the flow of information there. Pyramidal fall into over a few classes, regardless of the enormous amount of information they have to deal with. The functional repertoire of pyramidal cells is supported by the rich diversity of GABAergic interneurons. It's been shown that adding novel interneuron types to the old network even in small numbers can create a nonlinear expansion of qualitatively different possibilities (Buzsaki 2006). Therefore, GABAergic interneurons have diverse morphological, physiological and molecular characteristics, even though they are a minor population (~20%) in the cortex. Although interneurons are a heterogeneous group of neuronal cells, they often have common features that distinguish them from excitatory pyramidal neurons. These include aspiny dendrites and GABA as the main neurotransmitter. The inhibitory transmitter, GABA, is synthesized primarily by the action of two isoforms of glutamic acid decarboxylase (GAD65, GAD67). GABA binds to two different types of GABA receptors ($GABA_A$ and $GABA_B$ receptor). $GABA_A$ receptors are ionotropic receptors that selectively allow Cl^- ions to pass through their pores upon activation, resulting in hyperpolarization of the neuron and preventing

neurons from firing. $GABA_B$ receptors are metabotropic seven-transmembrane receptors for GABA that are linked via G-proteins (Gi/Go) to potassium channels and calcium channels, and elicit presynaptic and slow postsynaptic inhibition. $GABA_B$ receptors can also reduce the activity of adenylyl cyclase and decrease the cell's conductance to Ca^{2+} (Sivilotti and Nistri 1991).

1-4: Common Classification Methods of Cortical Interneurons

Each different class of GABAergic interneurons has a different functional role, and understanding each role is the key to describing the dynamic neural networks in the cortex. However, we still don't have unequivocal methods to classify interneurons, even after extensive discussion (Ascoli, Alonso-Nanclares et al. 2008). This is mainly because of the lack of agreement on criteria for what is necessary to define a cell type. Present classification methods depend on three categories: (1) morphology (anatomy) (2) neurochemical signature (3) electrophysiological properties. Most researchers used all or two categories to name the interneurons they were working on.

1-4-1: Morphological Criteria

Morphologies alone can provide basic information of interneurons' functional roles in the active neural networks. Each group varies in its somatic, dendritic, and axonal morphologies (Figure 1.2).

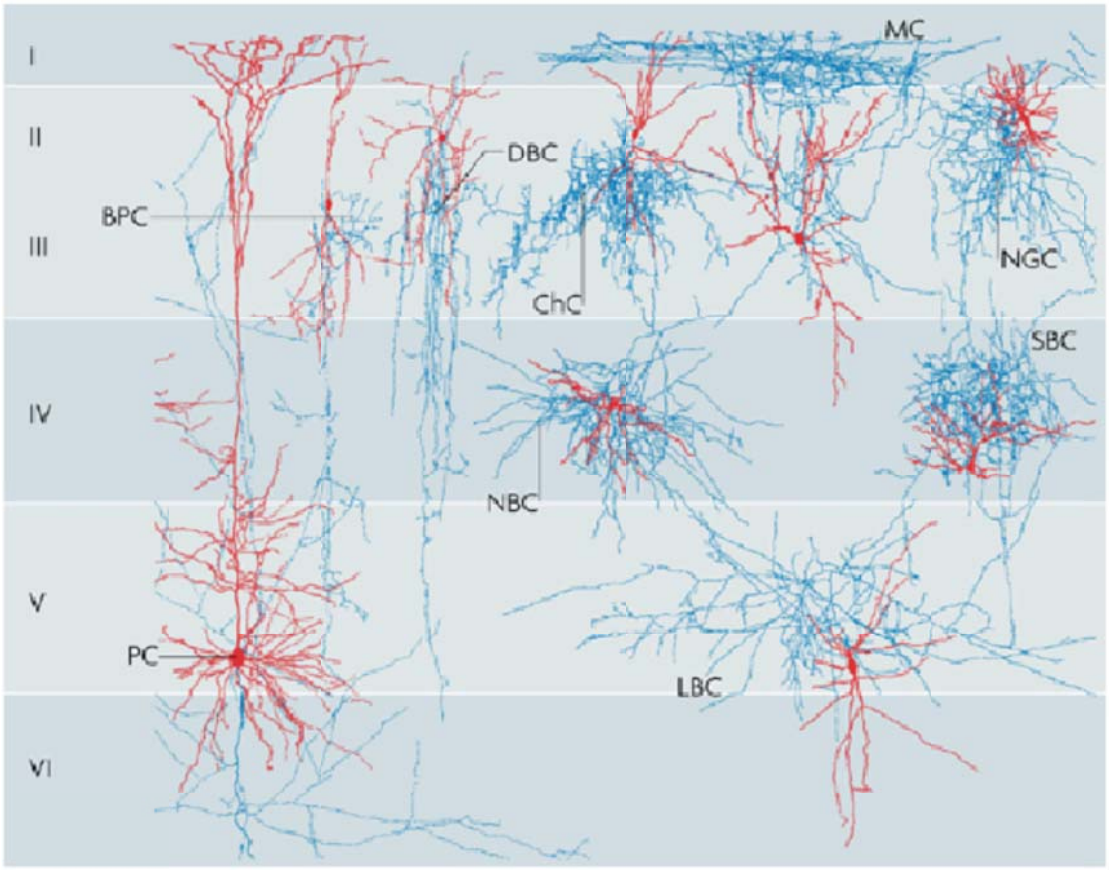

Figure 1.2: Major Interneuron Cell Types
Morphologies of major interneuron cell types. Layer 5 Pyramidal cell is pictured as a comparison. Axons are shown in blue and dedrites are shown in red. PC, Pyramidal cell; BPC, bipolar cell; ChC, Chandelier cell; NBC, nested basket cell; LBC, large basket cell; SBC, small basket cell; MC, Martinotti cell; DBC, double bouquet cell; NGC, Neurogliaform cell. Each cell type has distinct morphology, especially its axonal arbor (Huang, Di Cristo et al. 2007).

Dendritic morphology is the least reliable feature because of its variability. On the other hand, axonal arborizations are characteristic in each group and can suggest the information they are involved. However, some interneurons showed intermediate morphologies. Because there are no agreed criteria in the morphological classification, it

is hard to get a consensus among different researchers as to naming. Most of the time, other classification methods are required.

The major cell types are:

a) Basket cells – the biggest interneuron population in the cortex forms a basket-like nest in which a Pyramidal cell rest. Basket cells form multiple synaptic contacts on the somata and proximal dendrites of pyramidal neurons and control the timing and frequency of their action potentials. This regulation could also affect cellular and network synchronization, and they are known to be involved in θ and γ oscillations in the cortex (Curley and Lewis 2012). The majority of basket cells are Parvalbumin (PV) positive or Cholecystokinin (CCK) positive and never express Calretinin (CR) or Vasoactive intestinal peptide (VIP). PV basket cells discharge trains of short duration action potential at high frequencies, whereas CCK basket cells fire accommodating spike trains at moderate frequencies. Basket cells also can be subdivided into at least three subgroups based on their morphologies: the large, small and nest (Markram, Toledo-Rodriguez et al. 2004).
b) Chandelier cells – characterized by their axonal arbors with the terminals forming distinct arrays called "cartridges". They target the axon initial segment (AIS) of pyramidal neurons and control their output. It is still controversial, but some Chandelier cells were shown to provide GABAergic excitation due to the depolarized reversal membrane potential of AIS (Szabadics, Varga et al. 2006). Chandelier cells are located in all layers, but most abundantly in layer 2/3. They typically express PV.

c) Martinotti cells – defined by their ascending axonal collaterals with extensive branching in layer 1, where they inhibit the dendrites of the pyramidal neurons. Martinotti cells seem to connect with many surrounding pyramidal neurons to balance out the over-excitation in the same column (Fino and Yuste 2011). These cells are physiologically characterized by a moderate frequency of firing and significant spike frequency adaptation. They are somatostatin (SST) positive.

d) Neurogliaform cells – They are late spiking neurons characterized by a small round soma, a compact dendritic tree and dense axonal aborizations. Single Neurogliaform cells (NGF) can produce a dense cloud of GABA, inducing volume transmission by activating extrasynaptic GABA receptors (Olah, Fule et al. 2009). Therefore NGF cells can inhibit the activities of nearly all cells in a local region similar to Martinotti cells. They can evoke long lasting inhibition through atypically slow $GABA_A$ responses and slow $GABA_B$ mediated responses in the postsynaptic neurons. They are unique in that they form gap junctions with many different types of interneurons, whereas others form electrical synapses with neurons which belong to the same cell type. This implies NGF cells might be involved in the network synchronization of the cortex. NGF cells belong to reelin positive/SST-negative population and they also express Choline acetyltransferase (Chat), nitric oxide synthase (NOS) and the ionotropic serotonin receptor, Htr3a.

e) Bipolar cell/Bitufted cell – small cells with an oval-shaped somata and bipolar dendrites that extend vertically. They are dendritic targeted cells. Bitufted cells have adapting regular firing during large depolarization. Bipolar cells display fast

adapting firing pattern. Both are VIP positive. Bitufted cells are also CR positive, while bipolar cells are CR negative. Some also express Chat.

f) Double Bouquet cell – have characteristic long tightly interwoven vertical axon bundles and bitufted dendrites. They are VIP, CR, and Calbindin (CB) positive. They are located mainly in layer 2-3 (Somogyi and Cowey 1981). Their existence in rodent cortex is still questionable and Double Bouquet cells have suggested to be primate specific interneurons (Jones 2009).

g) Cajal-Retzius cells – They are layer 1 interneurons identified by Cajal. They possess long horizontal axons that inhibit dendrites of pyramidal neurons in layer 1. Most abundant during developmental stages. They are also reelin positive.

1-4-2: Neurochemical

Various Ca2+ binding proteins (PV, CB and CR) and neuropeptides (SST, VIP, neuropeptide Y (NPY), and CCK), have been used as molecular makers of cortical interneuron subtypes. These markers are useful for large scale functional studies and are good candidates for genetic approaches (Taniguchi, He et al. 2011). However, different types of morphologically defined interneurons could co-exist and overlap in a single neurochemically identified group. For example, expression of PV can be found in basket cells (Large, small, nested), Chandelier cells, and Multipolar Bursting cells. Each PV type has a different function in neural network (Blatow, Rozov et al. 2003; Woodruff, Anderson et al. 2010). Lack of better markers for each PV positive sub-group could cause confusion in functional studies (Kerlin, Andermann et al. 2010; Runyan, Schummers et al. 2010). SST positive interneurons were also suggested to be subdivided into more specific

cell types from the classification of their morphologies, localized layers, and firing pattern (Ma, Hu et al. 2006; McGarry, Packer et al. 2010). X94 cells were identified as a new SST positive cell types in transgenic mice with a random insertion of a GFP transgene under the small GAD67 promoter (Ma, Hu et al. 2006). They are located in layer 4 and 5B and often don't show axonal projections to layer 1. However, due to the absence of molecular markers for these cells, it is not possible to target these neurons genetically. It is still an open question whether they are really different from Martinotti cells. Another problem in neurochemical classification is the activity dependent changes in marker gene expression. Some of the markers such as PV or NPY can be regulated by the activity of neurons. If expression of these markers is not stable, it is hard to define cell types with them.

1-4-3: Physiological

Physiological properties of neurons (both passive and active) directly affect their functions in the network activity and computations. Therefore many studies have been performed to identify their passive or subthreshold responses, action potential reactions, firing patterns, gap junctions, and plasticity in slice cultures. These studies found correlations between some physiological properties and molecular markers or morphologies. For example, fast spiking neurons are usually either PV positive basket cells or Chandelier cells. That is expected because electrophysiological responses depend on the ion channel composition and neural morphology of neurons. However, physiological properties are dynamic and are easily affected by the state of neurons (such as neuromodulatory control) in vivo. The same physiological properties can be found in

morphologically distinct populations and vice versa. Therefore it is hard to predict cell types just based on physiological properties.

A simplified diagram showing correlations between different categories is in Figure 1.3 (Markram, Toledo-Rodriguez et al. 2004).

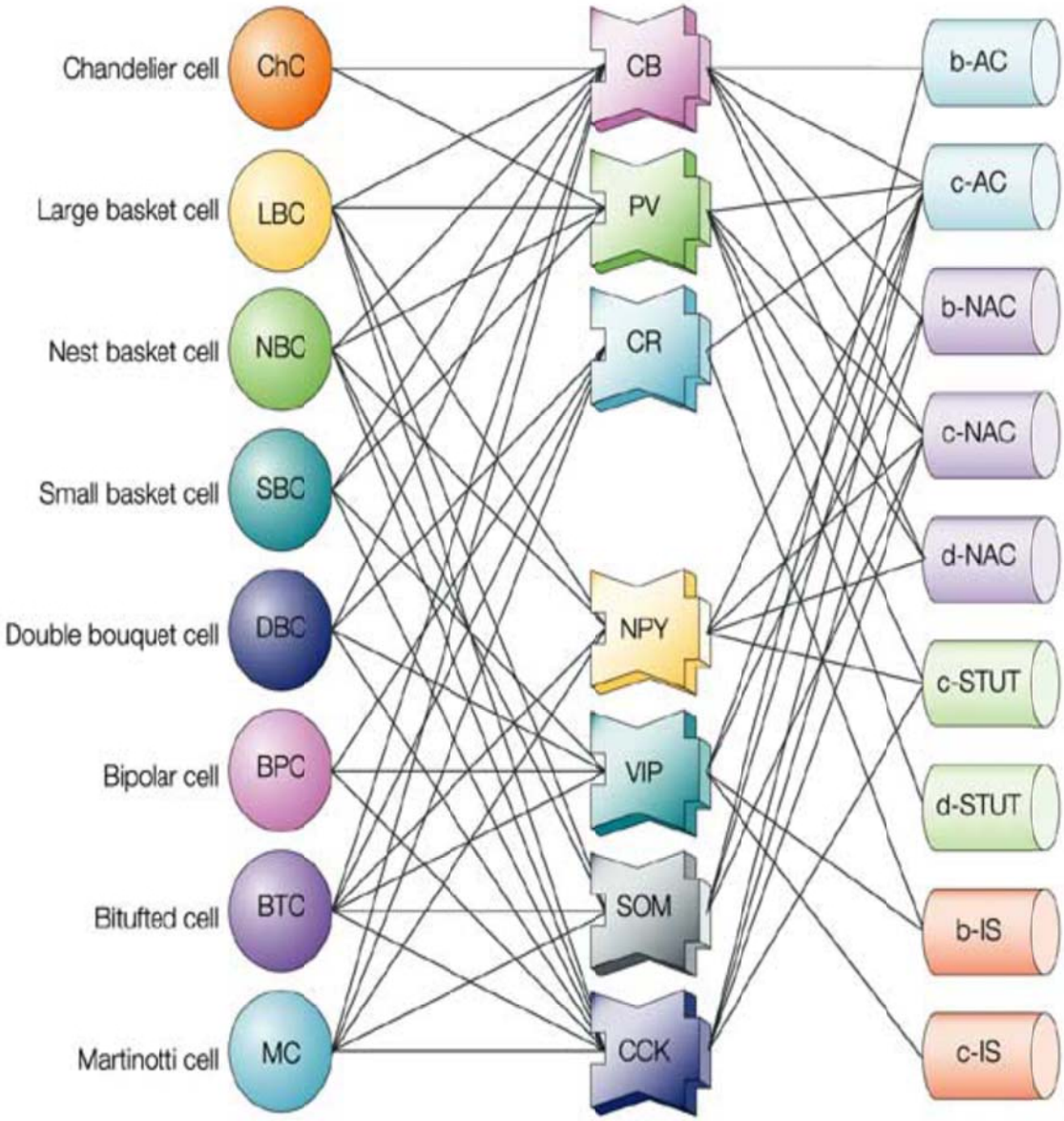

Figure 1.3: Expression of Known Markers in Interneurons

The relationship of neurochemical markers with morphologies and discharge responses at steady state. This diagram shows that each classification method can't predict other features. This means none of the methods is sufficient to identify interneuron cell type. Calbindin (CB); Parvalbumin, (PV); Calretinin, (CR); Neuropeptide Y, (NPY); Vasoactive Intestinal Peptide, (VIP); Somatostatin, (SOM); Cholecystokinin, (CCK); accommodating, (AC); burst subtype, (b); classic subtype, (c); delay subtype, (d); irregularspiking, (IS); non-accomodating, (NAC); stuttering, (STUT) (Markram, Toledo-Rodriguez et al. 2004).

1-5: Development of GABAergic Interneurons

Much pioneering work has been accomplished to understand the developmental mechanisms in the generation of cortical interneuron diversity (Wonders and Anderson 2006; Batista-Brito and Fishell 2009; Gelman and Marin 2010). Cortical interneurons are generated in the ventricular zone of the ventral ganglionic eminences and migrate tangentially into the developing cortex, while cortical projection neurons derive from the dorsal pallial telencephalon and migrate radially into the cortical mantle zone. One of the characteristic events of the GABAergic development is the shift of $GABA_A$ mediated responses from depolarizing to hyperpolarizing (Ben-Ari 2002). $GABA_A$ receptors are selectively permeable to Cl^- and their reversal potential is determined by the distribution of Cl^-. During development, profound sodium potassium chloride cotransporter (NKCC1) expressions were detected in the ventricular zone of the ganglionic eminences. NKCC1, driven by potassium and sodium gradients, increases the intracellular Cl^- concentration. Therefore, upon GABA binding, $GABA_A$ receptors transfer Cl^- outwards, which causes deporalization of neurons. Several days after reaching the cortex, migrating interneurons upregulate the expression of the potassium chloride exchanger (KCC2), which keeps the intercellular Cl^- concentration low and changes the reversal potential of $[Cl^-]$. This is the main factor of the shift in GABAergic responses towards hyperpolarization. Recently this switch has been shown to work as a stop signal of interneuron migration (Bortone and Polleux 2009).

Multiple studies suggest that each class of cortical interneurons is generated from defined progenitor cells by different groups of transcription factors. PV or SST positive interneurons are derived mainly from the medial ganglionic eminence (MGE) and other

interneurons including VIP or CR positive neurons are generated from the caudal ganglionic eminence (CGE). Both PV and SST positive interneurons require the expression of transcription factor, Nkx2.1 for their specification (Butt, Sousa et al. 2008) and Lhx6 for their migration (Alifragis, Liapi et al. 2004; Liodis, Denaxa et al. 2007). But no transcription factors are known which would differentiate PV and SST neurons. Although the dorsal MGE-SST and ventral MGE-PV spatial bias were confirmed, both subgroups originate from progenitors located throughout the MGE (Inan, Welagen et al. 2012). There is also evidence that the identity of interneurons can be influenced by their birth date (Miyoshi, Butt et al. 2007). MGE precursors can generate distinct subtypes of interneurons depending on the development time point at which they are generated. However CGE derived interneuron subtypes are not dependent on their birth date.

It is possible to speculate that regional and temporal patterns of transcription factor expression dictate the generation of interneurons' identities. However, we still can't eliminate all environmental effects on the decisions of their final identities. They might do final modifications on their morphology, physiological properties, positions or gene expressions that determine their final identities with local environmental cues after they reach the cortex.

1-6: Gene Expression Profiling Approach

As I mentioned in the previous sections, no clear correlations could be established among morphological, neurochemical, and electrophysiological classification methods. However there is a correlation between gene expression profile and the morphology or the

biophysical features of neurons. An individual repertoire of receptors and ion channels has major functional importance at the cellular and network level. To a large extent, the identity and physiological state of neuron types are determined by their patterns of gene expression (Nelson, Hempel et al. 2006; Hobert, Carrera et al. 2010). Therefore genome-wide gene expression profiling could be a sound and unbiased method for neuronal classification. Technically, single cell gene profiling from different cell types could be the answer, but this technology is a major challenge owing to the very small amounts of mRNA involved.

Pooling mRNA from multiple neurons without losing cell type specificity is necessary for replicable microarray or RNA-seq genome wide expression analysis. Recent technology advances make this profiling possible in adult mouse brain tissue where identities of cells are established (Sugino, Hempel et al. 2006; Doyle, Dougherty et al. 2008; Heiman, Schaefer et al. 2008). The method of Sugino et al and manual dissection and dissociation of cells could introduce potential stressors which could alter their transcription profile. Translating ribosome affinity purification (TRAP) was developed to overcome this problem by employing direct and rapid affinity purification for isolation of polysomal RNA from genetically targeted cell types (Doyle, Dougherty et al. 2008; Heiman, Schaefer et al. 2008).

These methodologies require specific labeling of functionally distinct cell types in mice. In the last 10 years, large scale efforts have been made into mapping the expression of thousands of genes in the CNS, most notably, Gene Expression Nervous System Atlas

(GENSAT), BGEM and Allen Brain Atlas (ABA) (Gong, Zheng et al. 2003; Hatten and Heintz 2005; Lein, Hawrylycz et al. 2007). ABA and BGEM produced a digital atlas of gene expression by in situ hybridization and GENSAT generated transgenic mouse lines that express EGFP or Cre protein under the transcriptional control of gene specific promoter using bacterial artificial chromosome (BAC) transgenesis technique. These large scale efforts have uncovered a wealth of information about the unique expression patterns of genes. Due to the diversity of neurons in the brain, it is unlikely that every cell type has a unique marker, but in a restricted area, there could be. Also reproducible fluorescently labeled neurons will cause less confusion among different research groups in their naming. In retina, ~100 GENSAT mouse lines turn out to have stratum or cell type specific GFP labeling (Siegert, Scherf et al. 2009). A similar approach has been taken in interneurons using promoters of known neurochemical markers (Taniguchi, He et al. 2011). 18 Cre or inducible CreER knock-in driver lines were generated, targeting major classes and lineages of GABAergic neurons. These mouse lines will be very useful for functional and developmental studies. However, the populations they are targeting are known to be heterogeneous and more specific mouse lines will be required to describe the diversity of interneurons.

1-7: Functional Studies on Specific Interneuron Population

Functional studies could give us better understanding of the function of each cell type. Cre transgenic/knock-in mice for specific cell types could be a breakthrough for functional studies, especially of minor cell types. With recent technological developments,

we now can identify connections and regulate activity in vivo to determine the functional differences in Cre positive neurons.

1-7-1: Cre/loxP System

Development of the Cre/loxP system for mouse genetics expanded the possibilities of functional studies of specific cell types. Cre recombinase is a DNA recombinase enzyme derived from the P1 Bacteriophage. This enzyme carries out site specific recombination between specific DNA target sequences, namely loxP sites that are otherwise absent in the mouse genome. The Cre gene and loxP sites can be introduced into transgenes, viruses or genomic locator. Cre and loxP transgenic lines are developed separately and crossed to produce the Cre-loxP mouse line. The systematic approach to generate cell type specific Cre driver transgenic lines has been taken by GENSAT and ABA. By crossing Cre lines with different loxP reporter lines, we can delete a gene or express a reporter or modulator in the same Cre positive cells. However Cre expression is not usually restricted to a unique population throughout the brain and recombination can occur with transiently expressed Cre proteins during developmental stages, which can causes broader transgene expression in adults. Thus, the recent development of Cre dependent Adeno-Associated Viral (AAV) carrying a reversed and doubled-floxed transgene increases the usefulness of Cre driver mouse lines. AAV can control regional and temporal gene expression by local injection of the virus in the brain. It is hard to achieve cell specificity using AAV due to the short cell type-specific promoters that are compatible with the limited packaging capacity of the virus. Therefore intersectional genetic approach is taken with Cre transgenic mice and Cre dependent AAV. Different

Cre dependent AAV systems have been set up for loss of function/gain of function of specific proteins, gene profiling, silencing/activation, or retrograde/anterograde tracing in specific Cre populations.

1-7-2: Cre-dependent Anterograde/Retrograde Tracing Virus System

Connectivity can be another factor to reveal cell identity. Anterograde and retrograde neuronal tracers can reveal the locations of neurons projecting to or from a target area. The swine pathogen pseudorabies virus (PRV), as well as human pathogens herpes simplex virus type 1 (HSV-1) and rabies virus (RV) are the three transsynaptic viral strains used for defining circuitry of neurons in mouse CNS. Unlike most conventional chemical retrograde tracers such as Cholera Toxin B, the viral tracers reliably move from one neuron to another neuron via synapses and also they can amplify signals at each step by viral replications. They are genetically targetable, too. Especially the recent development of Cre-dependent cell type specific retrograde and anterograde viral or lectin tracing could be very useful in understanding the anatomical neural circuits of minor populations such as interneurons. Although most of these transsynaptic tracers can cross multiple synapses, Glycoprotein gene-deleted rabies virus pseudotyped with the avian sarcoma leucosis virus glycoprotein EnvA was designed to label only direct, monosynaptic inputs onto defined cell populations with the help of Cre dependent helper virus (Wall, Wickersham et al. 2010). Helper viruses express rabies glycoproteins and TVA, EnvA receptor, in a Cre dependent manner. TVA is needed for modified rabies virus to infect neurons and Glycoproteins are necessary for the spread of modified rabies through synapses (Wickersham, Lyon et al. 2007). Therefore modified rabies can only

infect Cre positive neurons expressing TVA and amplify themselves only in Cre positive neurons with G-proteins and their monosynaptic direct inputs.

Recently, another cell type specific monosynaptic retrograde tracing technique was developed utilizing endogenous receptor for the neuregulin (NRG), ErbB4 (Choi and Callaway 2011). ErbB4 is expressed in inhibitory neurons in the cortex, and NRG dependent rabies infections were focused on PV/SST non-expressing interneurons in the cortex (Choi, Young et al. 2010). By coupling EnvB pseudotyped rabies virus and lentivirus with the fusion proteins of the avian viral receptor TVB and NRG, the fusion proteins could infect rabies virus to ErbB4 expressing non-PV/SST interneurons and their direct monosynaptic inputs only. This method can be very useful to animals for which transgenesis is not applicable, especially if it can be generated to other classes of neurons.

Cre dependent transsynaptic anterograde tracers based on the H129 strain of herpes simples virus (HSV) were recently reported (Lo and Anderson 2011). They could successfully label Cre positive neurons and polysynaptic anterograde outputs of Cre neurons in the cerebellum, the olfaction system and the visual system. This tracer would be useful to examine the flow of information from peripheral neurons. However, it is not useful to follow connections of neurons with dense interactions in the local circuit like interneurons, because it crosses multiple synapses.

1-7-3: Cre-dependent Activation/Silencing System

Electrical stimulation, lesions, and inactivation of brain areas have allowed functional mapping of discrete regions and nuclei. However, classical lesion studies are invasive and lack cell specificity. Microstimulation also activates all different kinds of neurons including both excitatory neurons and inhibitory neurons as well as fibers of passage. Therefore much effort has been made for the development of activity manipulation methods for genetically targeted specific cell groups in vivo to understand how they contribute to particular behaviors and neural networks. Selective neuronal death has been carried out with Diphtheria Toxin A (Buch, Heppner et al. 2005), Herpes Simplex Virus 1, Thymidine Kinase and nucleoside analogs (Borrelli, Heyman et al. 1988). Techniques for manipulating neural activities include inward rectifying potassium channel (Kir) channel (Johns, Marx et al. 1999), *Drosophila* Allatostatin receptor (Tan, Yamaguchi et al. 2006), ivermectin-gated chloride channel (GluCl) from *Caenohabditis elegans* (Lerchner, Xiao et al. 2007), membrane tethered-toxin of Na^+ channel (Ibanez-Tallon, Wen et al. 2004), Capsaicin receptor (Arenkiel, Klein et al. 2008), Designer GPCRs (Armbruster, Li et al. 2007) and ion channels (Magnus, Lee et al. 2011), and optogenetics (Boyden, Zhang et al. 2005; Han and Boyden 2007; Zhang, Wang et al. 2007). Optogenetics in particular is heavily used and studied carefully due to the high temporal precision in the order of milliseconds. The light gated cation channel, Channelrhodopsin (ChR2), is distributed on the membrane surfaces including axons and dendrites, and can be targeted to axonal projections by injecting viruses at the location of neuronal cell bodies and delivering light to the target region harbouring ChR2 expressing axonal processes. Inhibition of transmitter release is another way to perturb their specific

functions. Inhibition of neurotransmitter techniques includes the tetanus toxin light chain (TeTxLc) (Nakashiba, Young et al. 2008), Molecular systems for inducible and reversible inactivation of synaptic transmission (MISTs) (Karpova, Tervo et al. 2005) and membrane-tethered voltage gated Ca2+ channel toxins (Auer, Sturzebecher et al. 2010).

1-8: Psychiatric Diseases and Cortical Interneurons

Interneurons are the key regulators in the cortex. Not only balancing the activity in the cortex, they can control the timing and the context of information in the cortex. They also play a vital role in synchronous and oscillation network activity. Dysfunction of the GABAergic system is thought to play a part in neurological and psychiatric diseases, such as epilepsy, schizophrenia, autism, and Rett's syndrome (Lisman, Coyle et al. 2008; Chao, Chen et al. 2010; Marin 2012). Mouse genetics are becoming more important in psychiatric disease studies with the generation of many different mouse disease models. It is known that in schizophrenia, certain classes of interneurons (mainly subtypes of PV neurons) are affected. Therefore defining cell types in mice, and creating cell type specific mouse lines will greatly improve our understanding the pathophysiological mechanisms underlying psychiatric diseases. Also identification the molecular fingerprint of a particular cell type will help us to study other mammals such monkeys or human. We can apply these molecular signatures to determine whether abnormalities occur in the mouse cortex also occur in human patients.

Chapter 2

Creation of BacTRAP Mouse Lines for Known Markers and Gene Profiling of Targeted Neurons

A major obstacle for the study of cortical interneurons is the lack of specific markers and good mouse lines for interneuron subtypes. It is unlikely that every cell type has a single gene to specify the population, but no systematic screening for interneuron subtype markers has been done. Considering that gene expression is highly correlated with subtype characteristic morphology and physiological properties, there could be a gene that represents more specific populations. The ABA in situ hybridization (ISH) atlas has been used to find markers in different brain areas or pyramidal cells in the cortex. ISH provides the location of neurons expressing a gene of interest by labeling their cell bodies. Interneurons are scattered throughout all cortical layers. There are some correlations between layers and interneuron subtypes; however it is impossible to distinguish the cell type from the location of cells. Therefore screening markers with ABA atlas is not the answer for interneurons. Instead, we have taken the BAC transgenesis and TRAP approach to find potential candidate markers for interneuron subtypes. BAC transgenic mice generated for TRAP will be referred to as bacTRAP lines. BacTRAP can provide us the expressing gene list of targeted neurons in adults. Tissue specificity can be achieved by dissecting one part of the brain when we collect RNAs, even if the same genes are expressing in different areas. We targeted subpopulations of interneurons using BACs

containing known interneuron marker genes. These subpopulations of interneurons are known to be heterogeneous and overlap one other. Therefore comparative analysis of gene lists for these targeted interneurons may suggest candidate marker genes expressing themselves in subpopulations of interneurons.

2-1: Generation of bacTRAP Mouse Lines

We generated bacTRAP mouse lines for known marker genes or genes chosen from the expression of GENSAT EGFP mice (Figure2.1). BACs can be used to express proteins of interest under the transcriptional control of a selected gene. The EGFP tagged ribosomal protein L10a gene was inserted about 500bp upstream from the translational start codon of a gene on BAC by the homologous recombination, in order to visualize the targeted neurons with EGFP and also to extract cell type specific transcripts for detailed analysis of the molecular profile of the cell type. Purified BAC cDNA was pro-nuclear injected to generate transgenic mice. Positive mice that have EGFP integrated into the genome (Founders) were identified with PCR. The size of BAC is about 200kb, and usually is long enough to cover all regulatory regions which are needed to express similar endogenous genes. However, they don't always fully recapitulate the expression patterns of endogenous genes, and mouse lines from different mouse founders may have a different expression pattern. Possible explanations are: the position effect from the genomic site of integration, low BAC copy number combined with transcription inefficiency of the promoter, high BAC copy number leading to ectopic expression, and the regulatory sequences from the gene not included in the corresponding BAC. But at

the same time, this ectopic or partial expression of the transgene can be useful to target specific populations without identifying a new marker (Ma, Hu et al. 2006)

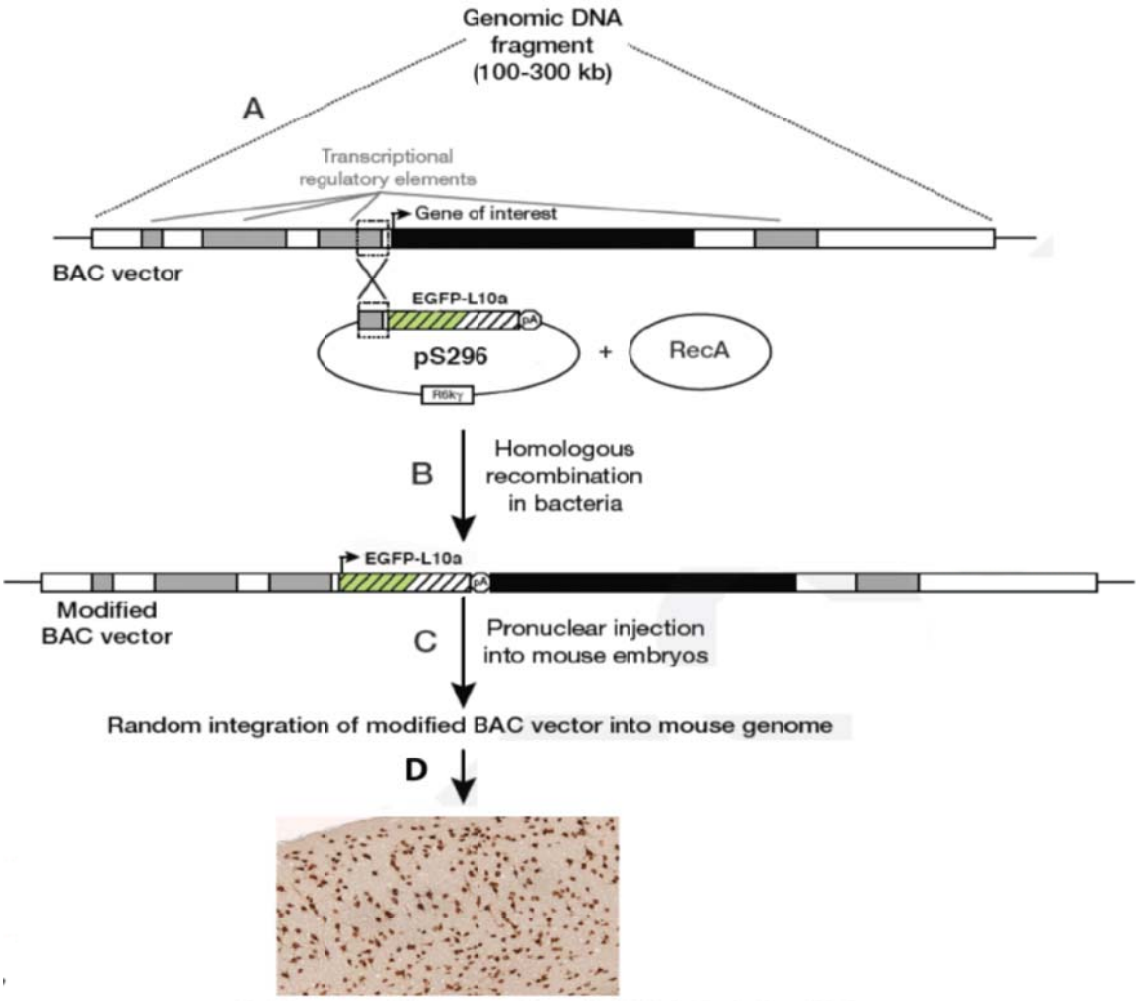

Figure 2.1 Generation of BacTRAP Line

(A) Bacterial Artificial Chromosome (BAC), including the gene of interest and surrounding genomic sequence which could produce transcriptional regulator, is modified using a homology region shared with the TRAP shuttle vector pS296. (B) RecA plasmid transformation renders the BAC carrying E.coli competent for recombination. (C) The modified BAC vector with the EGFP-L10a recombines immediately after the promoter is injected into the pronucleus of mouse oocytes. The modified BAC randomly integrates into the mouse genomes in variable tandem copies. (D) Progeny of the injected mice are screened for germline transmission of EGFP and such BAC founder lines are characterized for EGFP neuroanatomy.

Therefore once the BAC transgenic founder mice were made, we analyzed their expression using immunohistochemistry (IHC) of markers to evaluate how well the expression of reporter genes matches with the expected endogenous gene expression or targets specific populations of interneurons. Among the lines we made, mouse lines for distal-less homeobox 1 (Dlx1), PV, NPY, CCK, VIP, Cortstatin (Cort), Serotonin receptor 3a (Htr3a), LY6/PLAUR domain containing 6 (Lypd6), NIMA-related kinase 7 (Nek7), Dopamine receptor D1 (Drd1a) and Prepronociceptin (Pnoc) all had expression in interneurons. Among these, we selected 4 lines for further analysis, Dlx1 GM520, Cort GM130, Htr3a GM443, and Nek7 MN733, based on the specificity and their expression patterns.

2-2: Characterization of Selected 4 Mouse Lines

Dlx1 is a homeobox transcription factor which is required for the differentiation of GABAergic interneurons. Dlx1 is involved in maturation and survival of some interneuron subtypes (SST, NPY, nNOS etc.). Cort encodes a neuropeptide which has a similar structure to SST but has some role distinct from SST such as induction of slow-wave sleep. Htr3a is an ionotropic serotonin receptor and depolarizes neurons upon serotonin administration. Nek7 is serine/threonine-protein kinase that is required for proper spindle formation during cell division. The function of Nek7 in adult neurons is not known, but it is strongly expressed in GABAergic interneurons in the cortex. The design of each construct can be found in the Methods section. Dlx1 GM520 and Nek7 MN733 have expression across all layers in the cortex, whereas the expression of Cort is concentrated in lower layers and Htr3a expression is shifted to upper layers (Figure 2.2).

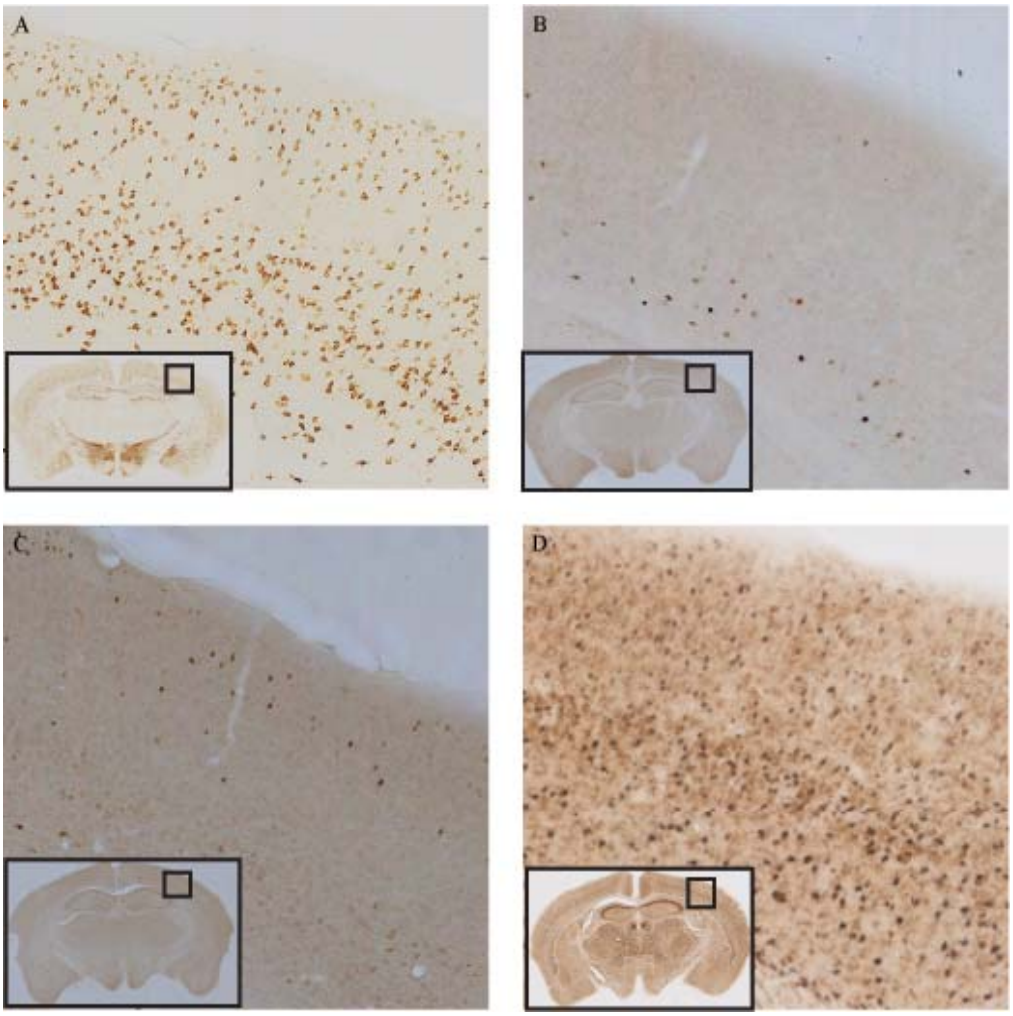

Figure 2.2: Expression Patterns of Four Interneuronal Mouse Lines in the Cortex

DAB immunohistochemistry with anti-EGFP antibody on coronal brain sections of each mouse line reveals a unique and specific pattern of expression of the EGFP-L10a transgene in the somatosensory cortex. Panels show the morphology and localization of cells expressing the transgene, while inset shows the locations of panel. EGFP expressions were localized in the cell bodies in neurons due to the L10a ribosome subunit protein attached to EGFP.
A) Dlx1 GM520, B) Cort GM130, C)Htr3a GM443, D) Nek7 MN733. A) Dlx1 GM520 shows scattered EGFP positive neurons in all layers. B) Cort GM130 has layer 6 localized EGFP expression. C) Htr3a GM433 has layer 1-3 scattered expression. D) Nek7 MN733 has EGFP transgene expression in the whole cortex, but has background in the cortex.

Nek7 has a high background, and high magnification image showed EGFP expression in glia. To elucidate the EGFP population double IHC was performed using anti EGFP antibody, and antibodies against known marker proteins in each transgenic line (PV, SST, CR, NPY, nNOS, VIP) in the somatosensory cortex of adult tissue (8-12weeks). Dlx1 GM520 labeled almost all CGE derived interneurons (92.5% of CR, 92.9% of VIP) and Sst (91.6%) however only 18.8% of PV were EGFP positive (Figure 2.3). On the other hand, Nek7 MN733 had expression in almost all PV cells (98.8%) and some SST cells (30%), but no CGE derived neurons were labeled (Figure 2.4). This suggests that almost all interneurons in the cortex can be covered by combining Dlx1 and Nek7 positive population. Cort GM130 is similar to Nek7 line, although only part of MGE derived PV (33.4%) and SST (35.4%) neurons are labeled; there are no CGE derived interneurons (Figure 2.5). Htr3a GM443 had EGFP expressions in almost all CGE derived neurons, but no MGE derived neurons (Figure 2.6). The expression pattern of these lines matched well with the previously reported expression of each gene (de Lecea, del Rio et al. 1997; Ferezou, Cauli et al. 2002; Cobos, Calcagnotto et al. 2005; Lee, Hjerling-Leffler et al. 2010). Htr3a bacTRAP line had slightly fewer VIP and CR labeled neurons compared to Htr3a-GFP BAC transgenic mice, even though we used the same BAC. However, the proportion of each group was the same. A summary of IHC results is in Table2.1.

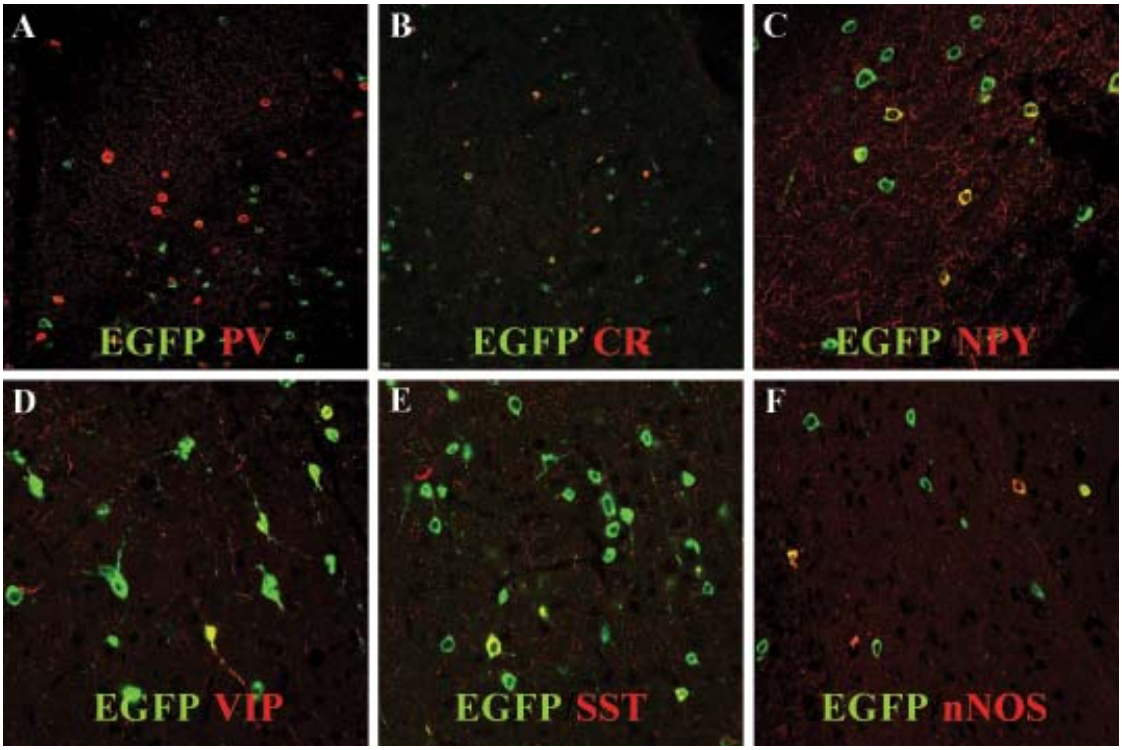

Figure 2-3: Colocalization of Transgenes and Interneuron Markers in Dlx1 GM520 Line

Fluorescent double immunostaining with anti-EGFP antibody (Green) and antibodies of interneuron markers (Red) in the somoatosensory cortex of Dlx GM520. (A) Parvalbumin (PV), (B) Calretinin (CR), (C) Neuropeptide Y (NPY), (D) Vasoactive intestinal peptide (VIP), (E) Somatostatin (SST), (F) Nitric oxide synthase (nNOS). Almost all red neurons in VIP, SST, NPY, nNOS and CR IHC are labeled with Green (EGFP), but most of PV red neurons are not labeled with Green. This suggests that EGFP neurons in Dlx1 GM520 label almost all interneurons except PV positive neurons.

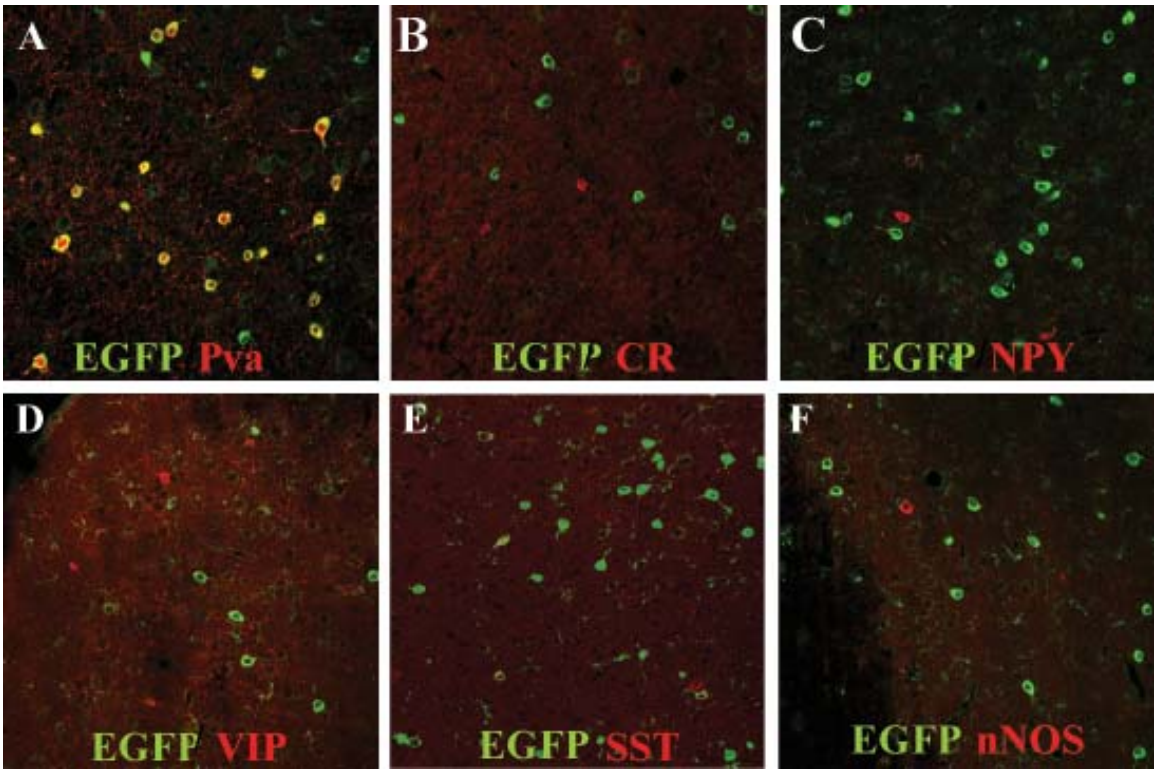

Figure 2-4: Colocalization of Transgenes and Interneuron Markers in Nek7 MN733 Line

Fluorescent double immunostaining with anti-EGFP antibody (Green) and antibodies of interneuron markers (Red) in the somoatosensory cortex of Nek7 MN733 BacTRAP line. (A) Parvalbumin (PV), (B) Calretinin (CR), (C) Neuropeptide Y (NPY), (D) Vasoactive intestinal peptide (VIP), (E) Somatostatin (SST), (F) Nitric oxide synthase (nNOS). EGFP positive neurons overlap with most of the PV neurons and some of the SST neurons but don't overlap with the CR, VIP and nNOS neurons. Almost all EGFP positive neurons are either PV or SST positive and no CGE derived neurons are labeled. Compared to Cort GM130, many more PV neurons are targeted in Nek7 line.

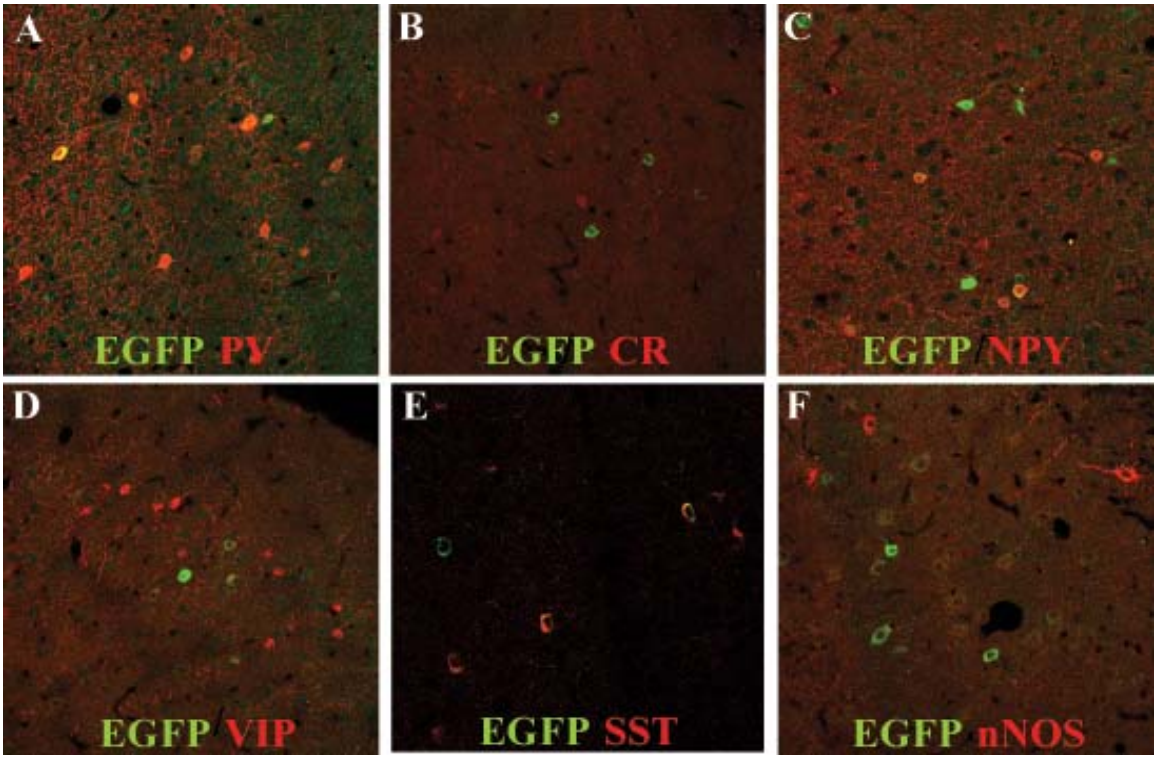

Figure 2-5: Colocalization of transgenes and interneuron markers in Cort GM130 Line

Fluorescent double immunostaining with anti-EGFP antibody (Green) and antibodies of interneuron markers (Red) in the somoatosensory cortex of Cort GM130 BacTRAP line. (A) Parvalbumin (PV), (B) Calretinin (CR), (C) Neuropeptide Y (NPY), (D) Vasoactive intestinal peptide (VIP), (E) Somatostatin (SST), (F) Nitric oxide synthase (nNOS). EGFP positive neurons overlap with some of the PV, NPY, and SST positive neurons but don't overlap with CR, VIP and nNOS labeling. Almost all EGFP positive neurons are either PV or SST positive while no CGE derived neurons are labeled.

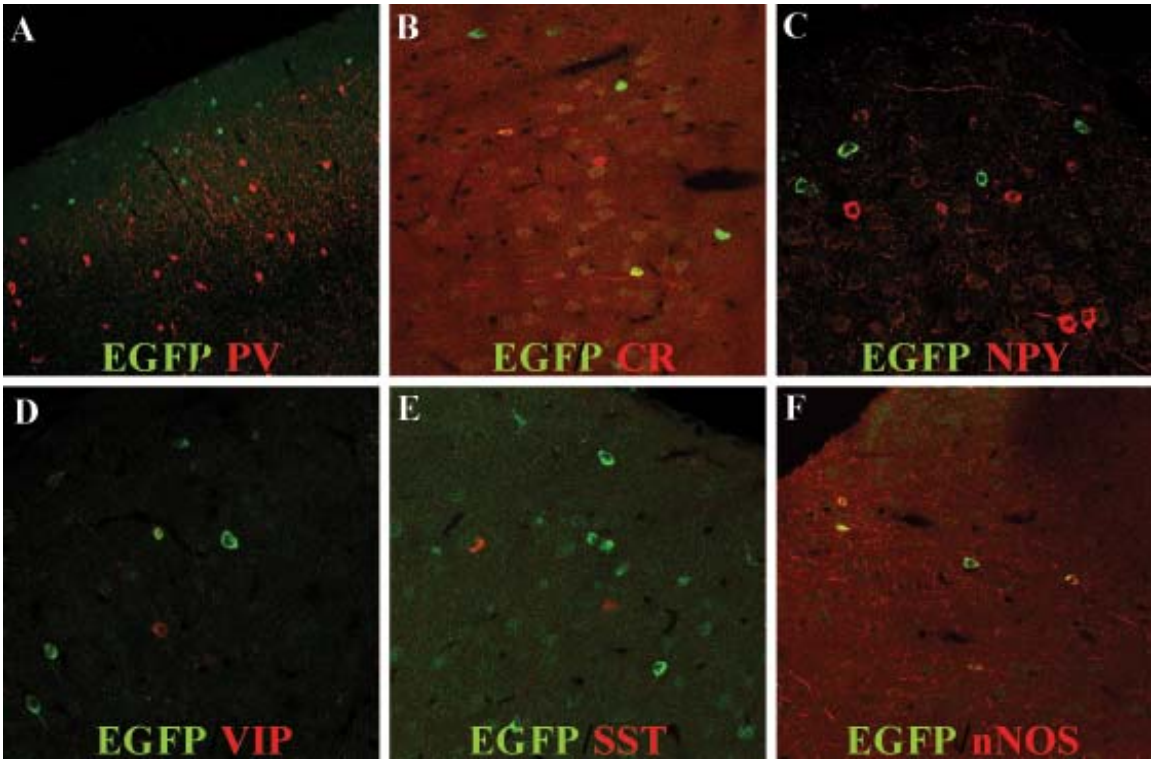

Figure 2-6: Colocalization of transgenes and interneuron markers in Htr3a GM443 Line

Fluorescent double immunostaining with anti-EGFP antibody (Green) and antibodies of interneuron markers (Red) in the somoatosensory cortex of Htr3a GM443 BacTRAP line. (A) Parvalbumin (PV), (B) Calretinin (CR), (C) Neuropeptide Y (NPY), (D) Vasoactive intestinal peptide (VIP), (E) Somatostatin (SST), (F) Nitric oxide synthase (nNOS). EGFP positive neurons overlap with many CR, VIP and nNOS neurons but don't overlap with PV and SST. Its pattern is opposite to Cort GM130 and no MGE derived interneurons are labeled in this line.

A

	PV	CR	NPY	VIP	SST	nNOS
Dlx1 GM520 (100%)	10.8% (17/157)	17.3% (40/235)	19.8% (27/141)	12.9% (13/104)	19.6% (24/123)	28.7% (25/117)
Cort GM130 (100%)	47.3% (38/86)	3.0% (2/81)	6.1% (3/53)	2.8% (1/47)	49.0% (18/38)	0% (0/86)
Htr3a GM443 (100%)	0.9% (3/232)	38.1% (61/165)	8.9% (15/193)	52.6% (114/198)	0% (0/55)	0% (0/65)
Nek7 MN733 (100%)	83.5% (279/341)	1.4% (3/143)	5.7% (7/324)	0% (0/98)	9.5% (50/526)	0% (0/383)

B

	PV (100%)	CR (100%)	NPY (100%)	VIP (100%)	SST (100%)	nNOS (100%)
Dlx1 GM520	18.8% (17/92)	92.9% (40/44)	100% (27/27)	92.9% (40/44)	91.6% (24/27)	98.2% (25/26)
Cort GM130	33.4% (38/131)	2.1% (2/83)	8.8% (3/42)	0.6% (1/80)	35.4% (9/21)	0% (0/37)
Htr3a GM443	0.9% (3/305)	39.8% (61/149)	13.8% (15/118)	77.4% (114/138)	0% (0/35)	0% (0/25)
Nek7 MN733	97.6% (279/285)	4.1% (3/70)	19.8 % (7/66)	0% (0/35)	30.9% (50/162)	0% (0/39)

Table 2.1 Summary of IHC

Proportion of each marker group in each line. All IHC was done on the somatosensory cortex of 4 mice for each line (A) showed the the percentage of EGFP/Marker positive neuron in marker positive populaton. (B) is the percentage of EGFP/Marker positive neurons in EGFP positive population

2-3: TRAP Methodology

The TRAP methodology was developed to collect translated mRNAs readily and reproducibly only from the EGFP tagged neurons (Figure 2.7) (Doyle, Dougherty et al. 2008; Heiman, Schaefer et al. 2008).

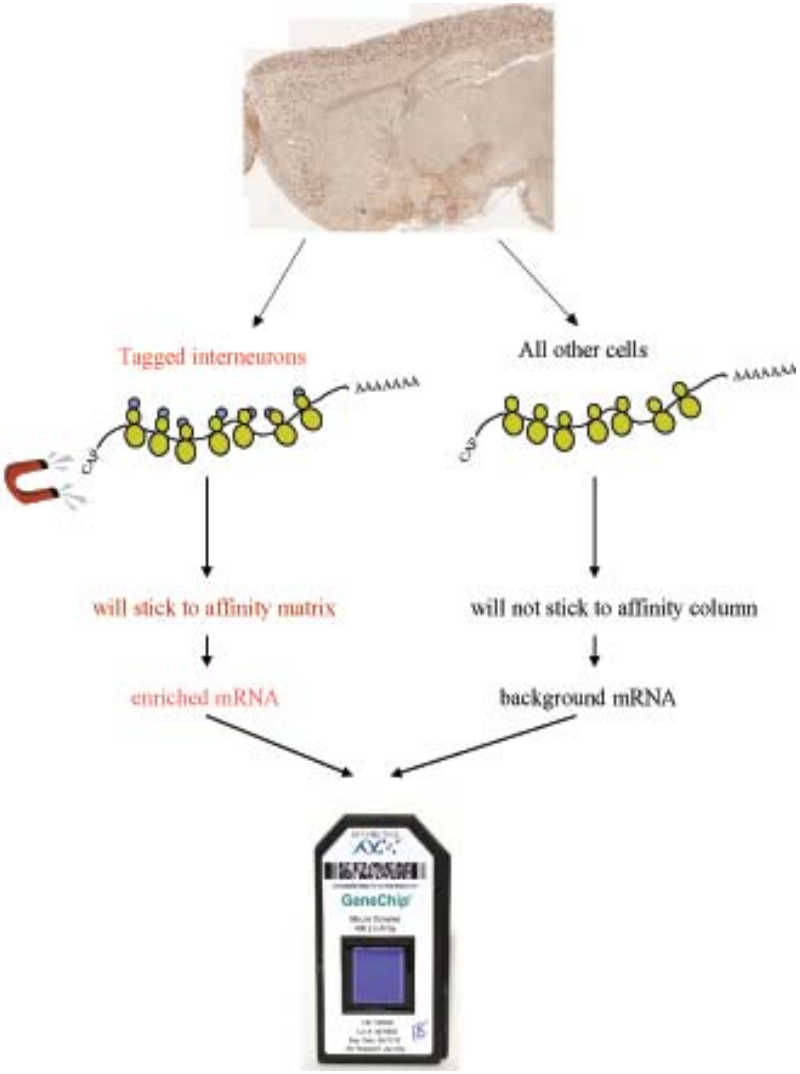

Figure 2.7: Scheme of BacTRAP Method

Cortical tissue of adult mice was dissected and subjected to polysomal immunoprecipitation using anti-EGFP antibody coated by magnetic beads to pull down tagged polysomes. Cell type specific polysomes (tagged) were affinity purified and subjected to RNA extraction. The extracted RNA was amplified and labeled before being hybridized on to the Mouse Genome 430 2.0 microarray chips, whereupon label signals were quantified and analyzed to generate cell-type specific translational profile.

This methodology requires EGFP-L10a expression in a specific population and this can be achieved by BAC transgenesis as showed previously. This EGFP tagged ribosome subunit can be incorporated into functional polysome in vivo and can be used to translate mRNAs into proteins. Therefore, mRNA is attached to the tagged polysome during translation process. Rapid extraction and immunoaffinity purification of the EGFP-tagged polyribosome complexes from intact brain tissue was optimized to give the least damage to the mRNA and to prevent transcriptional changes during this purification step. We dissected out the cortex in chilled buffer containing glucose, nuclease inhibitors and cycloheximide and homogenized in lysis buffer including magnesium, nuclease inhibitors and cycloheximide to maintain ribosome subunits on mRNA during purification. Then we solubilized rough endoplasmic reticulum-bonded polysomes under nondenaturing conditions with RNase inhibitors. Polysomes were affinity purified using monoclonal EGFP antibodies conjugated to Protein L followed by high salt washes to reduce background. The mRNAs bound to the polysomes were extracted and subjected to the genomic analysis.

Purified mRNA can be analyzed in three different ways: (1) RT-PCR, (2) Microarray, (3) RNA-seq. The RT-PCR method is useful to validate the enrichment of individual genes, but not for genome wide expression analysis. On the other hand, microarray and RNA-seq allows simultaneous enrichment analysis for thousands of genes. But both methods have their benefits and limitations. The microarrays used to be the most widely used methodology for transcriptome analysis and allow coincident detection of enrichment for 40,000 oligonucleotide cDNA probes. Microarrays are relatively inexpensive and

analysis methods are well established, however they face limitations such as incomplete coverage of all possible genes in the genome, inability to detect low abundance genes (less than 5 copies) and splice variants and high background levels owing to cross-hybridization. RNA-seq technology uses recently developed deep-sequencing technology. Short tagged cDNA converted from a pool of RNA is sequenced and mapped on the source genome to produce a genome-scale transcription map that consists of both the transcriptional and level of expression of each gene. RNA-seq gives a substantially higher coverage of the genome and more quantitive compared to the hybridization based approach (Wang, Gerstein et al. 2009). However, it's still a very expensive method, and the tools for analyzing the extensive sequence data are just being developed. In the current study, we have used microarrays to analyze transcriptional profiles of cortical interneurons, although we are shifting to RNA-seq. For microarrays, purified RNAs are amplified through two rounds of in vitro transcription and biotin-labeled anti-sense RNA was used to interrogate Affymetrix GeneChip Mouse Genome 430 2.0 arrays.

2-4: Gene Profiling of Selected 4 Lines

For each targeted population, data were collected from three independent biological replicates, each prepared from a cohort of 4 animals. Average RNA yields are Dlx1; 17.14ng/ul, Cort; Htr3a; 6.82ng/ul, and Nek7; 110.2ng/ul. The very high RNA yield from Nek7 line can be explained by glial contamination. Transcriptional replicates from each line gave nearly identical genome-wide translational profiles. (The average of Pearson's correlation between independent replicates is Dlx1: 0.991 Cort: 0.991 Nek7: 0.984 Htr3a: 0.986) We noticed that some probesets were consistently enriched in every data set

analyzed including the one from control mice with no transgene expression. Therefore we systematically eliminate these probesets from future analysis (Doyle, Dougherty et al. 2008).

To provide a measure of the enrichment, immunoprecipitated RNA was compared with RNAs (purified RNAs from the samples before immunoprecipitations) from the whole cortex (UB). GC-RMA normalized expression values from Affymetrix Mouse Genome 430 2.0 arrays for each line IP were plotted against the value of UB (Figure 2.8). To make initial judgments regarding the quality of a particular TRAP dataset, both known interneuronal markers enriched in IP more than 2 fold (blue dots) and known glial genes (red dots) as negative controls were plotted. Figure 2.9 showed IP/UB fold changes (log 2 base) of interneuron marker genes, driver genes, and glial genes in each data set.

Figure 2.8: Translational Profiles of Four Interneuron Cell Groups

Normalized expression values from Affymetrix Mouse Genome 430 2.0 array are plotted for A) Dlx1 GM520, B) Cort GM130, C) Htr3a GM443, D) Nek7 MN733 IP. The log signal intensity for the IP RNA is on the X-axis and the whole tissue RNA (UB) on the Y-axis. Middle diagonal line represents equal expression and the lines to each side represent 2.0-fold enrichments in either IP or UB. Blue circles indicate known interneuronal markers which were enriched in IP; side and red circles indicate probesets for known glial genes (negative controls). (A) As we expected, Dlx1 IP shows enrichments for most of the known interneuron markers including Dlx1, Nek7, Htr3a, and Cort. On the other hand, glial genes are on UB side. Dlx1 IP has the best signal/noise ratio among 4 lines. (B) Cort IP has high level of Cort, PV and SST genes. (C) Htr3a IP shows enrichments of VIP and Htr3a probesets. Glial genes are lined in the middle for both Cort IP and Htr3a IP even though positive controls are enriched in IP side. This is a typical IPvsUB plot with low RNA yield. (D) Nek7 IP also shows enrichments of Nek7 and PV. Nek7 also has glial genes aligned in the middle and IP side, but this is because EGFP-L10a is expressed also in glia of Nek7 Trap line. We have some glial gene contaminations in Cort, Htr3a and Nek7 IP. All positive controls are enriched in IP.

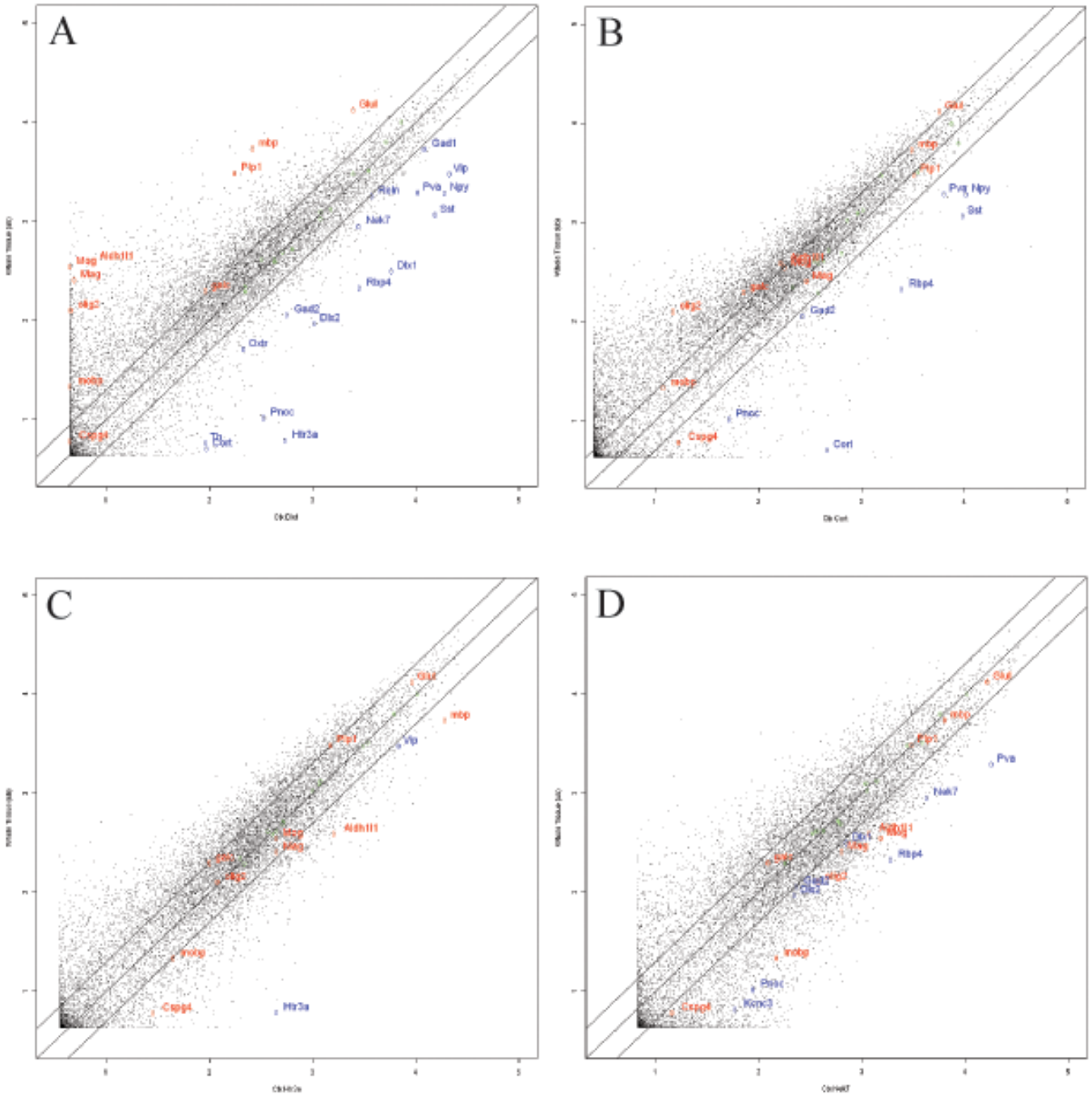
A
Glul
mbp
Gad1
Plp1
Vip
Rtn1n
Pvalb
Npy
Sst
Nnat
Mag
Aldh1l1
Dlx1
Rtbp4
Gad2
Dlx2
Cldn
Inabp
Pnoc
Cspg4
Th
Cort
Htr3a
B
Glul
mbp
Plp1
Pvalb
Npy
Sst
Rtbp4
Gad2
Inabp
Pnoc
Cspg4
Cort
C
Glul
mbp
Plp1
Vip
Aldh1l1
Inabp
Cspg4
Htr3a
D
Glul
mbp
Plp1
Pvalb
Nnat
Rtbp4
Inabp
Pnoc
Cspg4

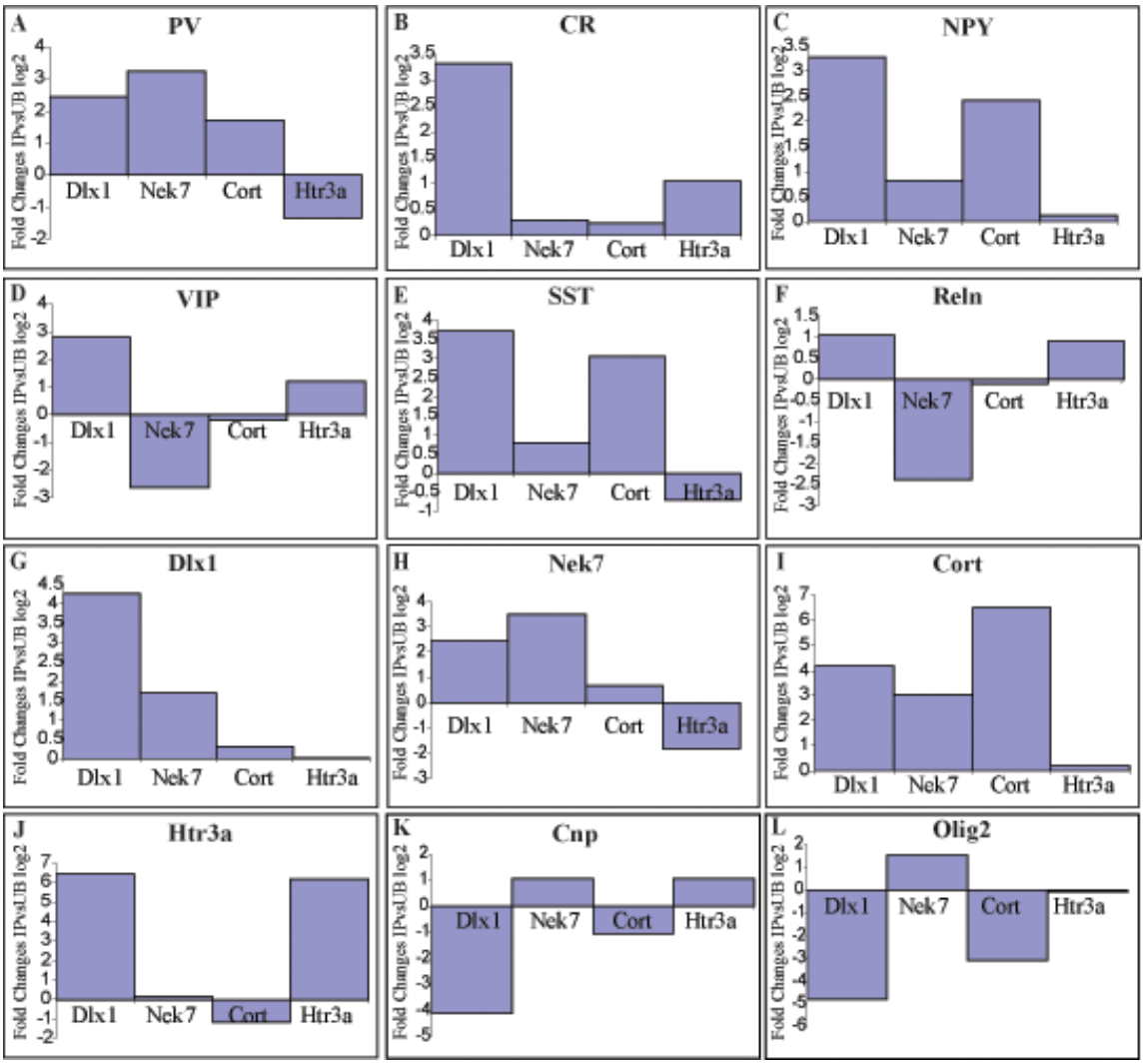

Figure 2.9: Expression Patterns of Interneuronal Markers

Log2 based fold changes of IP/UB for selected genes in each line. (A-F) known interneuron markers, (G-J) driver genes and (K-L) glial genes. The name of the transgenic mouse line for the list is on the x-axis and log2 based fold change is on the y-axis. The PV and SST probes are enriched in the Dlx1, Nek7 and Cort IP but not in the Htr3a IP. On the other hand, VIP and CR genes are expressed in only in the Dlx1 and the Htr3a IP. This matched with IHC results and proved that our BacTRAP methods successfully collected mRNA from targeted cells. Nek7 and Cort are enriched in both lines and Dlx1 gene was enriched in Htr3a IP and vice versa. This means Dlx1 and Htr3a EGFP populations overlapped and Nek7 and Cort EGFP share the same population. Glial genes are expressed in Nek7 IP and Htr3a IP.

Microarray results matched with previous IHC results and driver genes were enriched in the IP side of each list, which indicates that our TRAP method successfully collected RNAs from targeted cells. According to IHC results, almost the same number of SST cells was labeled in two lines, Nek7 and Htr3a. However only 15% of EGFP neurons in Nek7 EGFP-L10a neurons belonged to the SST positive population, while 49% of EGFP labeled interneurons were SST positive in Cort GM130. Therefore, the SST gene is more representative in Cort GM130. Due to the small number of EGFP neurons in the cortex of Cort and Htr3a line, the yield of RNAs for both lines was low. We observed a larger proportion of non-specific background RNA that came from unlabeled cell types of the tissue in low yield IPs (Dougherty, Schmidt et al. 2010). Therefore, probesets of glial genes (red dots in Figure 2.8) in Cort and Htr3a were shifted to the IP side, even though they showed remarkable enrichment of the positive control (Cort or Htr3a). Nek7 had a similar background, even though the RNA yield was high. We observed EGFP expressions in glia in Nek7 tissue, which could explain the background of glial genes in Nek7 gene list. This biological background could be avoided by making better lines or using better driver genes. However no other BACs we tried could target all the PV neurons in the cortex including the BAC containing endogenous PV gene, even though we could target subcortical PV populations well with this BAC. Also gene lists from Glial lines (Cnp, Olig2, Fthfd) showed enrichments of Nek7 in the IP side (data not shown), suggesting that transgene expressions in glia were not ectopic. Therefore it is hard to remove glia contaminations using the Nek7 construct.

Microarray results showed that Nek7 trap population and Cort trap population overlap each other but not with Htr3a trap. Dlx1 trap group overlapped with the other three lines, even though the Dlx1 gene was not so enriched compared to UB in Cort and Htr3a IP list. This is because genes expressing in many cells in the area were under-representative in IP/UB measurements. There were more Dlx1 positive interneurons in UB than Htr3a and Cort IP, even though UB included all other different types of cells. Expression values for Dlx1 probeset in Cort and Htr3a IP were about 10 times higher than the one from glial lines, which means Cort and Htr3a included Dlx1 positive population. On the other hand, fold changes of IP/UB for genes expressed only in rare cell types in the cortex were very high in IP of small number of cells. (such as Cort gene in Cort line, and Htr3a gene in Htr3a line). The genes we are looking for should label minor populations in the cortex. Therefore this bacTRAP approach is suitable for the search of marker genes for interneuron subtypes.

The summary image of the relationship of each group is in Figure 2.10. This doesn't contradict the previous IHC characterization results. Htr3a BAC transgenic mice only labeled CGE derived interneurons and Dlx1 BacTRAP lines labeled all CGE interneurons. Therefore targeted Dlx1 population can be subdivided by 2 with targeted Htr3a group. [Dlx1+, Htr3a-] population can further be subdivided into 3 or 4 different populations depending on how well Cort cell groups and Nek7 cell groups overlap. The rest of the [Dlx-, Nek7+] will be divided in 2 with Cort population.

In summary, 6 or 7 populations , (1) [Dlx1+, Htr3a+, Nek7-, Cort-], (2) [Dlx1+, Htr3a-, Nek7-, Cort-], (3) [Dlx1+, Htr3a-, Nek7+, Cort-], (4) [Dlx1+, Htr3a-, Nek7+, Cort+], (5) [Dlx1-, Htr3a-, Nek7+, Cort-], (6) [Dlx1-, Htr3a-, Nek7+, Cort+], ((7) [Dlx1+, Htr3a-, Nek7-, Cort+]) could exist and a comparative analysis of gene profiling of each line might be able to suggest potential marker genes for each subpopulation.

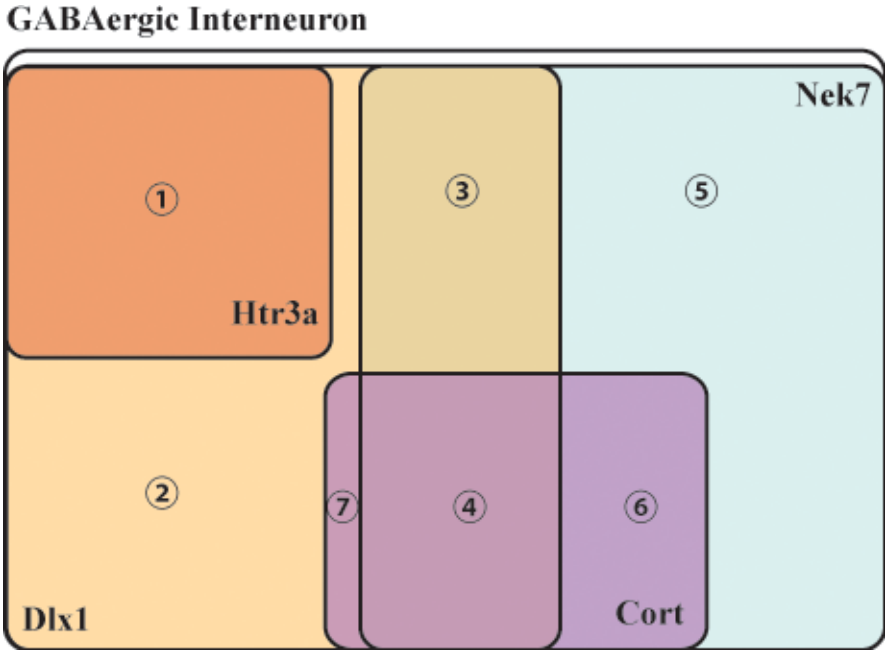

Figure 2.10: Summary of Four Interneuron Populations

GABAergic interneurons can be subdived by 6 or 7 subgroups by 4 inteneuronal lines. GABAergic Interneruons can be covered by two big populations of Nek7 and Dlx1. Each population can be subdiveded by Htr3a or Cort respectively.

(1) [Dlx1+, Htr3a+, Nek7-, Cort-] (2) [Dlx1+, Htr3a-, Nek7-, Cort-] (3) [Dlx1+, Htr3a-, Nek7+, Cort-] (4) [Dlx1+, Htr3a-, Nek7+, Cort+], (5) [Dlx1-, Htr3a-, Nek7+, Cort-], (6) [Dlx1-, Htr3a-, Nek7+, Cort+], (7) [Dlx1+, Htr3a-, Nek7-, Cort+]

2-5: Discussion

We successfully generated 4 distinct bacTRAP interneuronal lines which labeled different but overlapping population of interneurons. Gene profiling of the 4 lines was successful, even though there were some background issues for further analysis. We covered almost all interneurons in the cortex with Dlx1 and Nek7 trap population. Htr3a and Cort cell groups could subdivide each population and potentially we could get 6 or 7 different subpopulations of interneurons represented by differential expression pattern in 4 lines. It is possible that each subdivision wouldn't represent a more specific population. However, Dlx1, Htr3a and Cort are known to be involved in the function of cortical interneurons and it is likely that the existence of these genes' expressions is important for the identity of interneurons.

Chapter 3

Screening and Qualification of Candidate Marker Genes

Microarray technology is a hybridization based gene profiling method and doesn't directly measure the real number of transcripts. Comparing expression levels across different experiments requires good normalization and comparative analysis methods. We collected BacTRAP results from 4 lines to screen markers for more specific interneuron subtypes. Screening requires a number of steps. First, all non-enriched and glial background genes should be eliminated from the list. Second, we have to find genes that show differential enrichments in microarray results of 4 lines. Third, we have to check their expression patterns in adults by checking ABA ISH data. ISH results could tell us whether candidate marker genes have interneuron-like expression patterns (scattered in the cortex) and high expression level (high enough to be detectable by ISH) in adults. Finally, we checked their gene sizes. If the gene size is longer than one BAC, it is unlikely BAC transgenesis would work.

Another way to qualify markers is the "tiling" method. Tiling of axonal terminals and dendritic arbors and spacing of cell bodies in a cell type has been observed in many invertebrates and vertebrates (Wassle, Peichl et al. 1981; Gan and Macagno 1995; Sagasti, Guido et al. 2005; Fuerst, Koizumi et al. 2008). Tiling is critical to avoid functional

redundancy and to achieve complete coverage of the area for the same cell type of neurons. On the other hand, dendrites of different neuronal types can cover the same region to allow the sampling of different types of information from the same input. Although further studies will be required to understand the mechanism and the meaning of tiling and although not all cell types showed tiling features, clear identification of cell types could reveal more cell types with tiling. At the same time, if a group of neurons showed dendritic tiling or regular spacing of cell bodies, it is possible that this group would represent a functionally identical cell type.

3-1: Screening of Candidates

The whole procedure is summarized in Figure 3.1.

A. Specificity Index analysis with IP results of glial lines to filter out glial genes

Symbol	Ctx.olig2	Ctx.fthfd	Ctx.cnp	Nek7 ranking	P-value
Kcnj8	NA	NA	NA	109	0.00036
Akr1c18	NA	NA	NA	109.5	0.00036
Ctsh	NA	NA	NA	110	0.00036
Ncf4	NA	NA	NA	113.25	0.00039
Aif1	NA	NA	NA	118	0.00043
AF251705	NA	NA	NA	121	0.00048
Cbr2	NA	NA	NA	122.75	0.0005
Foxc2	NA	NA	NA	126.75	0.00053
P2ry13	NA	NA	NA	129.75	0.00056
Mafb	NA	NA	NA	131.25	0.00058

B. Get GCRMA normalized expression values of filtered genes for each line

	Ctx.cort	Ctx.Htr3a	Ctx.Dlx1	Ctx.Nek7
Sox18	3.0806	50.4577	5.3262	378.5374
Gpr34	3.1083	5.6882	5.3262	359.3451
Tmem119	4.4515	39.2453	5.3262	522.4352
Selplg	128.1090	217.1927	5.3262	1543.3866
Cox6a2	643.0868	115.3084	1046.2486	1964.2277
Anxa3	24.5150	184.0826	5.3262	773.0593
Fcgr3	28.9247	50.0978	5.3533	1151.7445

C. Divide each value with maxium expression value of each gene

	Ctx.cort	Ctx.Htr3a	Ctx.Dlx1	Ctx.Nek7
Sox18	0.0081	0.1333	0.0141	1
Gpr34	0.0086	0.0158	0.0148	1
Tmem119	0.0085	0.0751	0.0102	1
Selplg	0.0830	0.1407	0.0035	1
Cox6a2	0.3274	0.0587	0.5327	1
Anxa3	0.0317	0.2381	0.0069	1
Fcgr3	0.0251	0.0435	0.0046	1

D. Pick a template gene

	Ctx.cort	Ctx.Htr3a	Ctx.Dlx1	Ctx.Nek7
template gene A	0	0	1	1
template gene B	1	0	0	1
template gene C	0	0	1	0

E. Identify genes which have a similar expression pattern with the template gene using Genefilter (Bioconductor)

	Ctx.cort	Ctx.Htr3a	Ctx.Dlx1	Ctx.Nek7
Cdca7	0.046175793	0.06733791	0.77461594	1
Mypn	0.051581461	0.04725543	0.730138914	1
Gltpd1	0.101848481	0.13679355	0.902219339	1
Kcnc3	0.05529339	0.076775001	0.685687615	1
Tm6sf1	0.194251076	0.148546268	0.9291519	1
Cenpa	0.257528146	0.049338122	0.991749714	1

F. Examine expression patterns of each gene by ABA ISH database

Figure 3.1: Scheme of Microarray Analysis to Pick Candidate Marker Genes

(A) Specificity Index analysis with three glial lines was performed to filter out glial genes and we picked high ranked genes (p-value <.05) for each line (B) For selected genes, we got normalized expression values of four interneuroal lines and (C) divided them with maximum expression value for each gene. (D) Picking a template gene depending on which subpopulation we wanted to examine. (E) Ran Genefinder to find genes which have a similar expression pattern with the template gene. (F) Checked expression patterns of chosen genes by ABA database and selected genes with scattered expression in cortex.

3-1-1: Filtering out Background

We started either from the Dlx1 trap or the Nek7 trap, because all subdivisions were included in either one. To delete non-enriched and glial genes, we employed the Specific Index (SI) approach (Dougherty, Schmidt et al. 2010). SI could delete more glial gene background compared to other methods such as weighted gene co-expression network analysis (WGCNA) (Langfelder, 2008). The SI is an R-based generic algorithm for assessing the specificity of a given RNA in one sample relative to all other samples analyzed (Figure 3.2). First, GCRMA normalization was performed within replicates to remove non-biological variability. Global normalization to the biotinylated spike in controls provided by Affymetrix across all cell populations was carried out to make the expression value more comparable across all samples. Then genes which were enriched in the UB side (IP/UB < 1) or had low expression value (normalized expression value < 50) were deleted from the list. This filtered IP was compared to every other unfiltered sample (other IPs) in the dataset and the ratio was calculated for each probeset. Then the probesets were ranked from highest to lowest ratio within each comparison. For each probeset, its ranks across all comparisons were averaged to give the SI. Thus the SI is a measure of the specificity of expression for each probeset in a given cell type relative to all other cell types included in the analysis. The SI used a permutation based statistical approach to compensate for any irregularities in the distribution of the data, allowing direct comparison of P-values across samples with quite varied distributions. For each IP, the filtered expression values were randomly shuffled many times, and SIs were calculated for all probesets to determine the frequency of a particular SI value appearing. This created a simulated probability distribution.

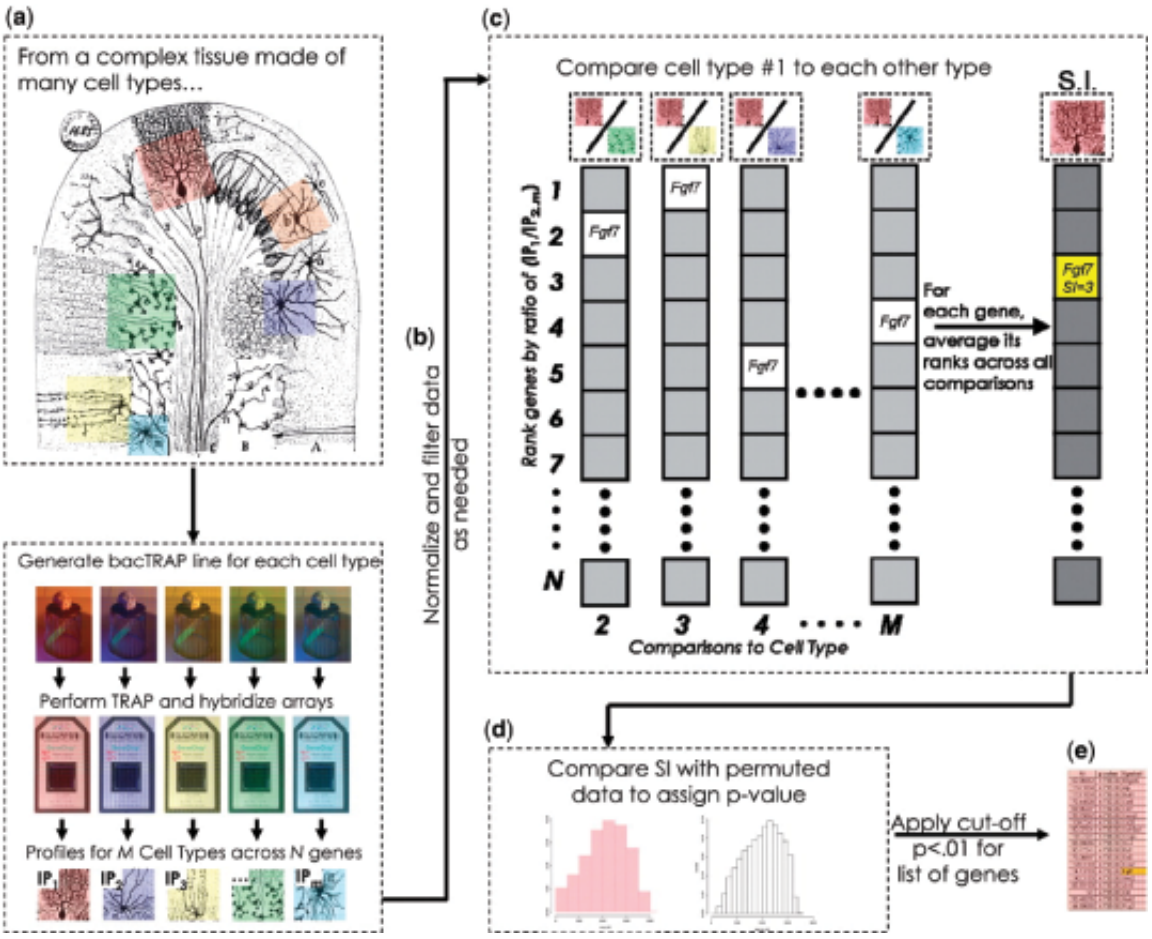

Figure 3.2: Algorithm for Calculation of SI

(a) Cellulary heterogeneous tissue such as cerebellum or neocortex can be analyzed for cell type specific translational profiles by generating bacTRAP transgenic lines for different cell types within the tissue. The TRAP data for M different cell types across N genes are obtained and (b) normalized and filtered as needed before being iteratively compared to each other on a gene-by-gene basis. (c) Ratios of enrichment vs every other cell type was calculated for any given gene; ranks were assigned based on the descending order of ratio in the list. For each gene, ranks were averaged across cell comparisons. (d) A P-value was assigned to a given SI value via permutation testing. (e) A list of genes significantly enriched in specific cell can be selected based on P-value (Dougherty, Schmidt et al. 2010)

The p-value for each ranking could be assigned by the probability of getting SIs from real data in this simulated probability distribution. These probabilities were comparable across samples.

We performed this SI analysis on the Dlx1trap or the Nek7 trap with trap IPs from the cortex of three glial BacTRAP lines, Cnp, Olig2 and Fthfd. Cnp, 2',3'-cyclic nucleotide 3'-phosphohydrolase, is a membrane associated enzyme that is present at high specific activity in glial and Schwann cells and in myelin. Olig2, oligodendrocyte transcription factor 2, is a marker for oligodendrocyte progenitors as well as mature oligodendrocytes. Fthfd, formyltertrahydrofoloate dehydrogenase, is expressed in mature astrocytes. Three transgenic lines for each gene (Cnp JD368, Fthfd JD130, Olig2 JD97) accurately target endogenous neuroglia population and have no ectopic expression in cortical neurons and microarray results confirmed this (data not shown). We selected only high ranked genes for Dlx1 trap or Nek7 trap with the p-value <.05. This process successfully removed most of glial and non-enriched genes from the Nek7 or the Dlx1 trap list.

3-1-2: Selection of Genes that Belong to Each Subdivision

We used the Genefilter program (Bioconductor) to screen genes which were expressed in each subdivision of interneuron groups. Genefilter is an R-based program which is designed to screen genes which have similar expression pattern to the gene of interest. To run Genefilter, we run through a couple of steps of preparation. First, we made all GC-RMA normalized and globally normalized expression values (same normalization method in SI analysis) for filtered genes in 4 interneuron lines. Then, we calculated the

ratio of expression by dividing by the maximum value for each gene. Now all the values were in the range of 0 to 1. We made the artificial template genes represent each subdivision (Figure 3.1). Then we ran Genefilter to find genes which had a similar pattern to the template gene. We picked the best 100 genes for each as candidate markers of each subdivision.

3-1-3: Screening in ABA

We were able to delete most of the glial genes by SI analysis with glial lines, but we discovered that the Nek7 trap also had microglia contaminations which we didn't have BacTRAP lines for. Therefore, to make sure these candidate genes are expressed interneurons, we needed to check the ISH expression pattern using ABA for the candidates and only picked genes with clear interneuron-like expression patterns in the cortex. Also, we included genes which were already known to be expressed in interneurons even when ISH is not working. After that, we checked their gene sizes and available BACs through UCSC genome browser.

Figure 3.3-5 shows the enrichment in each line for marker genes and ISH images from ABA. Mafb, Akr1c18, Rbp4, AI836003, Vwc2, Cox6a2 and Moxd1 all belong to [Dlx1+, Nek7+, Cort+, Htr3a-] group. As ISH images in Figure 3.3 show, even though these genes belong to the same group, their expression patterns are quite different. This could suggest more subdivisions in this group. Mafb is the bZIP transcription factor and is expressed in all PV and SST populations in adults. We kept this gene as a candidate to replace with the Nek7 bacTRAP transgenic mouse

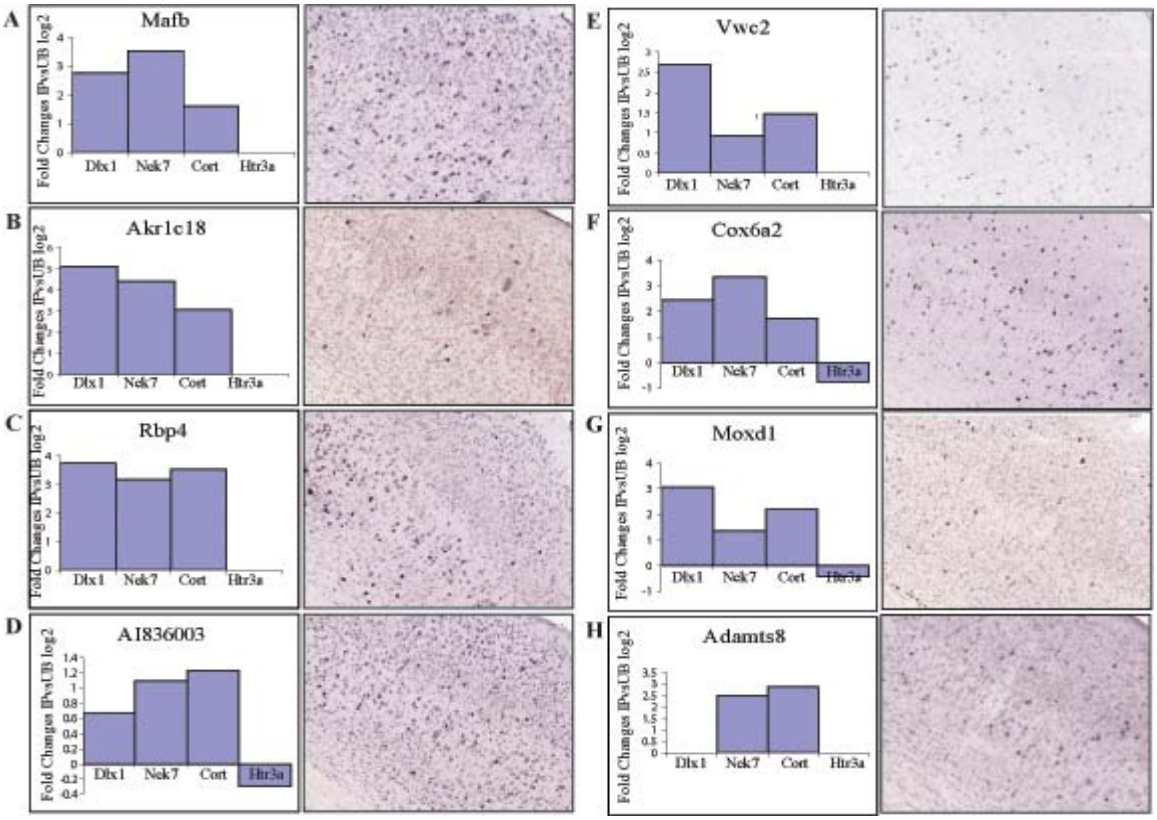

Figure 3.3: Microarray and ISH Results for Candidate Marker Genes for Subpoulation 4, and 6

Left panels showed the log2 based fold changes IP vs UB for the gene of interest in each line. Right panels showed ISH image of the somatosensory cortex from ABA. (A) Mafb (B) Akr1c18 (C)Rbp4 (D)AI836003 (E)Vwc2 (F) Cox6a2 and (G) Moxd1 all belong to subpopulation-4 [Dlx+. Htr3a-, Nek7+, Cort+]. Although they all belonged to the same subdivision, ISH images clearly showed that they are targeting different populations. Mafb had a similar pattern with PV or SST, but Cox6a2, Vwc2 and AI836003 seem to label slightly fewer neurons, although this might come from the ISH efficiency. Rbp4 had localized expressions in lower layers (layer 5-6) and Akr1c18 and Moxd1 probes only labeled a few neurons in the same area. Moxd1 is also expressed in subplate as previously reported. Adamts8 was in Nek7 and Cort list but not in Htr3a or Dlx1. (subpopulation 6 or mix with 5)

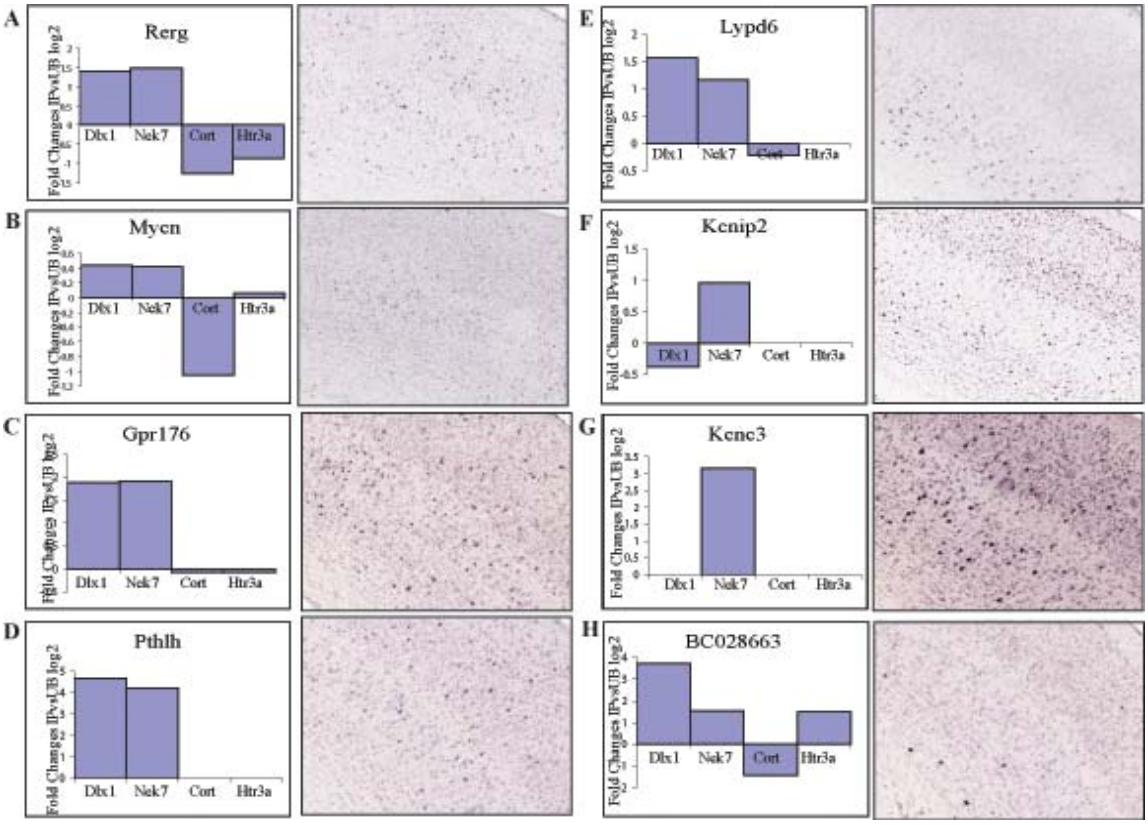

Figure 3.4: Microarray and ISH results for Candidate Marker Genes for Subpopulation 3, 5

Left panels showed the log2 based fold changes IP vs UB for the gene of interest in each line. Right panels showed ISH image of the somatosensory cortex from ABA. (A) Rerg (B) Mycn (C) Gpr176 (D) Pthlh (E) Lypd6 all belong to subpopulation-3 [Dlx+. Htr3a-, Nek7+, Cort-]. Again, they showed different patterns. Compared to Rerg, Gpr176 and Pthlh, Lypd6 shifted to lower layers similar to Rbp4. (F) Kcnip2 and (G)Kcnc3 were only enriched in Nek7 and showed interneruon-like ISH images. (H)BC028663 showed heterogenous-like microarray results, but ISH signals were localized in a few big neurons.

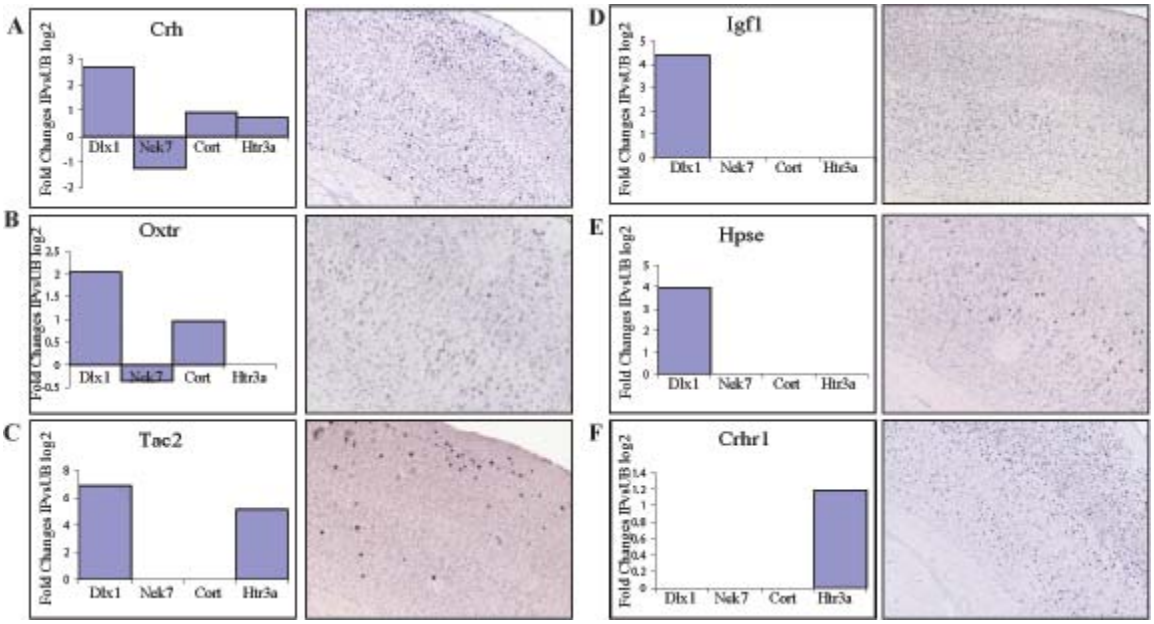

Figure 3.5: Microarray and ISH Results for Candidate Marker Genes for Subpopulation 1, 2 and 7

Left panels showed the log2 based fold changes IP vs UB for the gene of interest in each line. Right panels showed ISH images of the somatosensory cortex from ABA. (A) Microarray results showed Crh was heterogeneous but a few scattered neurons were labeled by ISH probe for Crh. (B) Oxtr was in subpopulation 7 (C) Tac2 belongs to subpopulation 1 and VIP like expression pattern (D) Igf1 and (E) Hpse were only in Dlx1 IP. Although ISH signals were weak, we could see interneuron-like small labeled neurons. (F) Crhr1 was only in Htr3a IP. This probably means small group of subpopulation 1 was targeted by Crhr1.

line which had a big background issue. Vwc2 encodes a BMP antagonist that may play a role in neural differentiation or adhesion process. Vwc2 was also enriched in Grm2 positive population, which represents granule cell layer interneurons in the cellebrum. We observed many genes from the list which were also expressed in GABAergic interneurons of other brain areas. Moxd1 is also a marker for subplate and the functions of Moxd1 in neurons are not known. However, because of the similarity to the dopamine beta-hydroxylase, it is possible to think it can produce a new transmitter in a specific population.

Adamts8 was enriched in the Nek7 and the Cort IP. Adamts8 expressed neurons might include two populations, ⑤ [Nek7+ Cort-], ⑥ [Nek7+, Cort]. However ISH showed much fewer neurons compared to the Nek7 ISH image and this could represent Dlx1 trap negative, subdivision of PV neurons. Rerg, Mycn, Gpr176 and Pthlh, Lypd6 could represent Cort trap negative, subpopulation of PV or SST neurons. Kcnip2 and Kcnc3 were only Nek7 trap positive, which probably means another subpopulation of PV. Kcnip2 encodes a voltage-gated potassium channel-interacting protein and may regulate the A-type current through Kv channel in response to changes in intracellular calcium. Kcnc3 protein is Kv channel subunit 3. Kcnip2 might be expressed in pyramidal neurons of upper layers, but expressions in layer 5-6 looks quite similar to the pattern of Kcnc3 which matched with our microarray results. The Kv3 family is characterized by positively shifted voltage dependence and very fast deactivation rates and these physiological properties enable neurons to fire repetitively at high frequency. Other Kv family members, Kcnc1 and Kcnc2, are required for fast firing of PV positive neurons

(Rudy and McBain 2001). Therefore, Kcnip2 and Kcnc3 could be working together to provide some unique firing properties in subpopulations of the PV neurons.

BC028663 and Crh, corticotropin-releasing hormone gene, have expression in both MGE and CGE derived interneurons, which mean they are probably targeting heterogeneous population. However, a very few scattered interneurons were labeled in the cortex using their ISH probes. Crh is known to be expressed in VIP or CR or SST neurons, which matches with our microarray results (Doyle, Dougherty et al. 2008). BC028663 was enriched in Nek7 and Htr3a, which represents MGE or CGE respectively, but as mentioned before, both lines have glial gene contamination. According to ISH results, a very few neurons were labeled by BC028663 probe. BC028663 might label a new interesting population in the cortex, such as long distance inhibitory neurons or interneurons and glia. Oxtr, Oxytocin receptor, represents more SST neurons, [Dlx1+, Cort+, Nek7-, Htr3a-], and Tac2 labels CGE derived interneurons. Igf1 and Hpse label [Dlx1+, Htr3a- Nek7-] population. Crhr1 was enriched only in Htr3a but that might be because the Crhr1 positive neurons are too rare in Dlx1 and the enrichment in Dlx1 couldn't be observed. (The expression value in Htr3a was also very low.)

3-2: Density Recovery Profiling (DRP)

DRP is a statistical measure of the cells' spatial autocorrelation, measuring the density of cell bodies as a function of distance from the reference cell (Rodieck 1991). Regularly spaced cells have a zone of exclusion for other homotypic cells, indicated by a below-average cell density at short distances. If the cells are randomly distributed, the density

profile would be flat regardless of the distance (Rockhill, Euler et al. 2000). Utilizing this method, it has been shown that GABAergic CCK neurons in upper layers seem to repel each other within 35um distance (Markus Meister, Allen Institute for Brain Science Symposium).

We ran DRP analysis on ABA ISH images for a number of genes. 100~400 labeled neurons were selected around the somatosensory cortex in coronal sections using Image J. A cell was taken as a reference cell and the distance from that cell to every other selected cell was measured and we repeated this procedure until we selected every cell as a reference cell. The results were binned along this distance and the overall density of cells at each distance from the reference cell was measured. This method required dense population; therefore we only selected Gpr176, Cox6a2 and Kcnc3 images from the candidates. Also as control, we selected Gad1, PV, and SST images. Gad1, glutamate decarboxylase 1, catalyzed the conversion of glutamate to GABA and expressed in all GABAergic interneurons in the cortex. As I mentioned earlier, GABAergic neurons are heterogeneous. The mixed population was known to have a random distribution which was represented by flat DRP like GAD1 DRP (Figure3.6A). This suggests that DRP analysis using ABA ISH images could detect random distribution. There are no known genes which could represent a specific cell type, therefore we tested PV and SST because PV and SST label more specific interneurons than Gad1 even though they are still mixed. PV and SST neurons showed weak repulsions at 20um (Figure 3.6 B, C). Compared to known markers, new candidate markers showed stronger exclusion at short distances. Gpr176, Cox6a2 and Kcnc3 showed strong repulsion within 20-30 um (Figure 3.6 D-F).

The size of the exclusion zone could depend on the dendritic field of each cell type and the cell soma size. However we already showed with microarray results that Gpr176 and Kcnc3 expressed in the Cort negative subpopulation of MGE derived neurons (PV and SST). Therefore, stronger repulsion compared to the PV and the SST population might suggest our new candidate markers are labeling more specific interneuron subtypes.

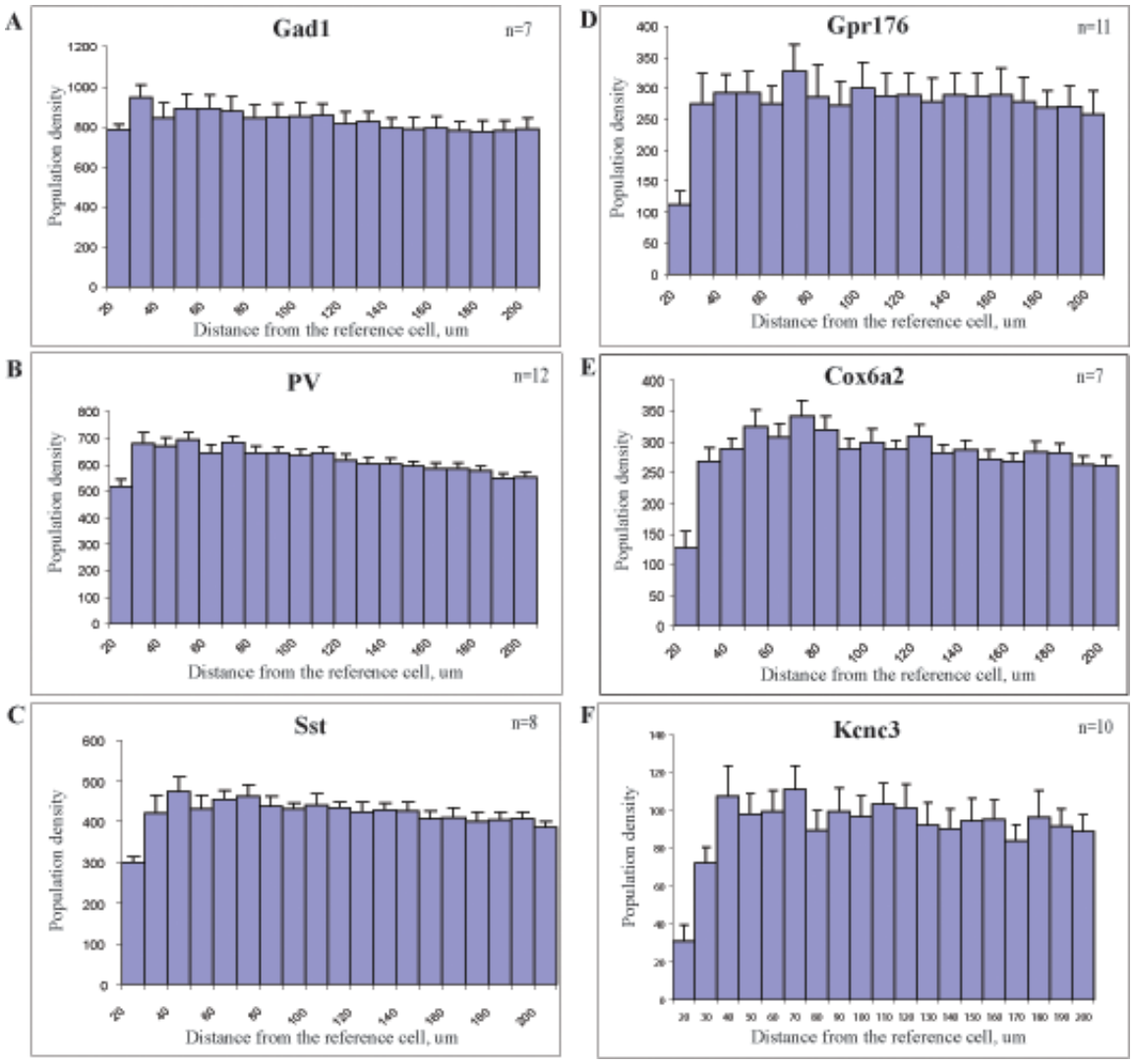

Figure 3.7: The Density Recovery Profiles of Interneuron Markers

The spacing of different interneuronal populations were measured by DRP methods. We used ABA ISH images around the somatosensory cortex to measure the spacing of each population. The distance between cells is on the X axis and the density of neurons in each distance is on the Y axis. All plots Mean +SEM.
(A) GAD1 and (B)PV showed random distributions. (C) SST showed some exclusion zone in 20um but this exclusion was more obvious in (D) Gpr176, (E) Cox6a2 and (F) Kcnc3 populations, which could suggest they are a more homotypic population.

3-3: Discussion

It is possible that the identity of interneuron cell types is defined by either the combinatorial expression of multiple genes or genes that are expressed only during the development stages. However the comparative analysis of microarray results found ~20 candidate genes for more specific interneuron BAC transgenic mice. ISH and microarray results suggest these genes might be expressed in more specific interneuron subtypes in the adult mouse cortex. Some candidate genes could change the firing patterns or output of the neurons and this should affect neurons' identities. Transgenic mice based on these genes could be very useful for various studies. bacTRAP transgenic mice lines for these genes and their gene expression profiling could provide clearer molecular explanation of cell phenotypes. Especially if these populations have a link to pathophysiological mechanisms underlying human brain disorder, by crossing with mouse disease models, bacTRAP lines could provide genetic factors of these human diseases. Cre transgene expression in candidate marker gene populations could be useful for further functional studies using virus in adult brains (Chapter 4).

Chapter 4

Characterization of New BAC Transgenic Lines

We generated either bacTRAP or Cre lines for all candidate genes. We characterized them using IHC of several markers and for Cre lines we injected AAV in adult brains to examine their specificity of Cre positive neurons in adults. Among them, we selected two lines, Rbp4 KL105 Cre and Oxtr ON82 Cre lines, for further studies based on their expression patterns in adults, specificity and gene functions.

As mentioned previously, the Cre system can be utilized for many different functional studies. We were able to use this system to elucidate the anatomical properties, gene profiling, and connectivity of Rbp4 Cre and Oxtr Cre cells. We also began functional studies using Cre-dependent silencing systems.

4-1: Molecular Characterization of Rbp4 Cre and Oxtr Cre Lines

Rbp4, retinol binding protein 4, is responsible for the transport of retinol (vitamin A). Retinol binds to Rbp4 in the blood and is taken up by target cells through an interaction with a membrane receptor for Rbp4, STRA6, and metabolized into all-*trans* RA. RA enters the nucleus and binds to a transcription complex which includes a pair of ligand-activated transcription factors comprising the RA receptor (RAR) – retinoic X receptor (RXR) heterodimer. RA can regulate the expression of more than 500 different genes including Reelin, calbindin D28K, and Chat. Under vitamin A (RA) deficient condition,

SST levels are severely reduced. RA signaling is known to be involved in neuronal plasticity in adults. RA receptor beta (Rarb) was identified as a regulator of cortical synchrony in the delta frequency during slow wave sleep (SWS). Rbp4 itself is known to be secreted from adipocyte cells, circulations in the blood, and induces insulin resistance in liver and skeletal muscle (Yang, Graham et al. 2005). However, the functions of Rbp4 in the brain are not known.

Oxtr is a member of the rhodopsin-type (Class I) G-protein (Gq/11α) coupled receptor and the receptor of Oxytocin. The neuropeptide Oxytocin has been implicated in anxiolytic mechanisms and a number of social behaviors, including maternal care, affiliation, social attachment trust and bonding. Oxytocin is a peptide hormone of nine amino acids and is made in the hypothalamic magnocellular neurosecretory cells of the supraoptic and in the paraventicular nuclei in the central nervous system. Oxytocin receptors are expressed in various regions including the neocortex, the olfactory system, the basal ganglia, the limbic system, the thalamus, the hypothalamus, the brain stem and the spinal cord. Many studies have been performed on Oxytocin receptors in the medial amygdala, the hypothalamus and the limbic system, but the cortical Oxtr positive neurons' functions are unknown. According to our microarray results, Oxtr genes are enriched in interneuron populations but not in excitatory neurons in the cortex (data not shown). Oxytocin is currently being tested as an effective treatment of autism's repetitive and affiliative behaviors.

The Cre expressions of new Cre driver lines were characterized by crossing with EF1a-EGFP-L10a (BacTRAP reporter line) to check EGFP expression (Figure 4-1).

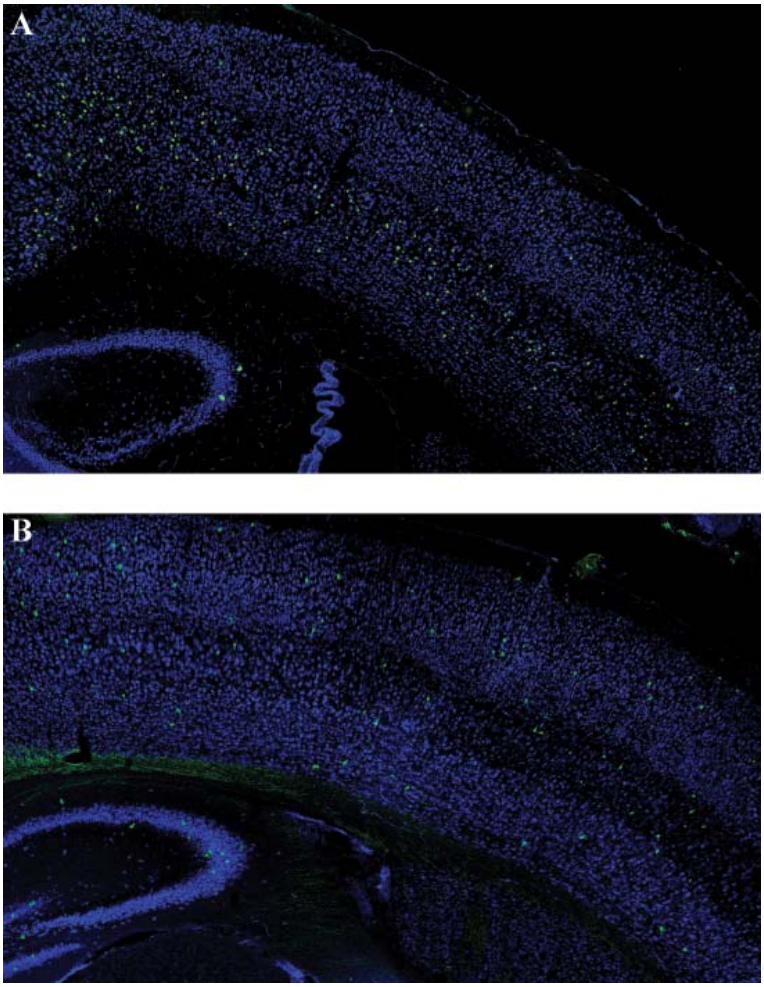

Figure 4.1: Distribution of EGFP-L10a positive Neurons in Rbp4 Cre and Oxtr Cre Lines

EGFP and NeuN co-immunostaining was done on brain sections of (A) Rbp4 KL105 Cre and (B) Oxtr ON82 Cre line crossed with EGFP-L10a reporter line. EGFP (Green) and NeuN (Blue). EGFP-L10a expression was localized in cell bodies of each Cre positive neuron. (A) Rbp4 Cre neurons were localized to layer 5, similar to ISH results. On the other hand, (B) Oxtr Cre neurons showed a scattered expression pattern in all layers.

Rbp4 Cre expression is mainly concentrated in lower layers (mainly layer 5), while Oxtr Cre expression is scattered in all layers. We performed double IHC to examine coexpression of known marker proteins and Cre-EGFPL10 proteins for both lines (Figure 4.2). Rbp4 Cre neurons could be labeled with SST (70%) and PV (10%). Almost no VIP or CR positive neurons were found among Rbp4 Cre neurons. Oxtr Cre neurons expressed SST (53%), PV (14%) or CR (10%). (Table 4.1)

Table 4.1: Summary of IHC Results on Rbp4 KL105 Cre and Oxtr ON82 Cre Crossed with EGFP-L10a Line

	PV (100%)	CR (100%)	VIP (100%)	SST (100%)
Rbp4 KL105 Cre	1% (7/692)	0% (0/103)	2% (8/398)	15.8% (115/728)
Oxtr ON82 Cre	3.1% (30/973)	9.6% (13/136)	1.3% (11/873)	27.4% (173/631)

	PV	CR	VIP	SST
Rbp4 KL105 Cre (100%)	9.86% (7/71)	0% (0/85)	2.78% (8/288)	69.3% (115/166)
Oxtr ON82 Cre (100%)	13.8% (30/218)	4.7% (13/276)	2% (11/512)	53.4% (173/324)

Proportion of each marker group in each line. Each IHC was done on the somatosensory cortex of 4 adult mice. (A) showed the percentage of EGFP/Marker positive neurons in marker positive population. (B) indicated the percentage of EGFP/ Marker positive neurons in EGFP positive population

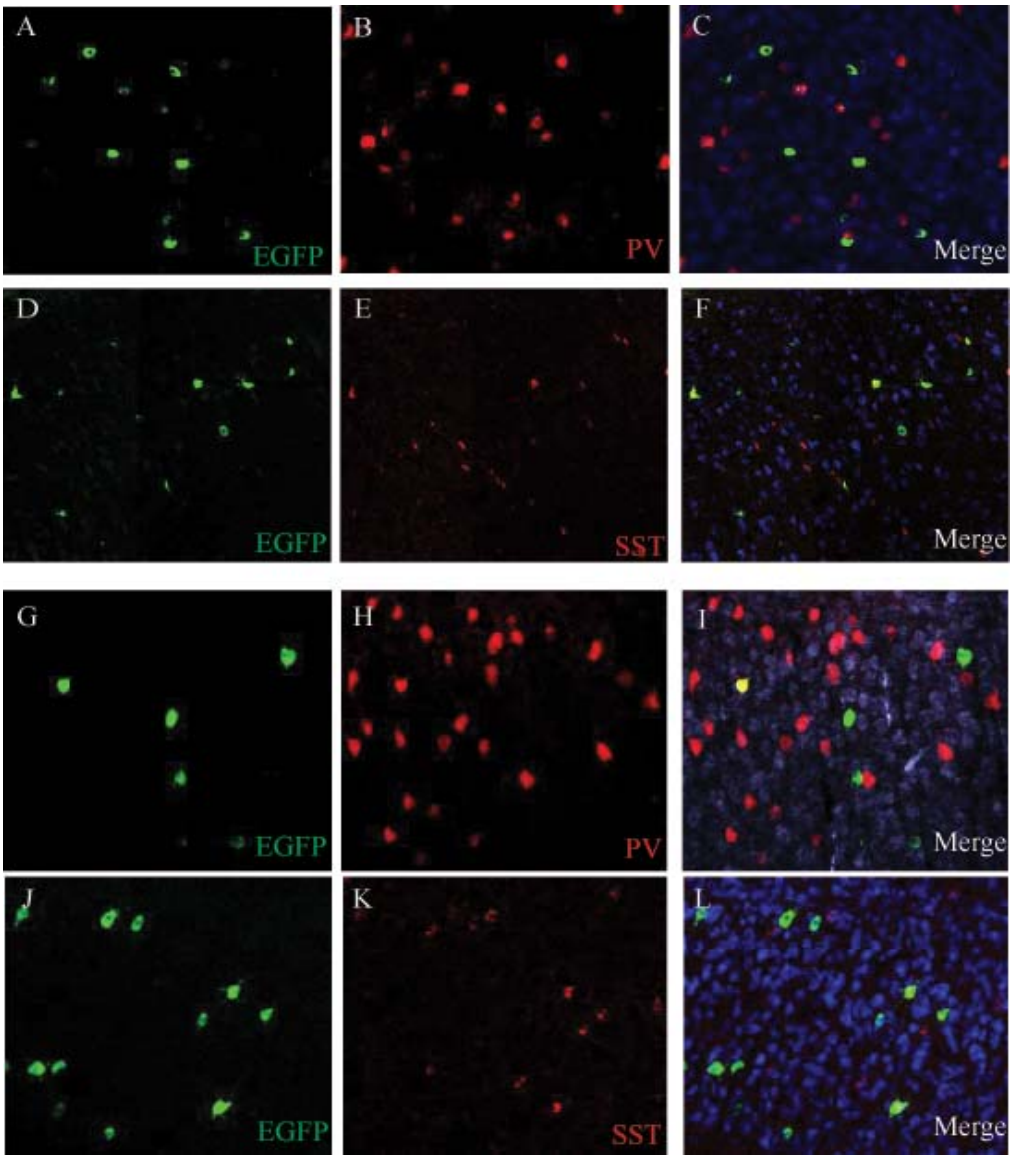

Figure 4.2: Colocalization of EGFP and Interneuron Markers

Triple Fluorecence immunostaining for EGFP, interneuron markers (PV or SST), and NeuN were done on Rbp4 Cre and Oxtr Cre crossed with EGFP-L10 rerporter line. (A-F) Rbp4 KL105 Cre (G-L) Oxtr ON82 Cre. (A-C) Some weak EGFP expression was found in PV positive neurons, but strong EGFP neurons rarely overlap with PV. (D-F) Most of the strong Rbp4 Cre-EGFP neurons overlapped with SST positive neurons. (G-I) A few Oxtr Cre - EGFP neurons were PV positive. (J-L) About half of the Oxtr Cre positive neurons were SST positive.

We also collected IPs from each Cre/loxP bacTRAP line and examined their expression profiles. Enrichment of each interneuron marker represented by fold changes of IP/UB matched well with the IHC results, which suggests that bacTRAP successfully collected RNAs from targeted neurons (Figure 4.3). bacTRAP results also showed very high enrichment of each driver gene compared to other lines (Figure 4.4). This result implies Cre transgenes were targeting endogenous Rbp4 or Oxtr expressing cortical population well. However we don't know exactly how well the endogenous populations overlap with each Cre positive neurons. Driver enrichments also suggest Rbp4 Cre population and Oxtr Cre population overlapped with each other but not with Htr3a positive neurons.

None of the retinoic acid signal cascade molecules were enriched in Rbp4 IP or other cortical interneurons. Although there are still possibilities that either the probesets for these genes were not good or they also expressed in other cell types at the same time, it seems there is no specific retinoic acid signaling in Rbp4 Cre population. At the same time, we couldn't find any other cell types which showed enrichment of these genes. Functions of Rbp4 in the adult brain are not known but it could be different from classical retinoic acid signaling.

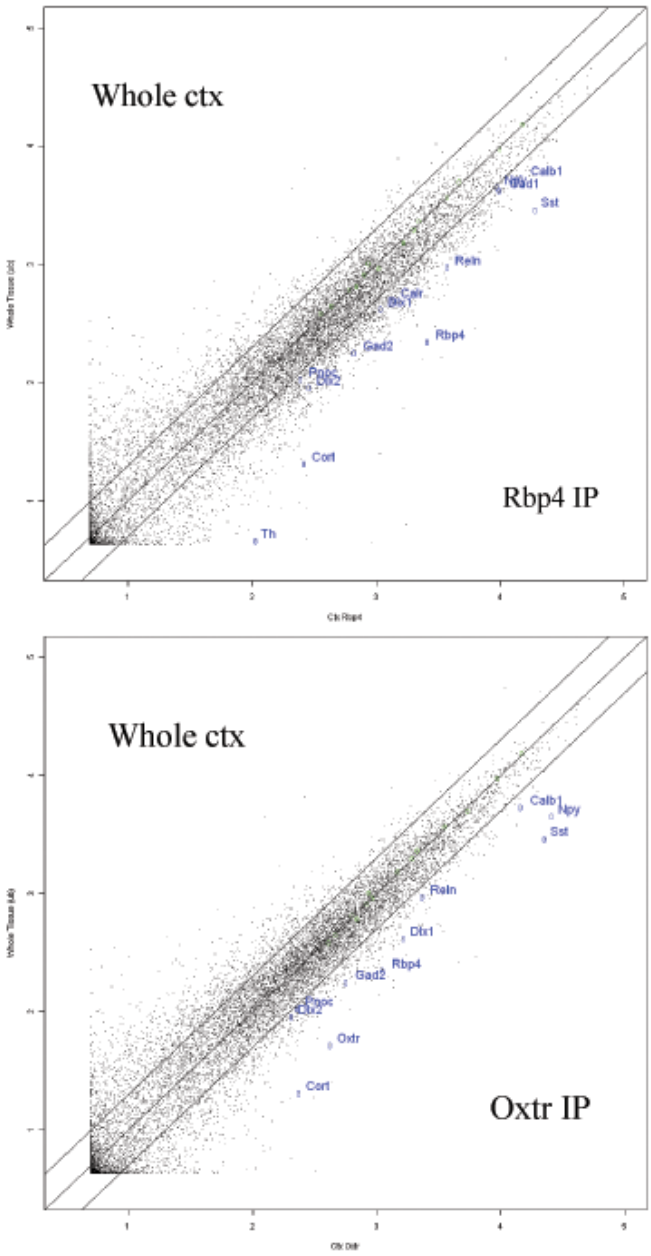

Figure 4.3: Scatterplots of Microarray Data for Rbp4 KL105 Cre/EGFP-L10a and Oxtr ON82 Cre/EGFP-L10a

Translational profiles of Rbp4 Cre and Oxtr Cre line. We crossed Cre lines with the EGFP-L10a reporter line and collected IP from the cortex of each line. Fluoresence signals of all 40,000 probesets for each IP (X) were averaged and plotted against total cortex input (Y) in an X-Y scatterplot. Grey lines show positions of 0.5, 1 and 2 fold changes. Blue dots represent enriched (more than 2-fold) known interneuronal markers. As expected from IHC results, SST is one of the most enriched genes in both IPs. Rbp4 is enriched in Rbp4 IP and Oxtr probe is enriched in Oxtr IP.

Figure 4.4: Enrichment of Marker Genes and Driver Genes in Rbp4 Cre and Oxtr Cre Trap Results

Log2 based fold changes of IP vs UB were plotted for (A-F) marker genes, and (G-I) driver genes in 6 lines. As a comparson, we includeed the previous microarray results of the original 4 lines. The transgenic lines' names are on the x-axis and log 2 based fold changes on the y-axis. (A.B) As expected from IHC results, SST and PV were enriched in both Rbp4 and Oxtr lines and (C) CR was enriched only in Oxtr line. (E, F) Reelin and NPY also showed enrichments in new lines, while (D) VIP gene didn't. This suggested our Cre dependent TRAP method using EGFP-L10a reporter line worked. (G, H)There are no reports on endogenous Rbp4 or Oxtr interneuron population in the cortex, but according to microarray results, Oxtr gene was enriched most in Oxtr Cre transgenic population compared to other mouse lines and Rbp4 showed the highest fold changes in Rbp Cre transgenic line, too.This suggests both Rbp4 and Oxtr Cre line have the highest proportion of endougenous driver gene populations among 6 lines. (I) Neither Cre lines expressed Htr3a gene, and (G, H) Htr3a IP list didn't show enrichments of Rbp4 and Oxtr probesets.

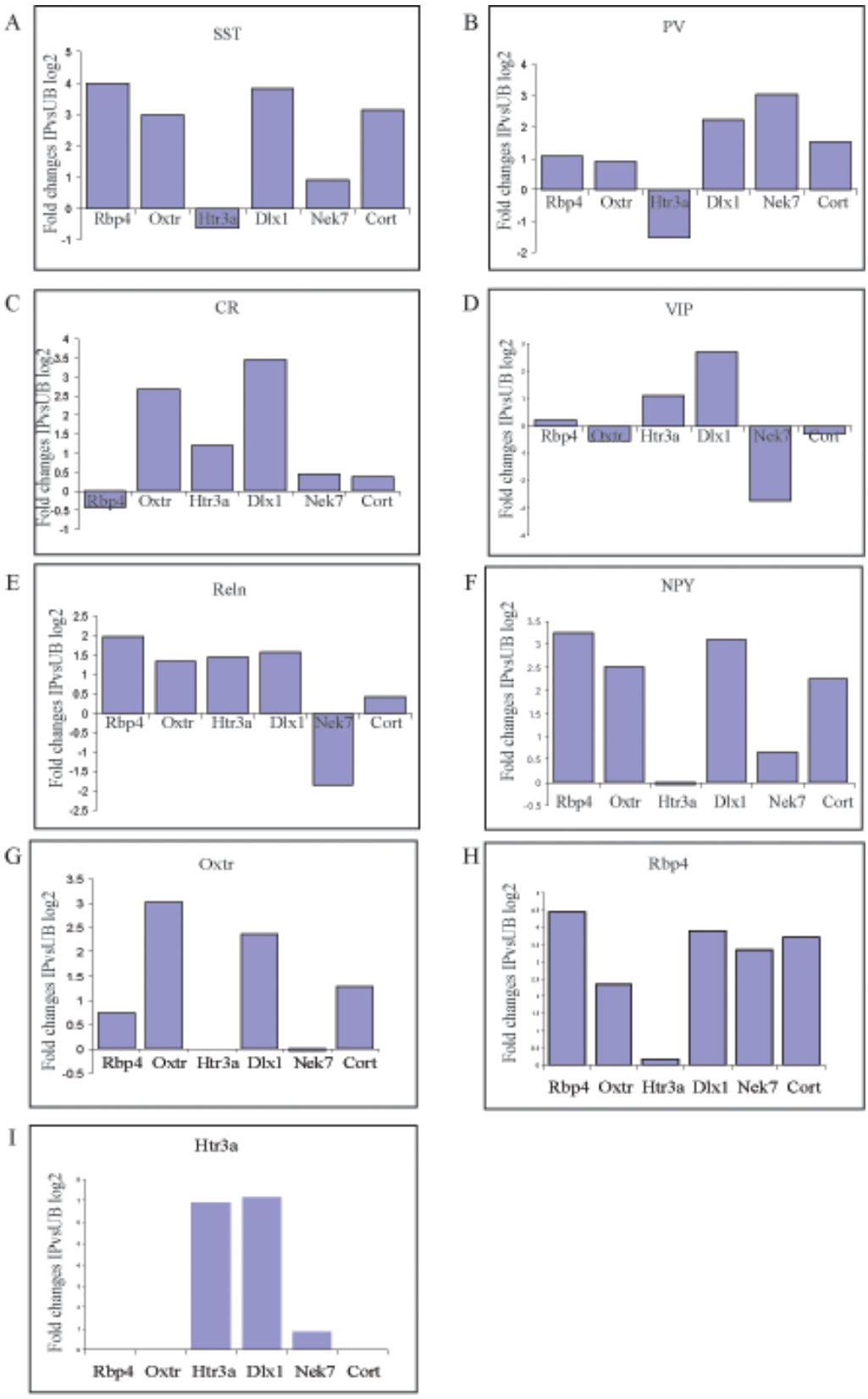
A
SST
Fold changes IPvsUB log2
Rbp4 Oxtr Htr3a Dlx1 Nek7 Cort
B
PV
Fold changes IPvsUB log2
Rbp4 Oxtr Htr3a Dlx1 Nek7 Cort
C
CR
Fold changes IPvsUB log2
Rbp4 Oxtr Htr3a Dlx1 Nek7 Cort
D
VIP
Fold changes IPvsUB log2
Rbp4 Oxtr Htr3a Dlx1 Nek7 Cort
E
Reln
Fold changes IPvsUB log2
Rbp4 Oxtr Htr3a Dlx1 Nek7 Cort
F
NPY
Fold changes IPvsUB log2
Rbp4 Oxtr Htr3a Dlx1 Nek7 Cort
G
Oxtr
Fold changes IPvsUB log2
Rbp4 Oxtr Htr3a Dlx1 Nek7 Cort
H
Rbp4
Fold changes IPvsUB log2
Rbp4 Oxtr Htr3a Dlx1 Nek7 Cort
I
Htr3a
Fold changes IPvsUB log2
Rbp4 Oxtr Htr3a Dlx1 Nek7 Cort

4-2: Tiling Properties of Cre Positive Neurons

We measured DRP for Rbp4 Cre/loxP EGFP-L10a and Oxtr Cre/loxP EGFP-L10a neurons. We cut 20um thick sections and stained with anti EGFP antibody. Labeled neurons around the somatosensory cortex were counted using ImageJ and the pairwise distance was measured (Figure 4.5). DRP results implied Rbp4 Cre seems to be distributed randomly even though expression was localized to layer 5. On the other hand, Oxtr Cre showed a zone of exclusion within 40um distance.

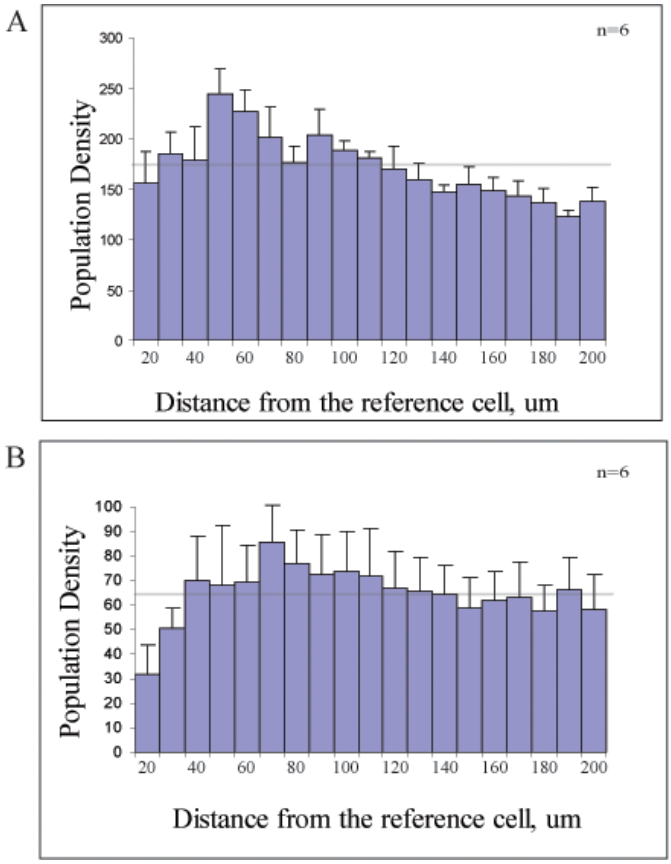

Figure 4.5: DRP Analysis on Rbp4 Cre and Oxtr Cre Lines Crossed with EGFP-L10 Reporter Line

We performed the DRP analysis on EGFP neurons in the somatosensory cortex of new Cre lines crossed with the EGFP-L10 reporter line. All Average + SEM. The light, shadowy line shows the average density. (A) Rbp4 Cre reached the average density from the shortest distance. (B) Oxtr Cre showed repulsion within <40um distance. SEM is higher due to the low number of EGFP neurons within 200um distance.

To examine adult Cre expression and targeted neurons' morphologies, we have used two recombinant AAVs: AAV2/5-EF1a-double floxed ChR2 (E123A)-EYFP-WPRE and AAV2/5-EF1a-double floxed ChR2 (E123A)-mCherry-WPRE. ChR2 is a light gated ion channel and is distributed along all the membranes including the dendrites and axons. Therefore EYFP or mCherry fused with ChR2 can visualize Cre positive neurons' morphologies. We carried out unilateral stereotaxic injections (400nl) of either pAAV-ChR2-EYFP or pAAV-ChR2-mCherry in the somatosensory cortex of Rbp4 Cre or Oxtr Cre lines at the age of 8-12 weeks. Recommended duration for Cre-inducible viral transgene expression is over 3 weeks. Hence after virus injection, we housed mice for 3-4 weeks and we sacrificed mice for neuroanatomical analysis. This volume of virus could spread about ~1mm in all directions of the cortex. Figure 4.6 shows much wider innervations from Oxtr Cre neurons compared to Rbp4 Cre neurons, even though the number of labeled neurons was almost the same. Rbp4 Cre positive neurons had dense axonal/dendritic projections in layer 5 and only a few sent the axon to the layer 1.

Both the innervation pattern and the spacing between cell bodies from DRP analysis suggest Oxtr Cre neurons might have a tiling property. Oxytocin gene knockout mice showed robust inductions of cFos in the whole somatosensory cortex after a social encounter (Ferguson, Aldag et al. 2001). cFOS has been used as an indirect marker for neuronal activity. This suggests Oxytocin dependent inhibition through Oxtr expressing interneurons affect the whole area of the somatosensory cortex. Therefore, Oxtr interneurons might develop a tiling mechanism to cover the whole area effectively.

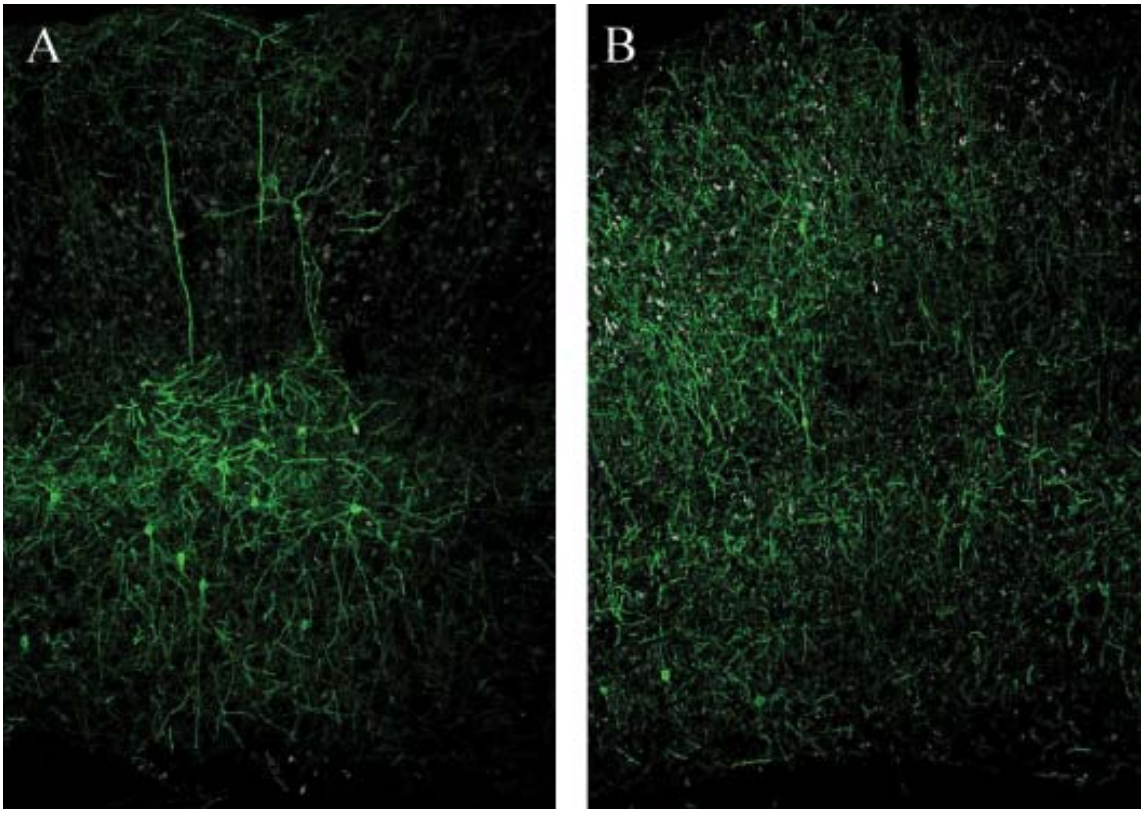

Figure 4.6: Morphologies of Rbp4 KL105 Cre and Oxtr ON82 Cre Positive Neurons

We injected AAV-dflox-ChR2-EFYP virus into the somatosensory cortex of each line to visualize neurons' dendrites and axons. ChR2-EFYP could express only in neurons expressing Cre proteins in adult. (A) Rbp4 KL105 Cre showed dense branches in the layer 5 and sometimes sent the axon to the upper layer. (B) Oxtr Cre positive neurons's branches covered the whole area, even though the number of cell bodies was relatively small.

4-3: Cre-dependent Retrograde Neuronal Tracing with a Modified Rabies Virus

We employed cre-dependent monosynaptic rabies system to elucidate the differences of their anatomical inputs of each line (Figure 4.7).

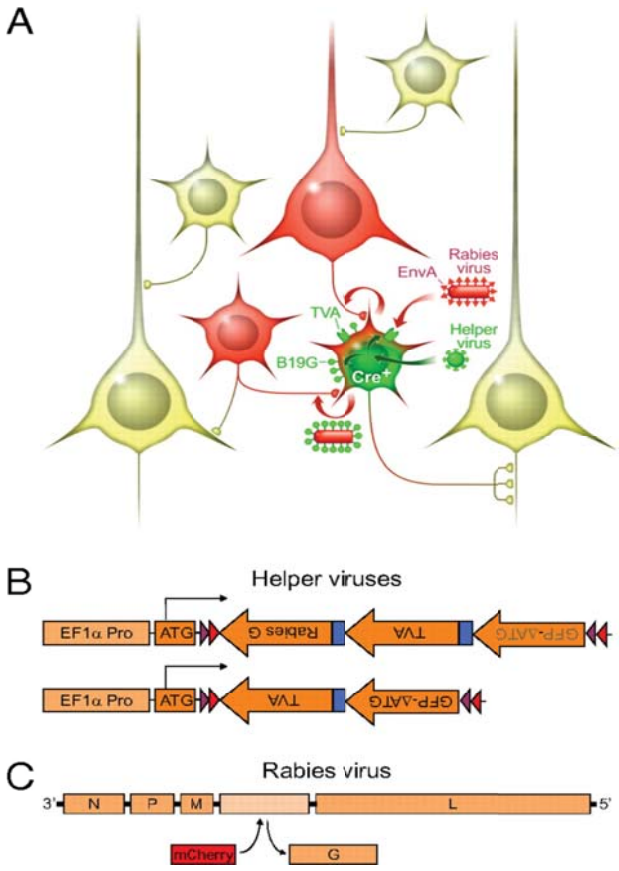

Figure 4.7: Cre-dependent Monosynaptic Retrograde Tracing System Using Modified Rabies Virus

(A) The image of tracing system. (B) Cre-dependent helper virus with the upper construct could express TVA, the rabies glycoprotein, and GFP only in Cre positive neurons around the injection site. ATG start codon from all genes were deleted and a single Kozak sequence was added outside the dflox cassette to avoid leaky expressions (C) Rabies Glycoprotein gene replaced with fluorescence (mCherry of EYFP) gene in the rabies genome. The rabies could no longer express Glycoproteins by itself. Also, the rabies virus was pseudotyped with EnvA. (A) Modified rabies virus could only infect TVA expressing neurons (Green) and requires rabies glycoprotein expressions to be transferred through synapses retrogradely. Cre negative presynaptic inputs (Red) on Green neurons don't express glycoproteins. Therefore the spread of rabies would stop there.

First we injected the helper virus (AAV2/9 pEF1a-doublefloxed-GFP-2A-TVA-2A-Glycoprotein) to express rabies glycoproteins and TVA, EnvA receptor, in Cre positive neurons. 2A elements allow productions of multiple proteins from a single ORF. After waiting ~2 months for TVA/Glycoprotein/GFP expression, modified rabies were injected into the same area. Modified rabies virus can't infect neurons unless TVA was expressed. TVA is absent in mammalian cells unless introduced with helper virus. Glycoproteins are necessary for the spread of modified rabies beyond the initially infected neurons through synapses. Modified rabies virus is designed not to produce its own glycoproteins. Therefore modified rabies can only infect Cre positive neurons expressing TVA and newly synthesized modified rabies virus can complement with the glycoprotein expressed in these cells, allowing the modified rabies virus to spread retrogradely across synaptic contracts, directly labeling presynaptic neurons. Because presynaptic neurons don't express rabies glycoprotein, these cells can't produce infectious rabies virus particles, restricting infections to the targeted cell type and its direct monosynaptic inputs. Rabies infected cells are labeled by either EFYP or mCherry transgene in the rabies genome.

We used this system to elucidate inputs to specific Cre interneuron subtypes. As a control, we also used Htr3a Cre NO152 line to compare with Rbp4 Cre and Oxtr Cre. Htr3a Cre NO152 adult Cre expressions matched with Htr3a BacTRAP GM433 line and barely overlapped with Rbp4 and Oxtr Cre population as we mentioned before. We examined the inputs of each Cre population in the primary somatosensory cortex and the medial prefrontal cortex.

The somatosensory cortex is one of the most well studied areas in the mouse cortex. The barrel cortex has played an especially important role in the studies of cortical micro circuit, due to its distinctive cytoarchitechtonics, functional significance and clear and easily modifiable inputs. Sensory information from facial whiskers is transferred to the primary somatosensory cortex (S1) through two parallel anatomical pathways: the lemniscal pathway which ascends via the principal nucleus (PrV) of the brainstem and the ventroposterior medial thalamic nuclei (VPM), and the paralemniscal pathway which runs via interpolar nucleus of brainstem and the posterior thalamic nucleus (POm). Thalamacortical (TC) neurons from VPM mainly project to layer 4 of S1, while TC neurons from PO diffusely target layer 5 of S1. These different pathways are thought to transmit different modalities of sensory information from the whisker. S1 processes tactile vibrissae information to perceive spatial and textural features of the immediate surroundings and guide rodents to move accordingly by sending sensory information to the motor cortex.

The prefrontal cortex (PFC), on the other hand, received much attention from the neuroscience field because of its involvement in psychiatric diseases. The executive functions of PFC are the set of control processes that serve to optimize performance including social behaviors, decision making processes, and goal directed attention. In mice, there are three distinct regions in the PFC: 1) medial PFC, 2) anterior cingulate, 3) orbitofrontal cortex. The medial prefrontal cortex is believed to play an important role in the regulation of social cognition which might involve top-down control of subcortical structures including the amygdala. Recently, elevation of excitatory/inhibitory imbalance

in medial prefrontal cortex was shown to cause social deficit and psychiatric disease like phenotypes. Therefore inhibitory systems in medial prefrontal cortex might be critical to understanding the cause of psychiatric diseases, especially for autism and schizophrenia. We focused our injections to the medial prefrontal cortex (prelimbic, infralimbic and cingulate cortex).

For each line, we injected 400nl of helper virus either in the somatosensory cortex or the prefrontal cortex. After 2 months, 400nl of modified rabies virus either with EFYP or mCherry transgene were injected into the same cortical area. Then we waited for another 2 weeks for transsynaptic transfer of modified rabies virus and the accumulation of fluorescence proteins. The mice were sacrificed and brain tissues were processed for IHC. We also injected modified rabies virus without helper virus to confirm there was no leaky expression from modified rabies virus. And we didn't observe any labeling from rabies without TVA or EnvA (data not shown) as previously reported (Wall, Wickersham et al. 2010). Helper virus infected neurons were visualized by GFP and as expected GFP expression was similar to Cre expression pattern of each line, which suggests Cre dependent infections of helper virus (Figure 4.8). Some AAV serotypes were taken up by axonal terminals and retrogradely label neurons. However we didn't observe any helper virus infected neurons outside of our injection sites. Therefore we could ignore this possibility. Not every green labeled neuron was infected by modified rabies virus. Yellow neurons in Figure 4.8 represented neurons which were infected by both viruses. The spread of rabies virus to neurons presynaptic to yellow interneurons resulted in only

mCherry expression in numerous pyramidal neurons and interneurons locally near the injection site (Figure 4.8).

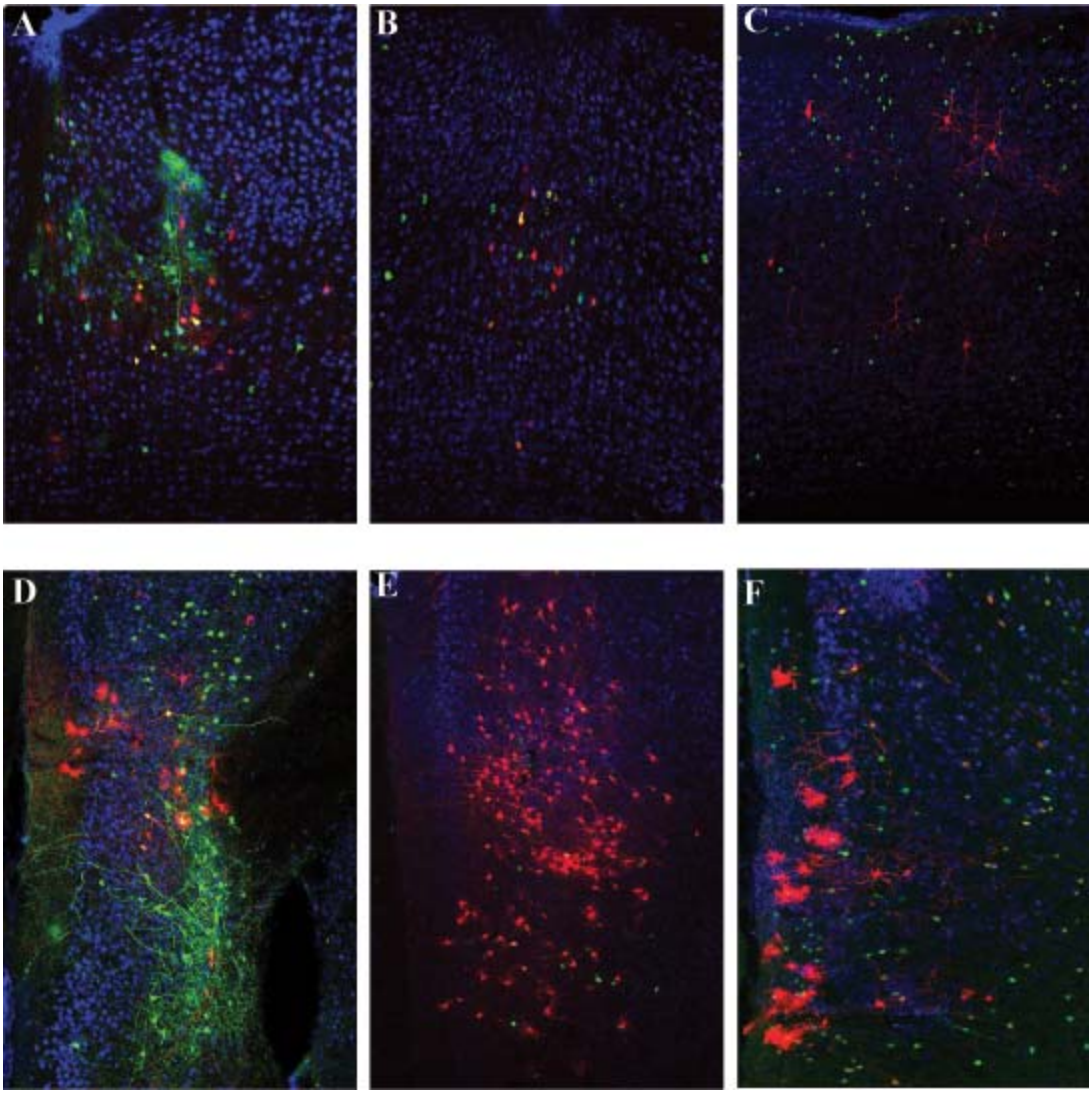

Figure 4.8: Helper Virus and Rabies Virus Expressions in Injection Sites

Helper virus could infect each Cre positive interneuron in injection sites and label neurons with GFP. Modified rabies virus could be taken up by GFP positive neurons and monosynaptically label their presynaptic inputs with rabies fluorescence. (either mCherry or EYFP). (A) Rbp4 Cre S1 (B) Oxtr Cre S1 (C) Htr3a Cre S1 (D) Rbp4 Cre PFC, (E) Oxtr Cre PFC (F) Htr3a Cre PFC. Red: mCherry expressing rabies virus, Green: GFP from helper virus, Yellow: mCherry Rabies + Helper virus

RV expressions were observed in all three lines in the pyramidal neurons of the ipsilateral secondary somatosensory cortex separated by a clear gap containing no intervening labeled neurons (Figure 4.9B). In Htr3a Cre neurons, we also observed many innervations from the primary motor cortex (M1) and contralateral S1 (Figure 4.9A). We also counted the number of subcortical neurons labeled by the expression of fluorescent reporter (EFYP or mCherry) from the modified rabies genome. Both Rbp4 and Oxtr Cre positive neurons in S1 received innervation from the ipsilateral ventral posterior nucleus (VPM) and the posterior nucleus (PO) in the thalamus (Figure4.10A, B). We also observed innervation from the ventral lateral thalamic nucleus, which is known to transfer information from basal ganglia to M1. On the other hand, we only found a few RV transferred neurons in M1 for Rbp4 and Oxtr Cre lines. They also received projections from ipsilateral nucleus basalis of meynert (NBM) which is known to be the main cholinergic input to the neocortex (Figure4.10C, D). Cre positive neurons in S1 of three different lines seem to receive innervation from the same places, but the preference was different. Rbp4 Cre neurons received more innervations from subcortical and S2 than M1 and collateral S1. Oxtr Cre neurons mostly interact with subcortical areas but do not get many inputs from other cortical areas. Htr3a line had many inputs from all areas but less cholinergic inputs from NBM.

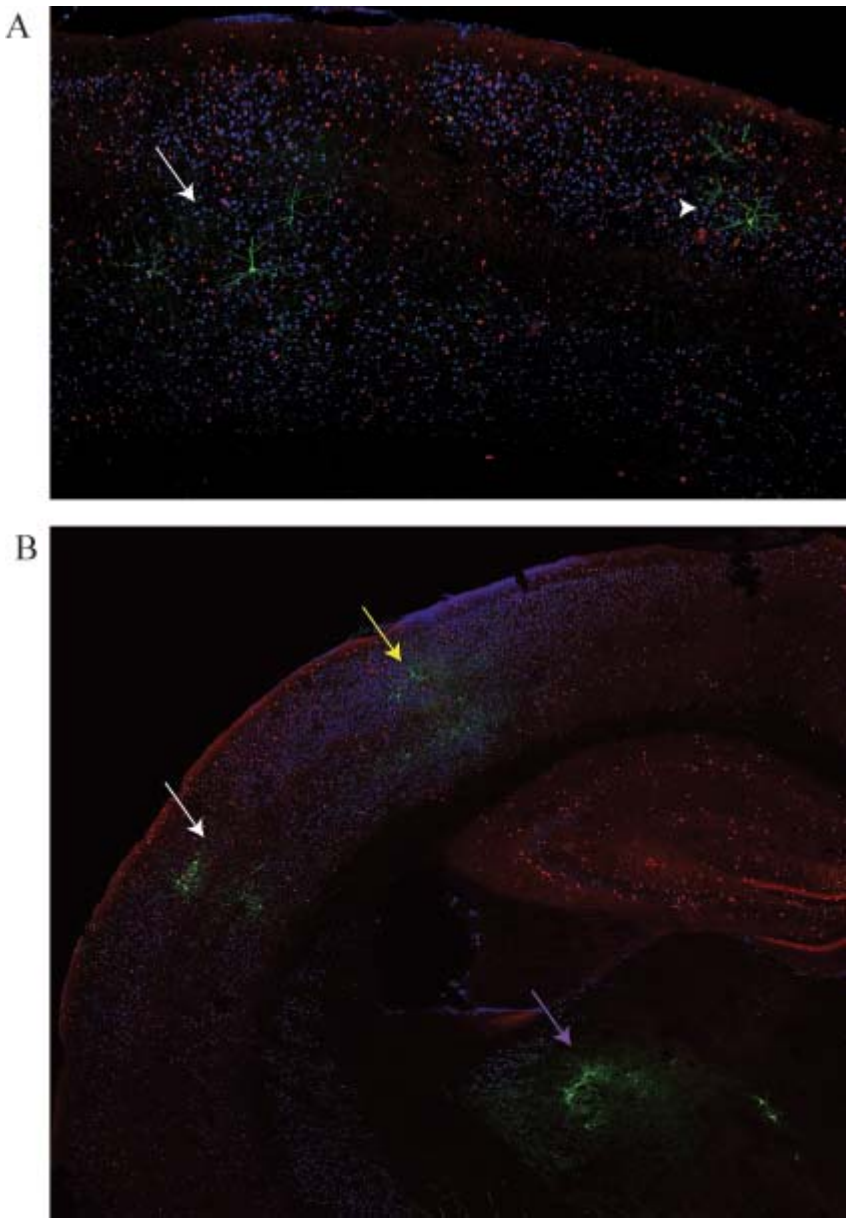

Figure 4.9: Cortical Projections to Htr3a Cre Positive Neurons in S1

S1 Htr3a Cre neurons received innervation from the pyramidal neurons of (A) the primary motor cortex (M1) and (B) the secondary somatosensory cortex (S2). (A) Arrow indicates the rabies infected pyramidal neurons in the M1 and arrowheads points to S1 pyramidal neurons connected with S1 Htr3a Cre interneurons. (B) White arrow shows the S2 pyramidal neurons infected by Rabies. Yellow arrow indicates Pyramidal neurons in S1Barrel cortex. Purple arrow points to Rabies infected neurons in VPM, PO, and VL.

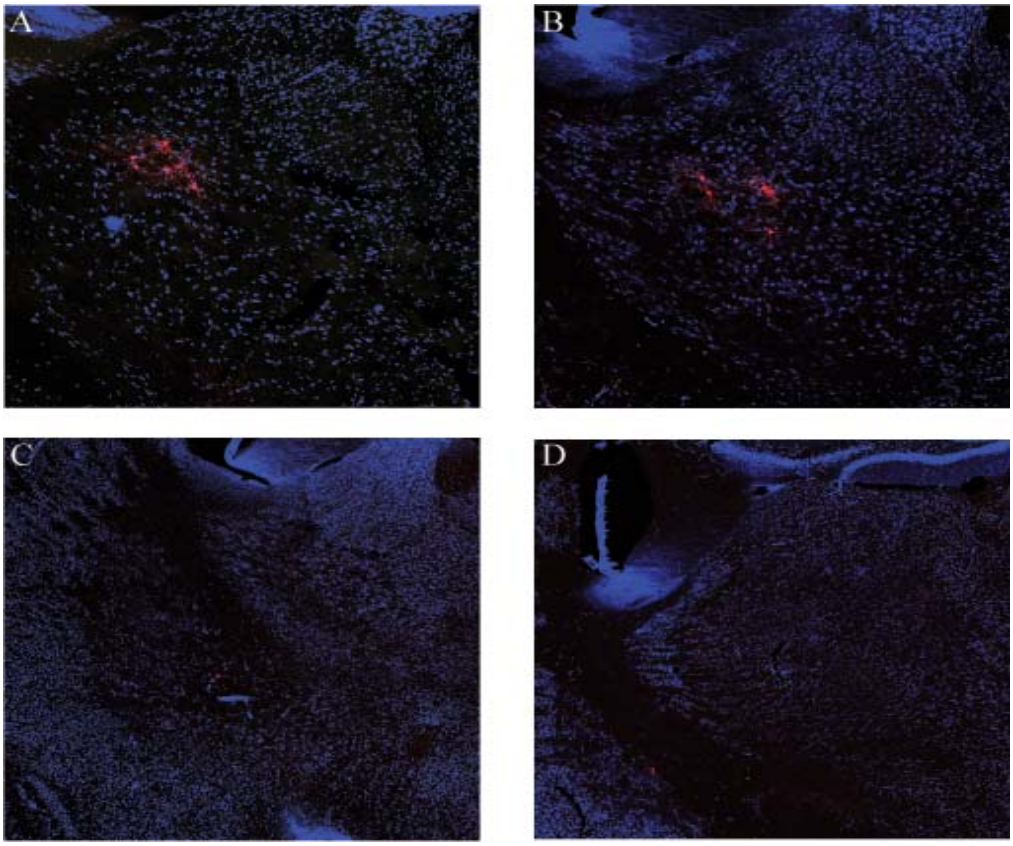

Figure 4.10: Subcortical Projections to Cre Positive Neurons in S1

Rabies virus was transferred trans-synaptically to ventral thalamic nuclei and Nucleus basalis of Meynert (NBM) in all three lines. (A) EYFP rabies expression in Ventral posterior medial nucleus (VPM) from S1 injection on Rbp4 Cre line. (B) mCherry expressing rabies virus in ventral lateral thalamic nucleus (VL) from S1 Oxtr Cre neurons. (C, D) NBM is expressing mCherry in (C) Rbp4 Cre and (D) Oxtr Cre lines.

Injection of helper virus and modified rabies virus in PFC resulted in different subcortical RV expressions to the somatosensory cortex. The anterior thalamic nuclear group, the mediodorsal thalamic nucleus (MD), and the midline thalamic nuclear group were the main projections sites in the thalamus to Cre positive neurons in PFC for all three lines (Figure 4.11). They belong to so-called association thalamic nuclei, and are known to be connected to the association cortical area. The anterior thalamic nuclei are known to receive inputs from hippocampus indirectly via mammilllary body and directly via fornix and project to cingulate cortex (Shibata 1993). Lesions of anterior thalamic nuclei caused spatial learning deficits. While anterior thalamic nuclei have strong connections with the hippocampal system, MD has strong reciprocal connections with PFC in addition to the basal ganglia networks. MD is involved in learning and the generation of goal-directed behavior. The midline thalamic nuclei and the intralaminar thalamic nuclei were once thought to have a non-specific global arousal effect on the whole brain. But now due to their specific connectivity, they are believed to be involved in more specific cognitive functions (Van der Werf, Witter et al. 2002). All three Cre lines received innervation from the midline thalamic nuclei.

The biggest projections to PFC Cre neurons were cholinergic neurons from NBM and the horizontal limb of the diagonal band (HDB) for all three lines (Figure 4.12). We also observed pyramidal neurons which were trans-synaptically infected with modified rabies virus in PFC, are projecting to HDB. Similar reciprocal connections were found in the lateral hypothalamus.

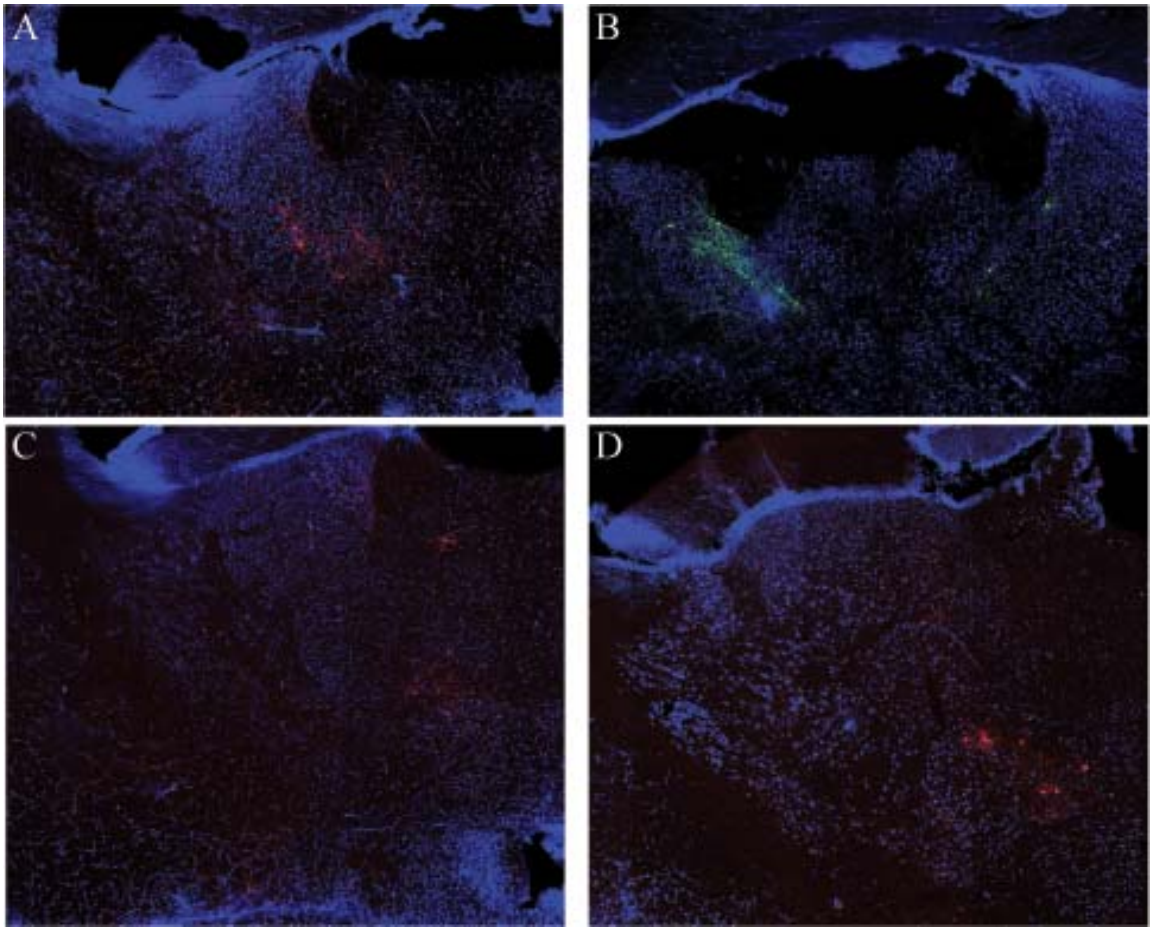

Figure4.11: Thalamic Inputs to Cre Neurons in PFC

Anterior thalamic nuclei projected to PFC in (A) Rbp4 Cre and (B) Oxtr Cre. We observed EFYP rabies virus expression in the ipsilateral anterior thalamic neucleus of Oxtr Cre line. This is probably because helper virus and rabies virus were spread to the ipsilateral side when we injected virus in PFC. Midline thalamic nuclei were also innervating to the PFC of (C) Rbp4 Cre and (D) Oxtr Cre.

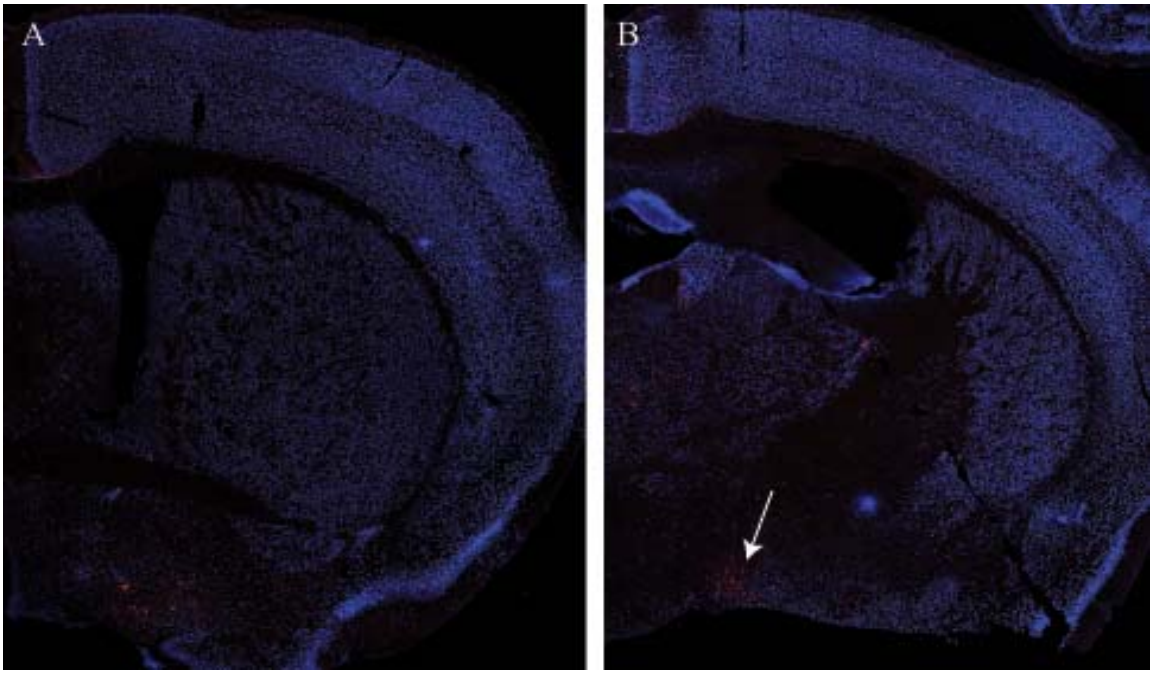

Figure 4.12: Innervations from HDB and PLH

(A) HDB innervations to Rbp4 Cre neurons in PFC (B) PLH innervations to Htr3a Cre neurons in PFC (white arrow). mCherry expressing rabies virus was also present in Anterior dorsal thalamic nucleus, Anterior medial thalamic nucleus (anterior thalamic nuclear group) and submedial thalamic nucleus (midline thalamic nuclear group). Similar observations were obtains in all three Cre lines.

On the other hand, innervations from the hippocampus and dopaminergic neurons seem to be line specific (Figure 4.13). We observed projections from hippocampus only in Rbp4 Cre and Htr3a Cre, but not in the Oxtr Cre line. Ventral CA1/Subiculum projections to prefrontal cortex have been previously reported (Jay and Witter 1991). The PFC neurons were known to be phase-locked to the hippocampal theta rhythm and this correlation is stronger during tasks requiring spatial working memory, which allows the integration of hippocampal spatial information into a broader, decision-making network (Jones and Wilson 2005). Projections to specific cortical interneurons from the hippocampus can facilitate the synchronizations between these two areas.

Interestingly two dopaminergic brain areas, VTA (ventral tegmental area) and Rli (the rostral linear nucleus) projected only to Htr3a Cre positive neurons in PFC but not to the Rbp4 and Oxtr Cre neurons. Dense dopaminergic inputs to PFC have been reported and they have received a lot of attention especially from schizophrenia studies, because of the indications on pathological involvements of both PFC and dopamine in schizophrenia. If dopaminergic neurons are innervating serotonin responsive interneurons selectively in PFC, this could be a site of crosstalk place between two different neuromodulatory systems.

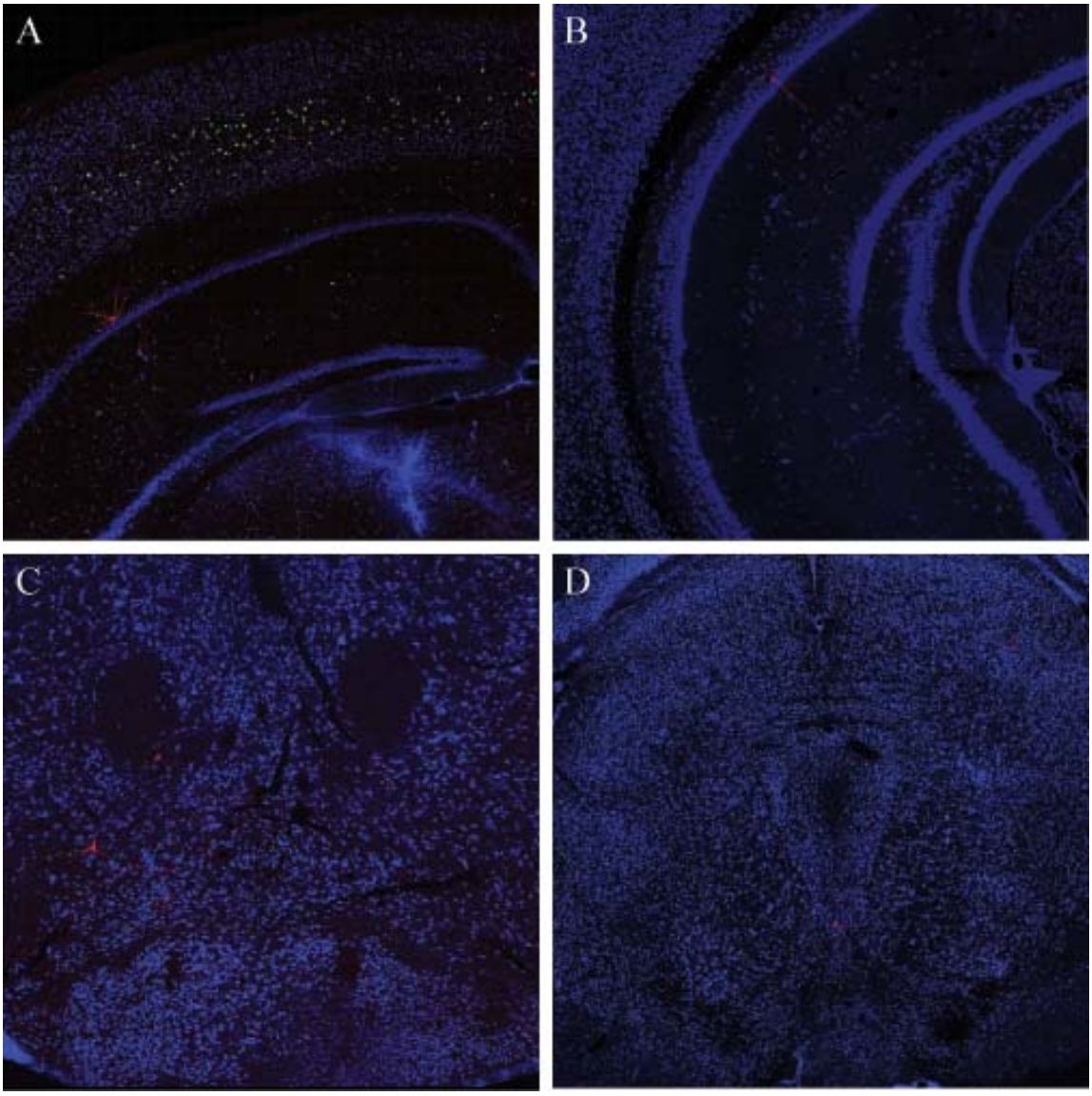

Figure 4.13: Selective Innervation from CA1 and Dopaminergic Neurons

(A,B) CA1 projections to Cre neurons in PFC of Rbp4 Cre line (A) and Htr3a Cre line (B). No CA1 neurons labeled Oxtr Cre neurons. (C) VTA and (D) Rli projections were observed only after mPFC rabies injections in Htr3a Cre neurons.

Although the Drd1a (dopamine receptor D1A) gene was not enriched in any of the interneuron lines including Htr3a Cre according to our TRAP results, other dopamine receptors were not represented on the microarray chip. Dopamine receptor 4 (Drd4) is known to be enriched in the prefrontal cortex, and Drd4 might be the main receptor of dopaminergic signaling in PFC. Future RNA-seq studies combining with TRAP could reveal the complete set of receptors which are expressing in each population. Another possibility is that this projection is either GABAergic or glutamatergic. In both VTA and Rli, dopaminergic neurons intermingled with GABAergic and glutamatergic neurons. GABAergic neurons in VTA are known to project to GABAergic neurons in the PFC (Carr and Sesack 2000). Therefore, this could be a dual inhibitory system to regulate the balance of the dopamine system and the serotonin system.

Again, the innervation preference to Cre positive PFC neurons was different depending on the lines. Rbp4 Cre line preferably connected to cholinergic neurons, while Oxtr Cre neurons received inputs almost equally from the anterior/midline thalamic nuclei and HDB. Both lines had only a few interactions with the MD thalamic nucleus. Htr3a Cre received more inputs from thalamic nuclei, in addition to CA1 and uniquely from dopaminergic neurons.

Figure 4.14 is a Summary Figure.

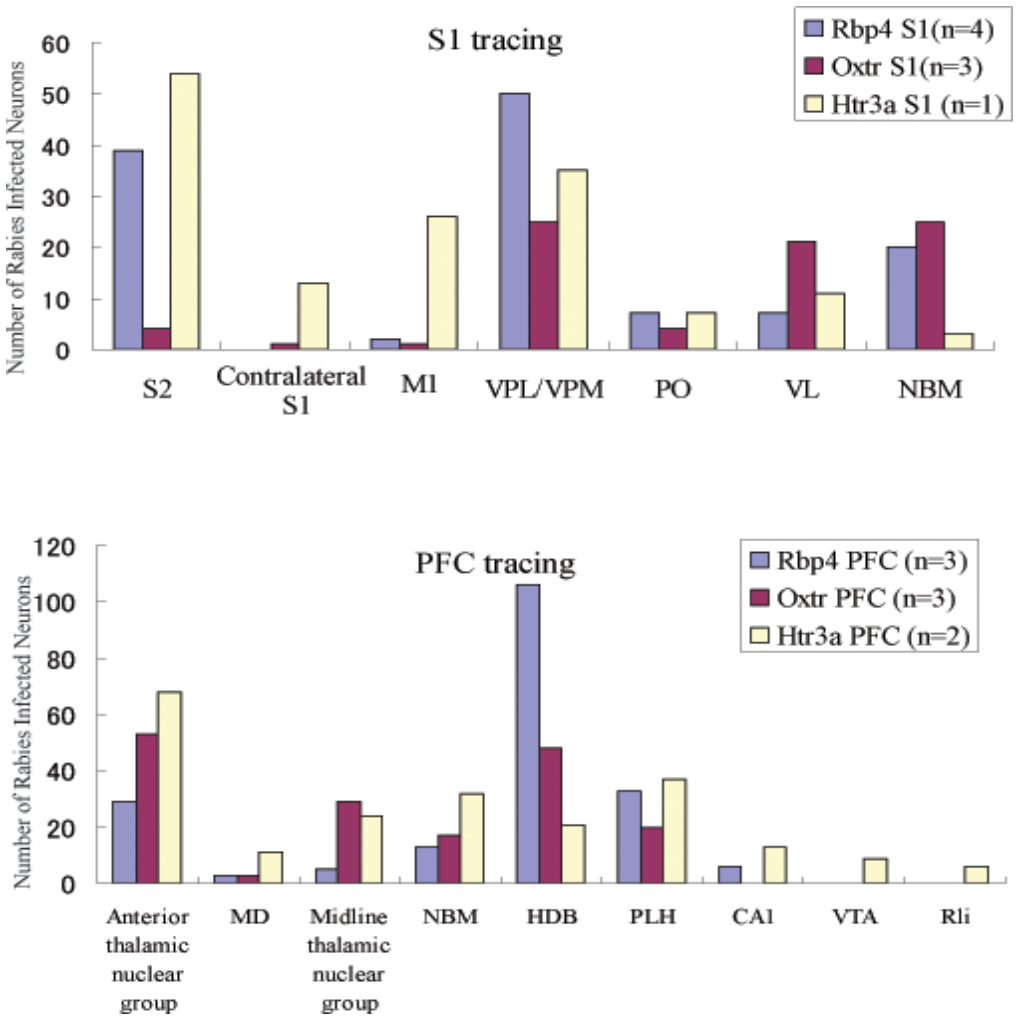

Figure 4.14: Summary of Tracing from S1 and PFC in 3 Cre Lines

(A) Tracing from S1. Major inputs to Rbp4 Cre neurons in S1 were S2 pyramidal neurons, Ventral thalamic neurons and NBM. Fewer innervations from contralateral S1 and ipsilateral M1 were observed in Rbp4 Cre and Oxtr Cre. On the other hand, Htr3a showed more innervation from these two cortical areas. Oxtr Cre didn't interact with other cortical areas as well, and received more innervation from subcortical areas. (B)Tracing from PFC. Rbp4 received more inputs from cholinergic neurons in HDB and NBM than thalamic neurons. Rbp4 and Htr3a Cre got innervations from CA1 but Oxtr Cre did not. Only Htr3a Cre received innervation from dopaminergic neurons.

Table 4.2 Number of Labeled Neurons in Locations Providing Input to S1 or PFC of Each Cre Mouse

A

S1	S2	colateral S1	M1	VPL/VPM	PO	VL	NBM
Rbp4 #1	7	0	0	2	2	0	4
Rbp4 #2	9	0	0	4	0	0	2
Rbp4 #3	16	0	2	37	0	0	12
Rbp4 #4	7	0	0	7	5	7	2
Oxtr #1	2	0	0	9	0	0	5
Oxtr #2	2	1	0	5	2	17	13
Oxtr #3	0	0	1	11	2	4	4
Htr3a #1	54	13	26	35	7	11	3

B

PFC	Anterior thalamic Nuclei	MD	Midline thalamic nuclei	NBM	HDB	PLH	CA1	VTA	Rli
Rbp4 #1	25	3	1	1	10	26	4	0	0
Rbp4 #2	0	0	1	0	46	5	1	0	0
Rbp4 #3	4	0	3	12	50	2	1	0	0
Oxtr #1	18	0	19	4	17	15	0	0	0
Oxtr #2	33	0	5	2	22	5	0	0	0
Oxtr #3	2	3	6	11	9	0	0	0	0
Htr3a #1	36	7	12	29	13	34	4	8	6
Htr3a #2	32	4	12	3	8	3	9	1	0

4-4: Discussion

4-4-1: Gene Profiling and IHC Studies

Gene profiling or IHC studies with EGFP-L10a reporter line might include cells which transiently express Cre during development and might be different from a group of neurons which were being targeted by AAV in adults. However the proportion of subtypes determined by IHC similar between labeled neurons with EGFP-L10a reporter line and targeted neurons by Cre dependent AAV-ChR2-EFYP in adults (data not shown) in these Cre lines. Therefore we ignored most of the effects from the development stages.

4-4-2: AAV Injections

AAV (ChR2-EFYP) injections into the somatosensory cortex of the adult Rbp4 Cre mouse line showed that most SST neurons in Rbp4 Cre lines rarely send axons to layer 1 (with some exceptions). This suggests Rbp4 Cre positive neurons label X94 like SST interneurons, even though they don't localize in layer 4. It is hard to define the clear morphologies and cell identity without electrophysiology and single cell labeling, but Rbp4 Cre may be preferably labeling a subtype of SST interneurons and Rbp4 could be a good marker for the study of X94 neurons. Rbp4 gene was also listed as one the most enriched genes in X94 cells compared to Martinotti cells in the comparative single cell PCR experiments (personal communication with Dr. Rudy).

4-4-3: Tiling of Oxtr Neurons

We observed a tiling-like phenomenon in the Oxtr Cre line. This could be controversial, because the Oxtr Cre population is heterogeneous according to IHC studies (at least mix

of SST and PV population). So far only adhesion molecules expressed in the same cell type and their downstream molecules were identified as tiling genes and there are no reports on the tiling of heterogeneous groups. It is doubtful that Oxtr itself could be involved in the spacing, but there a couple of reports suggesting Oxytocin's role in the maturation of interneurons. Oxytocin was shown to mediate the excitatory-to-inhibitory switch of GABA activity that occurs before birth in the GABAergic interneurons in the hippocampus (Tyzio, Cossart et al. 2006). This switch reduced neuronal activity, thereby protecting fetal neurons from hypoxia. As mentioned before, KCC2 can stop migration of neurons by excluding intercellular Cl^- and triggers the inhibitory switch in GABA signaling. If Oxytocin could stop migration like KCC2, oxytocin signaling through Oxtr might be involved in the positioning of Oxtr positive interneurons and spacing of them. It is too early to make a detailed hypothesis now, but there could be unknown tiling mechanisms for heterogeneous populations from different lineages.

4-4-4: Retrograde Tracing

Even though injection sites for every mouse were slightly different and the efficiency of virus infection was not identical either, subcortical locations of trans-synaptically RV infected neurons were quite consistent among different mice for each line. This supports the reliability of our methods, in spite of low number of infected neurons in subcortical regions. There could be a couple of reasons for the low efficiency. One reason comes from the size of the transgene inserted in helper virus. Compared to the maximum packaging size for AAV (5kb), transgene is oversized (7kb). Therefore recombination of Cre didn't happen efficiently compared to other Cre-dependent AAV viruses, even

though we waited for 2 months for the recombination. Also, if the injection site of AAV and rabies virus were slightly off, the number of neurons infected by modified rabies virus would be small due to the limitations of the virus spread. Therefore we collected data from a couple of mice with successful injections for each line.

Although Rbp4 Cre and Oxtr Cre population don't overlap completely, inputs to them were quite similar both in the somatosensory cortex and the prefrontal cortex. Surprisingly similar results were obtained from the Htr3a Cre line which suggests there are no big differences in their innervations among different cell types. However, it is possible that if we use a more specific line, we might be able to see clearer differences of innervations. Also, most of neuromodulatory inputs were not labeled by rabies virus, because they don't usually make synapses. This is why we couldn't observe Oxt neurons inputs in Oxtr Cre or Dorsal Raphe inputs to Htr3a Cre. Neuromodulatory inputs could be the major differences between different cell groups.

Modified rabies virus system using ErbB4-NRG interactions showed a similar innervation pattern to the Ht3a Cre line (Choi and Callaway 2011). This method targeted non PV/SST interneurons like Htr3a Cre line. Therefore, innervation patterns to Htr3a Cre neurons were confirmed with two different methods.

Reciprocal connections between S1 and M1 have been reported (Matyas, Sreenivasan et al. 2010) and this connection is critical for sensory-motor integration. However, only a few neurons in M1 were trans-synaptically labeled by modified rabies in Rbp4 and Oxtr

Cre line. This is not due to the selective transfer of rabies, because when helper virus was infected to pyramidal neurons, we observed many rabies infected neurons in M1 (data not shown). Also Htr3a Cre showed more innervations from M1. This suggests that inputs from M1 preferably connected to either pyramidal neurons or Htr3a positive population.

Chapter 5

Summary and Future Directions

The brain is considered to be the command center of our movements and thoughts, and evolved into a very complicated system to deal with all the situations animals could face. Scientists have taken a reductionist approach and designed several artificial neural network models to understand how local events happening in the brain could affect its computation outputs. However, most of the models simplified systems too much and lost the dynamicity of biological neural networks. One of the biggest obstacles these models face is the lack of information concerning the elementary unit of the system, “cell types” of neurons.

There is always a discussion whether there are many cell types or a continuum of a single class. At the anatomical level, interneurons are generally accepted as having distinct classes that correlate with their functional specializations. At the molecular level, the issue is more complicated. There are correlations of markers and some distinct classes, but this relationship is not always one to one. Different anatomically distinct classes share the same marker gene expression and the interneurons that belong to the anatomically same class could have different marker expression. This could suggest either that three are better molecular markers in each cell type or the more subtypes could exist in the class. If we consider the coverage factor of interneurons as 1 in the cortex, theoretically

~1000 different cell types could exist. This potential diversity just lends more confusion to the interneuron research when there is no clear method to differentiate cell types.

Two approaches could give us a better understanding of cell types. First, it should be understood how the brain groups neurons into different functional units, such as tiling mechanisms. We need more examples of cell types to understand how this works. Second, methods need to be created to manipulate functions of a specific group selectively and to examine their potential roles as cell types. Recent advances in the modern mouse genetic and in genomic tools could help us tackle these problems. What we need to know is the way to single out a group of neurons that carry out a distinct task and also to know the methods to label neurons which belong to the same group.

Many different transgenic/knock-in mice helped functional studies of interneurons (Ma, Hu et al. 2006; Taniguchi, He et al. 2011). However, these lines were not designed to help us understand the diversity of interneurons because target genes were known to label heterogeneous groups, and specific labeling by random insertions of transgenes can't be reproducible. Then the question is whether it is possible to target more specific populations by transgenesis. We have to find genes which are more correlated with the identity of the interneuron cell group. However, no efforts have yet been made to find potential interneuron markers in adult mouse brains.

By exploiting BacTRAP methods, we identified several candidate marker genes for more specific cortical interneuron subtypes and showed the possibilities of the existence of

molecular fingerprints for specific cell types. Without gene targeted mice, it is hard to qualify them as a marker, but both ISH and DRP results showed the possibility of targeting new specific cell groups. We discovered that BAC transgenesis was sometimes tricky when it came to targeting cortical interneurons. Many BAC transgenes showed correct subcortical expressions but not in the cortex. In the future, knock-in techniques could be used for these candidate marker genes which didn't target the endogenous group with BAC transgenesis. These lines could make huge progress in our understanding of interneuron cell types especially when they are combined with new gene profiling methods and Cre dependent functional studies.

Gene expression is highly correlated with cell identities and functions. However it is very hard to find out in which interneuron group a gene of interest is expressed. Not every protein has good antibodies, and double ISH methods often require a number of optimizations for each probe and it is hard to compare among different probes, because ISH signal is easily affected by sequences of probes. Gene profiling methods especially with RNA-seq could provide us with a complete list of expressing genes in a single experiment. With this list, we could hypothesize their inputs/outputs by the expression of receptors and neuropeptides. We could also easily distinguish different cell groups.

Cre lines can be used to reveal their connectivity. It was impossible to clarify the projections to a minor group by classical tracers. However, the new Cre dependent monosynaptic rabies virus system could label presynaptic inputs of only Cre positive neurons. We could successfully set up this technique to elucidate inputs to interneurons in

PFC and S1. We could find the input differences between different interneuron populations for the first time. This connectivity suggests potential functional roles of each interneuron group.

DRP studies on new Cre lines also suggest a new way to group interneurons. DRP analysis could be the only unbiased criteria for cell types, even though not all cell types have the tiling property. No new cortical neurons are born in adults, therefore they might need some functional redundancy to compensate for the potential loss of specific cell types. If the interneurons have 10-fold functional redundancy, the expected number of interneuron cell types is 35 (Stevens 1998) which is more reasonable number. However, we could observe tiling properties in Oxtr Cre neurons in adults. This might be difficult to accept because of the heterogeneity of Oxtr Cre neurons. But c-FOS studies on Oxytocin knock-out mice suggest the wide spread innervation of Oxtr neurons which we found by ChR2-EFYP AAV injections could be necessary to create the Oxytocin dependent cortical state.

To understand the oxytocin dependent cortical state, we are currently setting up a behavioral assay for Oxtr Cre neurons in PFC. We silenced Oxtr Cre positive interneurons in PFC by Cre-dependent membrane tethered toxins for Ca^{2+} channels (Auer, Sturzebecher et al. 2010) and examined their behavioral abnormalities after the social exposure when oxytocin was activated. We observed abnormal hyperactivity only after the social exposure, which suggests state dependent Oxytocin roles in the cortex. We need to do more control experiments to show that this phenomenon was created by

deficits of oxytocin control in the cortex, but this result suggests their homogenous role under the oxytocin influence. Although it is possible that homogenous subtypes in Oxtr Cre were good enough to silence the cortex after the social exposure, this could be the reason why heterogeneous groups need to show the tiling properties to influence the whole cortex.

Our research gave us new insights into interneuron properties and functions. Our unbiased systematic approach of the comparison of different interneuron subtypes has never been used before. Functional studies based on mouse lines for new candidate marker genes will be necessary to understand the microcircuit in the cortex. This study will expand our understanding of cell types.

Chapter 6

Materials and Methods

6-1: Generation of BAC Transgenic Mice

6-1-1: Molecular Cloning and BAC Modification

The BAC modification and transgenesis were carried out as previously reported (Gong, Zheng et al. 2003). For each driver, an optimal BAC was selected using UCSC genome browser (Table 6.1). We selected BACs which contained genes of interest. A 500-800 bp region immediately upstream of translational start codon was selected as the homologous region 'A box' and amplified by PCR from each BAC (primers information is in Table 6.1). The A box was then cloned into the shuttle vector pS296 (BacTRAP) or pS175 (Cre) using AscI/NotI sites. Each vector had either EGFP-L10 or Cre incorporated into its backbone right after the Abox sequence, whereas the R6kY-ORI promoter drove the pi protein dependent replication of the shuttle vector in the pir1 cells. The cloned shuttle vector was electroporated into BAC competent cells for the gene relevant BAC. The BAC competent cells have been rendered recombination competent by the introduction of a RecA gene from a carrier vector.

Electroporations underwent recombination and incorporated the A box along with the transgene (EGFP-L10 or Cre). Proper recombinant BAC cointegrates were selected by using a combination of three antibiotics: ampicillin (shuttle vector), chloramphenicol (BAC) and tetracycline (RecA plasmid). Further BAC cointegration was confirmed in

Gene	BAC	Forward Primer	Reverse Primer
Dlx1	RP23-440L10	CTTCTCGCGGGGTCTGGGTGTG	CTGGTTGGTTTCTGGGGCGGGAAG
PV	RP23-233L7	CAACTGTTTGAGCGGGCAGAGCAAG	GCCTCTGCACAGAGGAGCTCTGATAGTC
Npy	RP24-386I9	GGATACAGAAGGCTCAGACTTGGAGATGCTG	CCAGGAACCCAGATTGCATGTGTGCTC
Cck	RP23-234I17	GCTATGGGAAGCAAAGGCGAGGAGAG	CAAGAGGAAACGCTGCTTCTGATCAGGG
VIP	RP23-25A8	GGCGCGCCGCTTGGGCCTTGG	GGCGCGCCGCTTGGGCCTTGG
Cort	RP23-281A14	GACGTGCTGAGGTCTGTGCTTGGTG	CCTTCCTTGCGACCTGGTGAACACTG
Htr3a	RP24-377A21	GGCAAGCTTCCCAGATGTGGGAG	CCAGTCACCTGCTTCACTAGGGACATC
Lypd6	RP23-14O24	GGCAGACTGGCGTGTCACTCATACAGAGG	GGCGCGCCCTGAGTCTAGCTCCTGCAGTTTGGTAT
Nek7	RP23-209N14	AGGTTTTCGACAACTCGTGTG	TCTGACTCAACTGGGACTTCAG
Drd1a	RP23-322H10	CTTCCAGAAGGAAAGCACTTCCGGTGGCTTAGCCC	GGCGCGCCGGACTTGTCCAGGGGGTGATGGGCTG
Pnoc	RP23-264L8	CAGTGGGAATCGGGAGGCTGAAACAAC	CGCCACACTCTGCACTTTGCAATCCTTAC
Rbp4	RP24-285K21	CTCACCCCGGAGTCTGCCCTGCGGGACA	GGCGCGCCACACCATGGCCACGTAGGCCTCCAG
Oxtr	RP23-40E10	GACCAACCGCGACCGCGACCGCGACCCT	GGCGCGCCTGACAGGAGAGGTGTAGGTTTG

Table 6.1: BAC and Abox primers for Each Contsruct

two steps: first by carrying out cointegrate PCR, where primers for the region further 5' from the A box and EGFP or Cre reverse primer (Reverse (3') EGFP: CGCCCTCGCCGGACACGCTGAAC, or Reverse(3')Cre:CAACTTGCACCATGCCGCCCACGAC) are used to screen colonies and second, by Southern blot using radiolabelled A box as a probe on frequently cutting enzyme restricted BAC DNA. The confirmed BAC cointegrates were purified by Qiagen Large-construct kit (QIAGEN, Cat#12462) and linearized by PIsceI enzyme. We dialyzed BACs in injection buffer on a filter (Millipore, Cat # VSWP02500). Finally we ran pulse field gels to ensure BAC integrity, size and concentration.

6-1-2: BAC Transgenesis

All animal protocols were carried out in accordance with the US National Institute of Health Guide for the Care and Use of Laboratory Animals and were approved by the Rockefeller University Institutional Animal Care and Use Committee. All mice were raised at 78F in 12h light: 12h dark conditions with food and water provided *ad libitum*.

BAC transgenic mice were obtained by pronuclear injections of fertilized mouse oocytes (FVB/N) with a purified BAC fragment, followed by transfer of the injected oocytes to pseudopregnant foster mothers. Their progeny were screened for germline transmission of the modified BAC by PCR genotyping for EGFP. EGFP genotyping was carried out using the EGFP primers (CCTACGGCGTGCAGTGCTTCAGC and CGGCGAGCTGCACGCTGCGTCCTC) or the Cre primers (GATCTCCGGTATTG

AAACTCCAGC and GCTAAACATGCTTCATCGTCGG). Mice that carried the modified BAC in their genome, inferred by the presence of EGFP, were referred to as BAC founders (FF). The BAC founders were bread to C57Bl/6J mice to produce F1 litters which were then characterized for neuroanatomy. The BAC founders that recapitulated the endogenous gene expression pattern in the CNS and express the reporter EGFP at high enough levels in adults were then selected and used for further studying.

6-2: Histology

For DAB immunohistochemistry, brains were processed identically with MultiBrain Technology (NSA, Neuro Science Associates, Knoxville, TN) with a 1:75,000 dilution of Goat anti-EGFP serum (Heiman, Schaefer et al. 2008) according to the Vectastain elite protocol (Vector Labs, Burlingame, CA). Serial sections were digitized with a Zeiss Axioskop2 microscope at 10x magnification.

For fluorescence IHC of EGFP, PV, CR, nNOS, CB or NPY antibodies, mice were deeply anesthetized using CO2 chamber and transcardially perfused with 20ml of phosphate buffered saline (PBS) followed by 30ml of cold 4% paraformaldehyde (PFA) in PBS. For SST and VIP IHC, we used 10ml 4% PFA instead. Brains were post-fixed in 4% PFA overnight or 1hour for SST and VIP immunostaining. After postfix, brains were cryoprotected with 30% sucrose in PBS and incubated at 4C with gentle agitation until brains sank to the bottom. Then brains were embedded in "Neg50" Frozen Section Medium (Thermo Fisher Scientific). 40um coronal sections or 12um coronal section for SST and VIP IHC were cut with a Leica cryostat. 40um sections were processed free

floating IHC and 12um sections were directly mounted onto slides and IHC was performed on slides.

For immunohistochemistry, sections were blocked in 5% Normal Donkey Serum (NDS) in PBS with 0.1% Triton X-100 for 30mins and incubated at room temperature overnight with primary antibody against EGFP (Abcam, chicken monoclonal, ab13790, 1:1000), PV (Swant, rabbit polyclonal, PV-28, 1:1000), SST (Chemicon, rat monoclonal, MAB354, 1:500), CR (Chemicon, rabbit polyclonal, AB5054, 1:1000), nNOS (Chemicon, rabbit polyclonal, AB5380, 1:1000), NPY (Immunostar, rabbit polyclonal, 22840, 1:500), VIP (Immunostar, rabbit polyclonal, 20077, 1:500), or NeuN (Chemicon, mouse monoclonal, MAB377, 1:1000) in the blocking buffer. On the next day, sections were washed 3 times with 1x PBS for 5mins and then incubated with the appropriate Alexa dye-conjugated seconday antibodies diluted 1:1000 in 1x PBS for 1-2 hours. Then after being washed 3 times with 1x PBS again, sections were mounted on the slides. Confocal imaging of all staining was done on Zeiss LSM 700.

6-3: TRAP Methodology

All immunoprecipitations were performed with a mix of two custom generated GFP monoclonal antibodies (19C8, 19F7). Four adult mice (7-10 weeks old) were euthanized with CO2 for each replicate sample and the whole cerebral cortex was dissected out using HEPES buffer. In each case, males and female mice were used, evenly balanced in each replicate. Each cell population was assayed in triplicate. The cortical tissue was homogenized and centrifuged at 2000 x g for 10 min. The supernatant from the

homogenate was then supplemented with a mix of detergents DHPC and NP-40 before a second centrifugation at 20,000 x g for 15 min. 30ul of supernatant was saved as UB at 4℃. The rest of the supernatant was incubated overnight at 4℃ with pre-washed Streptavidin My-One Dynabeads conjugated with Protein-L and a mix of monoclonal anti-EGFP 19C8 and 19F7 antibodies. On the following day, the RNAs bound to the beads, referred to as immunoprecipitate (IP), were washed with high salt buffer (0.35M KCl) three times. RNA was extracted and purified using Absolutely NanoPrep RNA purification kit (Stratagene) for both IP and UB. RNA quantity and quality were determined using a Nanodrop 1000 spectrophotometer (Wilmington, DE) and Agilent 2100 Bioanalyzer (Foster City, CA). For each sample, 20ng of total RNA was amplified with Affymetrix two-cycle amplification kit and hybridized to Affymetrix 430 2.0 microarrays according to the manufacturer's instructions.

6-4: Microarray Normalization and Analysis

Replicate array samples were normalized within groups with quantile normalization (GCRMA) and between groups by global normalization to Affymetrix biotinylated spike-in controls. Data were filtered to remove those probesets with low signal (<50) from analysis, as well as those probesets identified as monoclonal background (Doyle, Dougherty et al. 2008). Biological replicates were averaged. Each IP was then compared to the UB from the same tissue to calculate the ratio of IP/UB as a measure of 'enrichment' and x-y scattered plot were created for 40,000 probesets.

The scripts used for calculation of SI are available on the BacTRAP website (www.bacTRAP.org). The IP was iteratively compared to each other and a ratio was calculated for each probeset. The probesets were ranked in accordance with the ratio and a statistical measure, p-value, is calculated based on how likely it is for a given probeset to have the rank by chance. SI analysis with IPs from three glial lines was done on Nek7 or Dlx1 IPs. Lists of statistically significant genes ($p<0.05$) for either Nek7 or Dlx1 IPs were generated and used for further analysis. For genes in each list, normalized expression values for 4 lines, (Dlx1, Cort, Nek7, Htr3a), were obtained and each divided by the maximum value among 4 lines for each gene. Genefilter from Bioconductor were performed to find a gene which has similar expression pattern as a template gene. Template genes were assigned for each subpopulation of 4 lines. Euclid distance was used to measure the differences. Top 100 genes were listed and processed to the ABA screening. Gene size and available BACs for candidate genes were checked in UCSC genome browser.

6-5: DRP Analysis

ABA ISH images around the somatosensory cortex were downloaded for GAD1, PV, SST, Cox6a2, Gpr176, and Kcnc3 genes. Confocal images of 20um thick coronal sections for Rbp4 Cre or Oxtr Cre line crossed with EGFP-L10a reporter line were also obtained for DRP analysis. 100~400 labeled neurons were selected using Image J and coordinates for each selected neuron were retrieved. Pairwise distance for every pair was calculated based on their coordinates and binned at 10um intervals. We ignored the data

for 10um because most of cell bodies of interneurons are about 10um wide. For each bin, density of selected cells was calculated by dividing with area for each bin.

6-6: Stereotactic Intracranial Injections

All animals were anesthetized by intraperitoneal injection of a cocktail of ketamine (100mg/ml) and xylazine (1mg/ml) at a volume equivalent to 10% of their body weights. Then the mice were mounted on a rodent stereotaxic instrument with head-fixing ear bars, a bite bar and a nose clamp. A small incision was made in the skin over the skull to expose the bregma, lambda, and desired injection site. A three-axis micromanipulator was used to measure spatial coordinates for the bregma and lambda. The stereotactic coordinates are S1: (AP-1.34, L-2.9, DV-0.3), and PFC: (AP-0.3. L-1.8, DV-1.5). All stereotaxic measurements were taken relative to Bregma and with the depth determined from the brain surface. A small drill hole was made in the skull over the injection site, exposing the brain. For the visualization of Cre positive neurons, a Hamilton needle (30G style #4, Hamilton company, NV) was loaded with either AAV2/5.EF1a.DIO.hChR2 (H134R)-EYFP.WPRE.hGH, or AAV2/5.EF1a.DIO.hChR2(H134R)-mCherry.WPRE .hGH from the Penn Vector Core in the University of Pennsylvania. 300nl of either virus was injected in S1 using Hamilton syringes. 3 weeks later mice were sacrificed to examine their expressions.

For retrograde tracing, pAAV2/9-EF1α-dflox-GTB were prepared by the Penn Vector Core. and EnvA-pseudotyped, G-deleted rabies virus were produced in a manner similar to that described previously (Wickersham, Lyon et al. 2007). First 400nl of helper AAV

virus were injected and 2 months later, 400nl of modified rabies virus were injected under the same condition in the same brain area. The rabies virus was allowed to replicate and spread for 2 weeks before perfusion and tissue processing.

References:

Alifragis, P., A. Liapi, et al. (2004). "Lhx6 regulates the migration of cortical interneurons from the ventral telencephalon but does not specify their GABA phenotype." J Neurosci **24**(24): 5643-5648.

Arenkiel, B. R., M. E. Klein, et al. (2008). "Genetic control of neuronal activity in mice conditionally expressing TRPV1." Nat Methods **5**(4): 299-302.

Armbruster, B. N., X. Li, et al. (2007). "Evolving the lock to fit the key to create a family of G protein-coupled receptors potently activated by an inert ligand." Proc Natl Acad Sci U S A **104**(12): 5163-5168.

Ascoli, G. A., L. Alonso-Nanclares, et al. (2008). "Petilla terminology: nomenclature of features of GABAergic interneurons of the cerebral cortex." Nat Rev Neurosci **9**(7): 557-568.

Auer, S., A. S. Sturzebecher, et al. (2010). "Silencing neurotransmission with membrane-tethered toxins." Nat Methods **7**(3): 229-236.

Batista-Brito, R. and G. Fishell (2009). "The developmental integration of cortical interneurons into a functional network." Curr Top Dev Biol **87**: 81-118.

Ben-Ari, Y. (2002). "Excitatory actions of gaba during development: the nature of the nurture." Nat Rev Neurosci **3**(9): 728-739.

Blatow, M., A. Rozov, et al. (2003). "A novel network of multipolar bursting interneurons generates theta frequency oscillations in neocortex." Neuron **38**(5): 805-817.

Borrelli, E., R. Heyman, et al. (1988). "Targeting of an inducible toxic phenotype in animal cells." Proc Natl Acad Sci U S A **85**(20): 7572-7576.

Bortone, D. and F. Polleux (2009). "KCC2 expression promotes the termination of cortical interneuron migration in a voltage-sensitive calcium-dependent manner." Neuron **62**(1): 53-71.

Boyden, E. S., F. Zhang, et al. (2005). "Millisecond-timescale, genetically targeted optical control of neural activity." Nat Neurosci **8**(9): 1263-1268.

Buch, T., F. L. Heppner, et al. (2005). "A Cre-inducible diphtheria toxin receptor mediates cell lineage ablation after toxin administration." Nat Methods **2**(6): 419-426.

Butt, S. J., V. H. Sousa, et al. (2008). "The requirement of Nkx2-1 in the temporal specification of cortical interneuron subtypes." Neuron **59**(5): 722-732.

Buzsaki, G. (2006). Rhythms of the Brain Oxford University Press.

Cajal, R. y. (1899). Histology of the nervous system of man and vertebrates.

Carr, D. B. and S. R. Sesack (2000). "GABA-containing neurons in the rat ventral tegmental area project to the prefrontal cortex." Synapse **38**(2): 114-123.

Chao, H. T., H. Chen, et al. (2010). "Dysfunction in GABA signalling mediates autism-like stereotypies and Rett syndrome phenotypes." Nature **468**(7321): 263-269.

Choi, J. and E. M. Callaway (2011). "Monosynaptic inputs to ErbB4-expressing inhibitory neurons in mouse primary somatosensory cortex." J Comp Neurol **519**(17): 3402-3414.

Choi, J., J. A. Young, et al. (2010). "Selective viral vector transduction of ErbB4 expressing cortical interneurons in vivo with a viral receptor-ligand bridge protein." Proc Natl Acad Sci U S A **107**(38): 16703-16708.

Cobos, I., M. E. Calcagnotto, et al. (2005). "Mice lacking Dlx1 show subtype-specific loss of interneurons, reduced inhibition and epilepsy." Nat Neurosci **8**(8): 1059-1068.

Curley, A. A. and D. A. Lewis (2012). "Cortical basket cell dysfunction in schizophrenia." J Physiol **590**(Pt 4): 715-724.

de Lecea, L., J. A. del Rio, et al. (1997). "Cortistatin is expressed in a distinct subset of cortical interneurons." J Neurosci **17**(15): 5868-5880.

Dougherty, J. D., E. F. Schmidt, et al. (2010). "Analytical approaches to RNA profiling data for the identification of genes enriched in specific cells." Nucleic Acids Res **38**(13): 4218-4230.

Doyle, J. P., J. D. Dougherty, et al. (2008). "Application of a translational profiling approach for the comparative analysis of CNS cell types." Cell **135**(4): 749-762.

Emoto, K., Y. He, et al. (2004). "Control of dendritic branching and tiling by the Tricornered-kinase/Furry signaling pathway in Drosophila sensory neurons." Cell **119**(2): 245-256.

Ferezou, I., B. Cauli, et al. (2002). "5-HT3 receptors mediate serotonergic fast synaptic excitation of neocortical vasoactive intestinal peptide/cholecystokinin interneurons." J Neurosci **22**(17): 7389-7397.

Ferguson, J. N., J. M. Aldag, et al. (2001). "Oxytocin in the medial amygdala is essential for social recognition in the mouse." J Neurosci **21**(20): 8278-8285.

Fino, E. and R. Yuste (2011). "Dense inhibitory connectivity in neocortex." Neuron **69**(6): 1188-1203.

Fuerst, P. G., A. Koizumi, et al. (2008). "Neurite arborization and mosaic spacing in the mouse retina require DSCAM." Nature **451**(7177): 470-474.

Gan, W. B. and E. R. Macagno (1995). "Interactions between segmental homologs and between isoneuronal branches guide the formation of sensory terminal fields." J Neurosci **15**(5 Pt 1): 3243-3253.

Gelman, D. M. and O. Marin (2010). "Generation of interneuron diversity in the mouse cerebral cortex." Eur J Neurosci **31**(12): 2136-2141.

Gong, S., C. Zheng, et al. (2003). "A gene expression atlas of the central nervous system based on bacterial artificial chromosomes." Nature **425**(6961): 917-925.

Han, X. and E. S. Boyden (2007). "Multiple-color optical activation, silencing, and desynchronization of neural activity, with single-spike temporal resolution." PLoS One **2**(3): e299.

Hatten, M. E. and N. Heintz (2005). "Large-scale genomic approaches to brain development and circuitry." Annu Rev Neurosci **28**: 89-108.

Heiman, M., A. Schaefer, et al. (2008). "A translational profiling approach for the molecular characterization of CNS cell types." Cell **135**(4): 738-748.

Hobert, O., I. Carrera, et al. (2010). "The molecular and gene regulatory signature of a neuron." Trends Neurosci **33**(10): 435-445.

Huang, Z. J., G. Di Cristo, et al. (2007). "Development of GABA innervation in the cerebral and cerebellar cortices." Nat Rev Neurosci **8**(9): 673-686.

Ibanez-Tallon, I., H. Wen, et al. (2004). "Tethering naturally occurring peptide toxins for cell-autonomous modulation of ion channels and receptors in vivo." Neuron **43**(3): 305-311.

Inan, M., J. Welagen, et al. (2012). "Spatial and temporal bias in the mitotic origins of somatostatin- and parvalbumin-expressing interneuron subgroups and the chandelier subtype in the medial ganglionic eminence." Cereb Cortex **22**(4): 820-827.

Jay, T. M. and M. P. Witter (1991). "Distribution of hippocampal CA1 and subicular efferents in the prefrontal cortex of the rat studied by means of anterograde transport of Phaseolus vulgaris-leucoagglutinin." J Comp Neurol **313**(4): 574-586.

Johns, D. C., R. Marx, et al. (1999). "Inducible genetic suppression of neuronal excitability." J Neurosci **19**(5): 1691-1697.

Jones, E. G. (2009). "The origins of cortical interneurons: mouse versus monkey and human." Cereb Cortex **19**(9): 1953-1956.

Jones, M. W. and M. A. Wilson (2005). "Theta rhythms coordinate hippocampal-prefrontal interactions in a spatial memory task." PLoS Biol **3**(12): e402.

Karpova, A. Y., D. G. Tervo, et al. (2005). "Rapid and reversible chemical inactivation of synaptic transmission in genetically targeted neurons." Neuron **48**(5): 727-735.

Kay, J. N., M. W. Chu, et al. (2012). "MEGF10 and MEGF11 mediate homotypic interactions required for mosaic spacing of retinal neurons." Nature **483**(7390): 465-469.

Kerlin, A. M., M. L. Andermann, et al. (2010). "Broadly tuned response properties of diverse inhibitory neuron subtypes in mouse visual cortex." Neuron **67**(5): 858-871.

Koike-Kumagai, M., K. Yasunaga, et al. (2009). "The target of rapamycin complex 2 controls dendritic tiling of Drosophila sensory neurons through the Tricornered kinase signalling pathway." EMBO J **28**(24): 3879-3892.

Lee, S., J. Hjerling-Leffler, et al. (2010). "The largest group of superficial neocortical GABAergic interneurons expresses ionotropic serotonin receptors." J Neurosci **30**(50): 16796-16808.

Lein, E. S., M. J. Hawrylycz, et al. (2007). "Genome-wide atlas of gene expression in the adult mouse brain." Nature **445**(7124): 168-176.

Lerchner, W., C. Xiao, et al. (2007). "Reversible silencing of neuronal excitability in behaving mice by a genetically targeted, ivermectin-gated Cl- channel." Neuron **54**(1): 35-49.

Liodis, P., M. Denaxa, et al. (2007). "Lhx6 activity is required for the normal migration and specification of cortical interneuron subtypes." J Neurosci **27**(12): 3078-3089.

Lisman, J. E., J. T. Coyle, et al. (2008). "Circuit-based framework for understanding neurotransmitter and risk gene interactions in schizophrenia." Trends Neurosci **31**(5): 234-242.

Lo, L. and D. J. Anderson (2011). "A Cre-dependent, anterograde transsynaptic viral tracer for mapping output pathways of genetically marked neurons." Neuron **72**(6): 938-950.

Ma, Y., H. Hu, et al. (2006). "Distinct subtypes of somatostatin-containing neocortical interneurons revealed in transgenic mice." J Neurosci **26**(19): 5069-5082.

Magnus, C. J., P. H. Lee, et al. (2011). "Chemical and genetic engineering of selective ion channel-ligand interactions." Science **333**(6047): 1292-1296.

Marin, O. (2012). "Interneuron dysfunction in psychiatric disorders." Nat Rev Neurosci **13**(2): 107-120.

Markram, H., M. Toledo-Rodriguez, et al. (2004). "Interneurons of the neocortical inhibitory system." Nat Rev Neurosci **5**(10): 793-807.

Masland, R. H. (2001). "Neuronal diversity in the retina." Curr Opin Neurobiol **11**(4): 431-436.

Masland, R. H. (2004). "Neuronal cell types." Curr Biol **14**(13): R497-500.

Matthews, B. J., M. E. Kim, et al. (2007). "Dendrite self-avoidance is controlled by Dscam." Cell **129**(3): 593-604.

Matyas, F., V. Sreenivasan, et al. (2010). "Motor control by sensory cortex." Science **330**(6008): 1240-1243.

McBain, C. J. (2012). "Cortical inhibitory neuron basket cells: from circuit function to disruption." J Physiol **590**(Pt 4): 667.

McGarry, L. M., A. M. Packer, et al. (2010). "Quantitative classification of somatostatin-positive neocortical interneurons identifies three interneuron subtypes." Front Neural Circuits **4**: 12.

Miyoshi, G., S. J. Butt, et al. (2007). "Physiologically distinct temporal cohorts of cortical interneurons arise from telencephalic Olig2-expressing precursors." J Neurosci **27**(29): 7786-7798.

Nakashiba, T., J. Z. Young, et al. (2008). "Transgenic inhibition of synaptic transmission reveals role of CA3 output in hippocampal learning." Science **319**(5867): 1260-1264.

Nelson, S. B., C. Hempel, et al. (2006). "Probing the transcriptome of neuronal cell types." Curr Opin Neurobiol **16**(5): 571-576.

Nelson, S. B., K. Sugino, et al. (2006). "The problem of neuronal cell types: a physiological genomics approach." Trends Neurosci **29**(6): 339-345.

Olah, S., M. Fule, et al. (2009). "Regulation of cortical microcircuits by unitary GABA-mediated volume transmission." Nature **461**(7268): 1278-1281.

Rockhill, R. L., T. Euler, et al. (2000). "Spatial order within but not between types of retinal neurons." Proc Natl Acad Sci U S A **97**(5): 2303-2307.

Rodieck, R. W. (1991). "The density recovery profile: a method for the analysis of points in the plane applicable to retinal studies." Vis Neurosci **6**(2): 95-111.

Rudy, B. and C. J. McBain (2001). "Kv3 channels: voltage-gated K+ channels designed for high-frequency repetitive firing." Trends Neurosci **24**(9): 517-526.

Runyan, C. A., J. Schummers, et al. (2010). "Response features of parvalbumin-expressing interneurons suggest precise roles for subtypes of inhibition in visual cortex." Neuron **67**(5): 847-857.

Sagasti, A., M. R. Guido, et al. (2005). "Repulsive interactions shape the morphologies and functional arrangement of zebrafish peripheral sensory arbors." Curr Biol **15**(9): 804-814.

Shepherd, G. M. (2003). "The Synaptic Organization of the Brain."

Shibata, H. (1993). "Efferent projections from the anterior thalamic nuclei to the cingulate cortex in the rat." J Comp Neurol **330**(4): 533-542.

Siegert, S., B. G. Scherf, et al. (2009). "Genetic address book for retinal cell types." Nat Neurosci **12**(9): 1197-1204.

Sivilotti, L. and A. Nistri (1991). "GABA receptor mechanisms in the central nervous system." Prog Neurobiol **36**(1): 35-92.

Somogyi, P. and A. Cowey (1981). "Combined Golgi and electron microscopic study on the synapses formed by double bouquet cells in the visual cortex of the cat and monkey." J Comp Neurol **195**(4): 547-566.

Stevens, C. F. (1998). "Neuronal diversity: too many cell types for comfort?" Curr Biol **8**(20): R708-710.

Sugino, K., C. M. Hempel, et al. (2006). "Molecular taxonomy of major neuronal classes in the adult mouse forebrain." Nat Neurosci **9**(1): 99-107.

Szabadics, J., C. Varga, et al. (2006). "Excitatory effect of GABAergic axo-axonic cells in cortical microcircuits." Science **311**(5758): 233-235.

Tan, E. M., Y. Yamaguchi, et al. (2006). "Selective and quickly reversible inactivation of mammalian neurons in vivo using the Drosophila allatostatin receptor." Neuron **51**(2): 157-170.

Taniguchi, H., M. He, et al. (2011). "A resource of Cre driver lines for genetic targeting of GABAergic neurons in cerebral cortex." Neuron **71**(6): 995-1013.

Tyzio, R., R. Cossart, et al. (2006). "Maternal oxytocin triggers a transient inhibitory switch in GABA signaling in the fetal brain during delivery." Science **314**(5806): 1788-1792.

Van der Werf, Y. D., M. P. Witter, et al. (2002). "The intralaminar and midline nuclei of the thalamus. Anatomical and functional evidence for participation in processes of arousal and awareness." Brain Res Brain Res Rev **39**(2-3): 107-140.

Wall, N. R., I. R. Wickersham, et al. (2010). "Monosynaptic circuit tracing in vivo through Cre-dependent targeting and complementation of modified rabies virus." Proc Natl Acad Sci U S A **107**(50): 21848-21853.

Wang, Z., M. Gerstein, et al. (2009). "RNA-Seq: a revolutionary tool for transcriptomics." Nat Rev Genet **10**(1): 57-63.

Wassle, H., L. Peichl, et al. (1981). "Dendritic territories of cat retinal ganglion cells." Nature **292**(5821): 344-345.

Wickersham, I. R., D. C. Lyon, et al. (2007). "Monosynaptic restriction of transsynaptic tracing from single, genetically targeted neurons." Neuron **53**(5): 639-647.

Wonders, C. P. and S. A. Anderson (2006). "The origin and specification of cortical interneurons." Nat Rev Neurosci **7**(9): 687-696.

Woodruff, A. R., S. A. Anderson, et al. (2010). "The enigmatic function of chandelier cells." Front Neurosci **4**: 201.

Yang, Q., T. E. Graham, et al. (2005). "Serum retinol binding protein 4 contributes to insulin resistance in obesity and type 2 diabetes." Nature **436**(7049): 356-362.

Zhang, F., L. P. Wang, et al. (2007). "Multimodal fast optical interrogation of neural circuitry." Nature **446**(7136): 633-639.